

การพัฒนาวิธีตรวจวัดซัลโฟนาไมด์โดยใช้อัลตราฟาสต์ลิควิดโครมาโทกราฟีร่วมกับการตรวจวัดทางเคมีไฟฟ้า

นางสาวณภัทรณีย์ ธัมมสุนทรีย์

วิทยานิพนธ์นี้เป็นส่วนหนึ่งของการศึกษาตามหลักสูตรปริญญาวิทยาศาสตรมหาบัณฑิต  
สาขาวิชาเคมี ภาควิชาเคมี  
คณะวิทยาศาสตร์ จุฬาลงกรณ์มหาวิทยาลัย  
ปีการศึกษา 2555

ลิขสิทธิ์ของจุฬาลงกรณ์มหาวิทยาลัย  
บทคัดย่อและแฟ้มข้อมูลฉบับเต็มของวิทยานิพนธ์ตั้งแต่ปีการศึกษา 2554 ที่ให้บริการในคลังปัญญาจุฬาฯ (CUIR)  
เป็นแฟ้มข้อมูลของนิสิตเจ้าของวิทยานิพนธ์ที่ส่งผ่านทางบัณฑิตวิทยาลัย

The abstract and full text of theses from the academic year 2011 in Chulalongkorn University Intellectual Repository (CUIR) are the thesis authors' files submitted through the Graduate School.

METHOD DEVELOPMENT FOR DETERMINATION OF SULFONAMIDES BY  
ULTRA FAST LIQUID CHROMATOGRAPHY COUPLED WITH  
ELECTROCHEMICAL DETECTION

Miss Nupattaraneer Thammasoontaree

A Thesis Submitted in Partial Fulfillment of the Requirements  
for the Degree of Master of Science Program in Chemistry

Department of Chemistry

Faculty of Science

Chulalongkorn University

Academic Year 2012

Copyright of Chulalongkorn University

Thesis Title                      Method development for determination of sulfonamides  
by ultra fast liquid chromatography coupled with  
electrochemical detection

By                                      Miss Nupattaraneer Thammasoontaree

Field of Study                      Chemistry

Thesis Advisor                      Professor Orawon Chailapakul, Ph.D.

---

Accepted by the Faculty of Science, Chulalongkorn University in Partial  
Fulfillment of the Requirements for the Master's Degree

.....Dean of the Faculty of Science  
(Professor Supot Hannongbua, Dr. rer. nat.)

#### THESIS COMMITTEE

.....Chairman  
(Assistant Professor Warinthorn Chavasiri, Ph.D.)

.....Thesis Advisor  
(Professor Orawon Chailapakul, Ph.D.)

.....Examiner  
(Assistant Professor Suchada Chuanuwatanakul, Ph.D.)

.....External Examiner  
(Anchana Preechaworapun, Ph.D.)

ณภัทรณีย์ ธัมมสุนทรีย์: การพัฒนาวิธีตรวจวัดซัลโฟนาไมด์โดยใช้อัลตราฟาสต์ลิควิดโครมาโทกราฟีร่วมกับเทคนิคการตรวจวัดทางเคมีไฟฟ้า(METHOD DEVELOPMENT FOR DETERMINATION OF SULFONAMIDES BY ULTRA FAST LIQUID CHROMATOGRAPHY COUPLED WITH ELECTROCHEMICAL DETECTION) อ. ที่ปรึกษาวิทยานิพนธ์หลัก: ดร. อรรพรรณ ชัยฉกากุล , 124 หน้า.

กราฟีน-วัสดุที่ประกอบด้วยอะตอมคาร์บอนเรียงตัวกันแบบสองมิติเป็นวัสดุที่กำลังได้รับความสนใจในงานทางเคมีไฟฟ้า เนื่องด้วยวัสดุดังกล่าวมี คุณสมบัติการนำไฟฟ้าสูง, มีความแข็งแรงคงทนสูง และมีราคาถูก ในงานวิจัยนี้ได้เตรียมส่วนผสมระหว่างวัสดุกราฟีนกับพอลิอะนิลีนและประสบความสำเร็จในการสร้างขั้วไฟฟ้าที่ดัดแปรผิวหน้าด้วยเทคนิคอิเล็กโทรสเปรย์ โดยขั้วไฟฟ้าดัดแปรนี้ได้ถูกนำไปเปรียบเทียบกับขั้วไฟฟ้าที่พิมพ์สกรีนคาร์บอนและขั้วไฟฟ้าฟิล์มบางเจือโบรอนและหลังจากนั้นได้นำไปประยุกต์ในการวิเคราะห์สารซัลโฟนาไมด์ทั้ง 8 ชนิดในคราวเดียวกัน ระบบอัลตราฟาสต์ลิควิดโครมาโทกราฟีร่วมกับการตรวจวัดด้วยแอมเพอโรเมตรีโดยการใช้ขั้วไฟฟ้าที่ดัดแปรผิวหน้าด้วยวัสดุกราฟีนกับพอลิอะนิลีนให้ผลการตอบสนองที่สูงและไวด้วยระยะเวลาในการแยกสารซัลโฟนาไมด์ทั้ง 8 ชนิด ภายใน 7 นาทีโดยใช้เฟสเคลื่อนที่ในการแยกคือ สารละลายโพแทสเซียมไฮโดรเจนฟอสเฟต(pH 3): อะซิโตนไตรรล์: เอทานอล ในอัตราส่วน 70: 25: 5 โดยเทคนิคแอมเพอโรเมตรีมีการให้ศักย์ไฟฟ้าในการตรวจวัดที่ 1.4 โวลต์ ค่าความเป็นเส้นตรงของระบบอยู่ในช่วง 0.01-10  $\mu\text{g mL}^{-1}$  โดยมีสัมประสิทธิ์สหสัมพันธ์ 0.99 และขีดจำกัดต่ำสุดในการตรวจวัดอยู่ในช่วง 1.162-6.127  $\text{ng mL}^{-1}$  สำหรับสารซัลโฟนาไมด์ทั้ง 8 ชนิด นอกจากนี้ระบบการวิเคราะห์แบบใหม่นี้ให้สภาพไวสูง รวดเร็ว และเลือกจำเพาะในการตรวจวัดสารซัลโฟนาไมด์ทั้ง 8 ชนิดได้ดี

ภาควิชา.....เคมี.....ลายมือชื่อนิสิต.....  
 สาขาวิชา.....เคมี.....ลายมือชื่อ อ.ที่ปรึกษาวิทยานิพนธ์หลัก.....  
 ปีการศึกษา.....2555.....

# # 537 2248 923 : MAJOR CHEMISTRY

KEYWORDS : ULTRA-PERFORMANCE LIQUID CHROMATOGRAPHY /  
SULFONAMIDES / GRAPHENE / POLYANILINE

NUPATTARANEE THAMMSOONTAREE: METHOD  
DEVELOPMENT FOR THE DETERMINATION OF SULFONAMIDES  
BY ULTRA FAST LIQUID CHROMATOGRAPHY COUPLED WITH  
ELECTROCHEMICAL DETECTION. ADVISOR: PROF. ORAWON  
CHAILAPAKUL, Ph. D., 124 pp.

Graphene (G) – a two dimensional sheet of  $sp^2$  carbon atom, has become an attractive materials in electrochemistry due to its high electrical conductivity, high mechanical strength and potentially low manufacturing cost. In this study, the nanocomposite of G and polyaniline (PANI) was prepared and was successfully modified on screen-printed carbon electrode by electrospraying technique. The G/PANI-modified electrode was compared with bare carbon and boron-doped diamond electrode and then applied for simultaneous determination of eight sulfonamides (SAs) using ultra fast liquid chromatography (UFLC). UFLC coupled with amperometric detection on G/PANI modified electrode offered high sensitivity and fast response with separation for all eight SAs within 7 minutes by using 70:25:5 (v/v/v) of potassium hydrogen phosphate solution (pH 3): acetonitrile: ethanol as mobile phase. Amperometric detection was performed at a detection potential of +1.4 V. The linearity of this system was obtained in a range of 0.01-10  $\mu\text{g mL}^{-1}$  with a 0.99 correlation coefficient, and the limit of detection was found in a range of 1.162-6.127  $\text{ng mL}^{-1}$  for all SAs. Overall, this novel system provides high sensitivity and rapid analysis for selective determination of eight SAs.

Department : .....Chemistry..... Student's Signature .....

Field of Study : .....Chemistry..... Advisor's Signature .....

Academic Year : .....2012.....

## ACKNOWLEDGEMENTS

Foremost, I would like to express my sincere gratitude to my advisor, Professor Dr. Orawon Chailapakul for the continuous support of my research, motivation, enthusiasm, and immense knowledge. Besides, I would like to thank the rest of my thesis committee, Assistant Professor Dr. Suchada Chuanuwatanakul, Assistant Professor Dr. Warinthorn Chavasiri and Dr. Anchana Preechaworapun for their encouragement, insightful comments, and excellent guidance in my thesis.

My sincere thanks also goes to Dr. Nadnudda Rodthongkum for excellent suggestion and encouragement. Her guidance helped me in all the time of my research. I specially thank my fellow lab members in Electrochemistry and Optical Spectroscopy Research Unit at Chulalongkorn University for their friendship, suggestion and impetus me on working.

Of course, this project would not have been possible without the financially supported by 72<sup>nd</sup> Birthday Anniversary of His Majesty the King's Scholarship.

Last but not the least, I would like to thank my family: my parents for giving birth to me at the first place and supporting me spiritually throughout my life.

## CONTENTS

	<b>PAGE</b>
<b>ABSTRACT (THAI)</b> .....	<b>iv</b>
<b>ABSTRACT (ENGLISH)</b> .....	<b>v</b>
<b>ACKNOWLEDGEMENTS</b> .....	<b>vi</b>
<b>CONTENTS</b> .....	<b>vii</b>
<b>LIST OF TABLES</b> .....	<b>xii</b>
<b>LIST OF FIGURES</b> .....	<b>xiii</b>
<b>LIST OF ABBREVIATIONS</b> .....	<b>xx</b>
<b>CHAPTER I INTRODUCTION</b> .....	<b>1</b>
1.1 Introduction.....	1
1.2 Objectives of research.....	4
1.3 Scopes of the research.....	4
<b>CHAPTER II THEORY</b> .....	<b>5</b>
2.1 Sulfonamide.....	5
2.2 Principle of chromatography.....	7
2.2.1 The basic of liquid chromatography methods.....	8
2.2.1.1 Liquid-liquid chromatography.....	8
2.2.1.2 Liquid-solid chromatography.....	9
2.2.1.3 Ion-exchange chromatography.....	9
2.2.1.4 Size exclusion chromatography.....	11
2.2.2 Basic factors of liquid chromatography.....	14
2.2.2.1 Retention time ( $t_R$ ).....	14
2.2.2.2 Resolution.....	16
2.3 Ultra fast liquid chromatography (UFLC).....	17
2.4 Ultra fast liquid chromatography configuration.....	18

	<b>PAGE</b>
2.4.1 Pumping unit and solvent delivery unit.....	19
2.4.2 Sample-injection unit.....	20
2.4.3 Separation unit.....	21
2.4.3.1 Number of theoretical plates (N).....	22
2.4.3.2 Height equivalent to a theoretical plate (H).....	23
2.4.4 Detection unit.....	25
2.5 Principles of Electrochemistry.....	26
2.5.1 Electrochemical cells.....	27
2.5.1.1 Galvanic cell.....	28
2.5.1.2 Electrolytic cells.....	29
2.5.2 Mass transports process.....	30
2.5.2.1 Diffusion.....	29
2.5.2.2 Convection.....	31
2.5.2.3 Migration.....	31
2.5.3 Voltammetric technique.....	32
2.5.3.1 Cyclic voltammetry.....	34
2.5.3.2 Amperometric detection.....	35
2.5.4 Instrument in electrochemistry.....	36
2.5.4.1 Working electrode.....	37
2.5.4.2 Reference electrode.....	39
2.5.4.3 Counter electrode.....	39
2.6 Solid phase extraction techniques.....	39
2.6.1 SPE procedure.....	40
2.7 Literature reviews.....	41
<b>CHAPTER III EXPERIMENTAL.....</b>	<b>46</b>
3.1 Chemicals and reagents.....	46



	<b>PAGE</b>
3.2 Instruments and apparatus.....	48
3.3 Preparation of chemicals and reagents solution.....	50
3.3.1 Preparation of solution for cyclic voltammetry.....	50
3.3.1.1 Preparation of 0.1 M KCl solution.....	50
3.3.1.2 Preparation of $K_3Fe(CN)_6$ and $K_4Fe(CN)_6 \cdot 3H_2O$ solution.....	50
3.3.1.3 Supporting electrolyte solution.....	50
3.3.1.4 Stock standard solution.....	51
3.3.1.5 Working standard solution.....	51
3.3.2 Preparation of solution for UFLC-ECD.....	51
3.3.2.1 Mobile phase.....	51
3.3.2.2 Stock standard solution.....	52
3.3.2.3 Working standard solution.....	53
3.3.3 Preparation of solution for sample preparation.....	53
3.3.3.1 $Na_2EDTA$ -Mallvaine's Buffer solution.....	53
3.3.3.2 Sample preparation of shrimp.....	53
3.4 Electrode preparation.....	54
3.4.1 Preparation of solution for graphene/polyaniline (G/PANI) modified electrode.....	54
3.4.1.1 Graphene solution.....	54
3.4.1.2 Polyaniline solution.....	55
3.4.1.3 Preparation of G/PANI solution.....	56
3.4.2 Preparation of screen-printed carbon electrode.....	56
3.4.3 Preparation of G/PANI-modified electrode.....	58
3.5 Procedure.....	59
3.5.1 Cyclic voltammetry study.....	59
3.5.1.1 Electrochemical investigation of G/PANI-modified electrode.....	59

	<b>PAGE</b>
3.5.1.2 Study the mass transfer process of G/PANI modified electrode.....	59
3.5.1.3 Comparison between G/PANI-modified electrode and unmodified electrode.....	60
3.5.1.4 Comparison between G/PANI modified electrode and BDD electrode BDD electrode.....	60
3.5.2 Ultra-fast liquid chromatography coupled with electrochemical detection.....	61
3.5.2.1 The effect of detection potential.....	61
3.5.2.2 The effect of pH.....	61
3.5.2.3 Optimal flow rate of mobile phase.....	61
3.5.2.4 Optimal condition for UFLC-ECD system.....	62
3.6 Analytical performance.....	63
3.6.1 Linearity.....	63
3.6.2 Accuracy and precision.....	63
3.6.3 Limit of detection (LOD) and Limit of quantification (LOQ).....	64
3.6.4 Comparison of the novel system UFLC-ECD and standard method.....	65
<b>CHAPTER IV RESULT AND DISCUSSION.....</b>	<b>66</b>
4.1 Characterization of G/PANI modified electrode.....	66
4.1.1 Surface morphology of G/PANI modified electrode.....	66
4.1.2 Electrochemical behavior of G/PANI modified electrode.....	68
4.1.3 The mass transfer process of G/PANI modified electrode.....	70
4.2 Cyclic voltammetry investigated for the determination of eight SAs	73
4.2.1 Cyclic voltammetry of eight SAs on G/PANI modified electrode compared to unmodified electrode.....	73

	<b>PAGE</b>
4.2.2 Cyclic voltammetry of eight SAs on G/PANI modified electrode compared to boron-doped diamond electrode.....	78
4.3 Optimal conditions of UFLC-ECD.....	83
4.3.1 Optimization of the detection potential for SAs.....	83
4.3.2 The effect of pH.....	85
4.3.3 Optimal flow rate of mobile phase.....	89
4.3.4 Optimal condition of the separation.....	91
4.4 Analytical performance.....	93
4.4.1 Calibration and linearity.....	93
4.4.2 Limit of detection (LOD) and limit of quantification (LOQ)...	97
4.5 Application in real sample.....	99
4.5.1 Determination of SAs in shrimp.....	99
4.5.2 Method accuracy and precision.....	101
4.5.3 Comparison of methods between the UFLC-ECD and UFLC- UV.....	104
<b>CHAPTER V CONCLUSIONS.....</b>	<b>106</b>
5.1 Conclusions.....	106
5.2 Suggestion for future work.....	108
<b>REFERRENCES.....</b>	<b>109</b>
<b>APPENDICES.....</b>	<b>118</b>
<b>APPENDIX A.....</b>	<b>119</b>
<b>APPENDIX B.....</b>	<b>122</b>
<b>VITAE.....</b>	<b>124</b>

**LIST OF TABLE**

<b>TABLE</b>	<b>PAGE</b>
3.1 Chemicals and reagents.....	46
3.2 Instruments and apparatus.....	48
3.3 Table of potassium hydrogen solution preparation.....	52
3.4 Conditions parameters of UFLC-ECD system for the detection of eight SAs.....	62
4.1 The UFLC-ECD conditions for the detection of eight sulfonamides.	91
4.2 Analytical performance of eight SAs including linear range (LR), limit of detection (LOD), slope (b), and limit of quantification (LOQ).....	98
4.3 Intra-day precision and recoveries of SAs detection in shrimp samples (n=3).....	102
4.4 Inter-day precision and recoveries of SAs detection in shrimp samples (n=3).....	103
4.5 Comparisons results of two methods in shrimp sample.....	105

## LIST OF FIGURES

<b>FIGURES</b>	<b>PAGE</b>
1.1 Structure of eight SAs in this work .....	2
2.1 Sulfonamide structure.....	5
2.2 Para-aminobenzoic acid (PABA) structure.....	6
2.3 Diagram of mechanism reaction (a) normal reaction of folic acid synthesis (b) antimetabolite of folic acid synthesis.....	6
2.4 Diagram display Tswett's experiment.....	7
2.5 Diagram of ion-exchange mechanism.....	10
2.6 Diagram of the separation of three molecules by Size Exclusion Chromatography (a) Size of black molecule is much smaller compared to the pore size of the solid particle and has total access to the pores (not excluded). (b) The size of green molecule is somewhat smaller compared to the pore size of the solid particle and has some access to the pores (partially excluded). (c) The size of purple molecule is larger than the pore size of the solid particle and does not have any access to the pores (totally excluded).....	12
2.7 Schematic of the four basic modes of liquid chromatography.....	13
2.8 Identification of analytes by retention time ( $t_R$ ).....	15
2.9 Diagram illustrating the van Deemter plot.....	17
2.10 Basic configuration of UFLC system.....	18
2.11 Solvent deliver unit (Shimadzu LC-20ADXR UFLC).....	19
2.12 Flow path of manual injector.....	20
2.13 Autosampler unit (Shimadzu LC-20ADXR UFLC).....	21
2.14 Diagram of galvanic cell.....	28
2.15 Diagram of electrolytic cell.....	29
2.16 A schematic cyclic voltammogram.....	35
2.17 Schematic thin layer flow cell (GL science).....	36
2.18 Schematic of potentiostat connected to an electrochemical cell.....	37

	<b>PAGE</b>
2.19 Schematic representation of SPE procedure.....	40
3.1 Homogeneous graphene (G) solution.....	54
3.2 Homogeneous polyaniline (PANI) solution.....	55
3.3 (Step I) in-house screen-printing technique for conductive pad.....	57
3.4 (Step II) in-house screen-printing technique for screen-printing carbon electrode.....	57
3.5 Schematic diagram of electrospray technique for preparation of G/PANI modified electrode.....	58
4.1 SEM images of G/PANI (1:1) nanocomposite, condition, No. needle; No.24 ( $\varnothing$ 0.45), voltage; 10kV, time; 5 min.....	61
4.2 Cyclic voltammograms of 1 mM $[\text{Fe}(\text{CN})_6]^{3-}$ / $[\text{Fe}(\text{CN})_6]^{4-}$ for (---) G/PANI- modified carbon electrode and (—) carbon bare electrode vs. Ag/AgCl with scan rate of 100 mV s <sup>-1</sup> .....	69
4.3 Cyclic voltammograms of $[\text{Fe}(\text{CN})_6]^{3-}$ and $[\text{Fe}(\text{CN})_6]^{4-}$ 1 mM for (---) G/PANI-modified carbon electrode vs. Ag/AgCl with scan rate of 10, 20, 50, 100 and 200 mV/s.....	71
4.4 The relationship between anodic current; $i_{ac}$ (a) and cathodic current; versus scan rate <sup>1/2</sup> of 0.1 mM $[\text{Fe}(\text{CN})_6]^{3-}/[\text{Fe}(\text{CN})_6]^{4-}$ in 0.1 M KCl solution.....	72
4.5 Cyclic voltammograms for (---) G/PANI-modified carbon electrode and (—) bare carbon vs. Ag/AgCl in 50 $\mu\text{g mL}^{-1}$ SMM, 0.1 M phosphate solution pH 3.0 with scan rate 100 mV s <sup>-1</sup> .....	74
4.6 Cyclic voltammograms for (---) G/PANI-modified carbon electrode and (—) bare carbon vs. Ag/AgCl in 50 $\mu\text{g mL}^{-1}$ SDM, 0.1 M phosphate solution pH 3.0 with scan rate 100 mV s <sup>-1</sup> .....	74
4.7 Cyclic voltammograms for (---) G/PANI-modified carbon electrode and (—) bare carbon vs. Ag/AgCl in 50 $\mu\text{g mL}^{-1}$ SG, 0.1 M phosphate solution pH 3.0 with scan rate 100 mV s <sup>-1</sup> .....	75

	<b>PAGE</b>
4.8 Cyclic voltammograms for (---) G/PANI-modified carbon electrode and (—) bare carbon vs. Ag/AgCl in 50 $\mu\text{g mL}^{-1}$ SDX, 0.1 M phosphate solution pH 3.0 with scan rate 100 $\text{mV s}^{-1}$ .....	75
4.9 Cyclic voltammograms for (---) G/PANI-modified carbon electrode and (—) bare carbon vs. Ag/AgCl in 50 $\mu\text{g mL}^{-1}$ SMX, 0.1 M phosphate solution pH 3.0 with scan rate 100 $\text{mV s}^{-1}$ .....	76
4.10 Cyclic voltammograms for (---) G/PANI-modified carbon electrode and (—) bare carbon vs. Ag/AgCl in 50 $\mu\text{g mL}^{-1}$ SSZ, 0.1 M phosphate solution pH 3.0 with scan rate 100 $\text{mV s}^{-1}$ .....	76
4.11 Cyclic voltammograms for (---) G/PANI-modified carbon electrode and (—) bare carbon vs. Ag/AgCl in 50 $\mu\text{g mL}^{-1}$ SDZ, 0.1 M phosphate solution pH 3.0 with scan rate 100 $\text{mV s}^{-1}$ .....	77
4.12 Cyclic voltammograms for (---) G/PANI-modified carbon electrode and (—) bare carbon vs. Ag/AgCl in 50 $\mu\text{g mL}^{-1}$ SMZ, 0.1 M phosphate solution pH 3.0 with scan rate 100 $\text{mVs}^{-1}$ .....	77
4.13 Cyclic voltammograms for (—) G/PANI-modified carbon electrode and (—) boron-doped diamond electrode vs. Ag/AgCl in 50 $\mu\text{g mL}^{-1}$ SDZ, 0.1 M phosphate solution pH 3.0 with scan rate 100 $\text{mV s}^{-1}$ .....	79
4.14 Cyclic voltammograms for (—) G/PANI-modified carbon electrode and (—) boron doped diamond electrode vs. Ag/AgCl in 50 $\mu\text{g mL}^{-1}$ SG, 0.1 M phosphate solution pH 3.0 with scan rate 100 $\text{mV s}^{-1}$ .....	79
4.15 Cyclic voltammograms for (—) G/PANI-modified carbon electrode and (—) boron doped diamond electrode vs. Ag/AgCl in 50 $\mu\text{g mL}^{-1}$ SMM, 0.1 M phosphate solution pH 3.0 with scan rate 100 $\text{mV s}^{-1}$ .....	80

	<b>PAGE</b>
4.16 Cyclic voltammograms for ( — ) G/PANI-modified carbon electrode and ( — ) boron doped diamond electrode vs. Ag/AgCl in $50 \mu\text{g mL}^{-1}$ SMX, 0.1 M phosphate solution pH 3.0 with scan rate $100 \text{ mV s}^{-1}$ .....	80
4.17 Cyclic voltammograms for ( — ) G/PANI-modified carbon electrode and ( — ) boron doped diamond electrode vs. Ag/AgCl in $50 \mu\text{g mL}^{-1}$ SMZ, 0.1 M phosphate solution pH 3.0 with scan rate $100 \text{ mV s}^{-1}$ .....	81
4.18 Cyclic voltammograms for ( — ) G/PANI-modified carbon electrode and ( — ) boron doped diamond electrode vs. Ag/AgCl in $50 \mu\text{g mL}^{-1}$ SSZ, 0.1 M phosphate solution pH 3.0 with scan rate $100 \text{ mV s}^{-1}$ .....	81
4.19 Cyclic voltammograms for ( — ) G/PANI-modified carbon electrode and ( — ) boron doped diamond electrode vs. Ag/AgCl in $50 \mu\text{g mL}^{-1}$ SDX, 0.1 M phosphate solution pH 3.0 with scan rate $100 \text{ mV s}^{-1}$ .....	82
4.20 Cyclic voltammograms for ( — ) G/PANI-modified carbon electrode and ( — ) boron doped diamond electrode vs. Ag/AgCl in $50 \mu\text{g mL}^{-1}$ SQ, 0.1 M phosphate solution pH 3.0 with scan rate $100 \text{ mV s}^{-1}$ .....	82
4.21 Hydrodynamic voltammetric results using our proposed UFLC-ECD system for $10 \mu\text{g mL}^{-1}$ of mixture of eight standard SAs (1) SG (2) SDZ (3) SMZ (4) SMM (5) SDX (6) SMX (7) SSZ (8) SDM at a flow rate of $1.5 \text{ mL min}^{-1}$ . The detection potential at 1.1 – 1.5 V vs. Ag/AgCl using G/PANI modified screen-printed carbon electrode.....	84



	<b>PAGE</b>
4.22 UFLC-ECD chromatogram of eight SAs $10 \mu\text{g mL}^{-1}$ at flow rate of $1.5 \text{ mL min}^{-1}$ with 70:25:5(v/v/v) of potassium phosphate solution (pH 3): acetonitrile: ethanol as the mobile phase. The detection potential was 1.4 V vs. Ag/AgCl using G/PANI modified screen-printed carbon electrode.....	86
4.23 UFLC-ECD chromatogram of eight SAs $10 \mu\text{g mL}^{-1}$ at flow rate of $1.5 \text{ mL min}^{-1}$ with 70:25:5(v/v/v) of potassium phosphate solution (pH 4): acetonitrile: ethanol as the mobile phase. The detection potential was 1.4 V vs. Ag/AgCl using G/PANI modified screen-printed carbon electrode.....	86
4.24 UFLC-ECD chromatogram of eight SAs $10 \mu\text{g mL}^{-1}$ at flow rate of $1.5 \text{ mL min}^{-1}$ with 70:25:5(v/v/v) of potassium phosphate solution (pH 5): acetonitrile : ethanol as the mobile phase. The detection potential was 1.4 V vs. Ag/AgCl using G/PANI modified screen-printed carbon electrode.....	87
4.25 UFLC-ECD chromatogram of eight SAs $10 \mu\text{g mL}^{-1}$ at flow rate of $1.5 \text{ mL min}^{-1}$ with 70:25:5(v/v/v) of potassium phosphate solution (pH 6): acetonitrile : ethanol as the mobile phase. The detection potential was 1.4 V vs. Ag/AgCl using G/PANI modified screen-printed carbon electrode.....	87
4.26 UFLC-ECD chromatogram of eight SAs $10 \mu\text{g mL}^{-1}$ at flow rate of $1.5 \text{ mL min}^{-1}$ with 70:25:5(v/v/v) of potassium phosphate solution (pH7): acetonitrile : ethanol as the mobile phase. The detection potential was 1.4 V vs. Ag/AgCl using G/PANI modified screen-printed carbon electrode.....	88

	<b>PAGE</b>
4.27 UFLC-EC chromatogram of standard mixture of eight SAs (10 $\mu\text{g mL}^{-1}$ ) (1) SG, (2) SDZ, (3) SMZ, (4) SMM, (5) SDX, (6) SMX, (7) SSZ and (8) SDM at G/PANI modified screen-printed carbon electrode with various of flow rate in the range of 0.5 – 2.0 $\text{mL min}^{-1}$ .....	89
4.28 UFLC-EC chromatogram of standard mixture of eight SAs (10 $\mu\text{g mL}^{-1}$ ) (1) SG, (2) SDZ, (3) SMZ, (4) SMM, (5) SDX, (6) SMX, (7) SSZ and (8) SDM at G/PANI-modified carbon screen-printed electrode. The mobile phase was 0.05 M potassium hydrogen phosphate solution (pH 3): acetonitrile: ethanol (70:25:5 v/v/v). The injection volume was 25 $\mu\text{L}$ , and the flow rate was 1.5 $\text{mL min}^{-1}$ .....	92
4.29 Calibration curve of SMZ by UFLC-ECD using G/PANI-modified screen- printed carbon electrode in the concentration range of 0.1 to 10 $\mu\text{g mL}^{-1}$ .....	93
4.30 Calibration curve of SMM by UFLC-ECD using G/PANI-modified screen- printed carbon electrode in the concentration range of 0.1 to 10 $\mu\text{g mL}^{-1}$ .....	94
4.31 Calibration curve of SG by UFLC-ECD using G/PANI-modified screen- printed carbon electrode in the concentration range of 0.1 to 10 $\mu\text{g mL}^{-1}$ .....	94
4.32 Calibration curve of SDZ by UFLC-ECD using G/PANI-modified screen- printed carbon electrode in the concentration range of 0.1 to 10 $\mu\text{g mL}^{-1}$ .....	95
4.33 Calibration curve of SDM by UFLC-ECD using G/PANI-modified screen- printed carbon electrode in the concentration range of 0.1 to 10 $\mu\text{g mL}^{-1}$ .....	95

	<b>PAGE</b>
4.34 Calibration curve of SSZ by UFLC-ECD using G/PANI-modified screen- printed carbon electrode in the concentration range of 0.1 to 10 $\mu\text{g mL}^{-1}$ .....	96
4.35 Calibration curve of SMX by UFLC-ECD using G/PANI-modified screen- printed carbon electrode in the concentration range of 0.1 to 10 $\mu\text{g mL}^{-1}$ .....	96
4.36 Calibration curve of SDX by UFLC-ECD using G/PANI-modified screen printed carbon electrode in the concentration range of 0.1 to 10 $\mu\text{g mL}^{-1}$ .....	97
4.37 UFLC-ECD chromatograms of (a) blank shrimp sample and (b) shrimp sample at spiked level 5 $\mu\text{g mL}^{-1}$ of (1) SG, (2) SDZ, (3) SMZ, (4) SMM, (5) SDX, (6) SMX, (7) SSZ and (8) SDM at G/PANI-modified carbon screen-printed electrode. The mobile phase was 0.05 M potassium hydrogen phosphate solution (pH 3): acetonitrile: ethanol (70:25:5 v/v/v). The injection volume was 25 $\mu\text{L}$ , and the flow rate was 1.5 $\text{mL min}^{-1}$ .....	100

## LIST OF ABBREVIATIONS

Ag/AgCl	Silver/silver chloride
AOAC	Association of Analytical Communities
BDD	Boron-doped diamond
CE	Capillary electrophoresis
CV	Cyclic voltammetry
CVD	Chemical vapor deposition
°C	Degree Celsius
$E$	Potential
$E^0$	Formal reduction potential
EB	Ethylparaben
EEC	European Economic Community
$E_{pa}$	Anodic peak potential
$E_{pc}$	Cathodic peak potential
G	Graphene
GC	Gas chromatography
HPLC	High performance liquid chromatography
IUPAC	International Union for Pure and Applied Chemistry
$i_{p,a}$	Anodic peak current
$i_{p,c}$	Cathodic peak current
L	Liter
M	Molar
mL	Milliliter
MS	Mass spectroscopy
min	Minute
N	Noise
n	Number of electron
nm	Nanometer
PANIB	Polyaniline
RE	Reference electrode

S	Signal
SD	Standard deviation
SDM	Sulfadimethoxine
SDX	Sulfadoxine
SDZ	Sulfadiazine
SEM	Scanning electron microscopy
SG	Sulfaguanidine
SMM	Sulfamonomethoxine
SMX	Sulfamethoxazole
SMZ	Sulfamerazine
SSZ	Sulfisoxazole
UPLC	Ultra-performance liquid chromatography
RSD	Relative standard deviation
WE	Working electrode
$\mu\text{A}$	Microampere

# CHAPTER I

## INTRODUCTION

### 1.1 Introduction

Sulfonamides (SAs) are one class of antimicrobial drug used in the treatment of bacterial infections. Antibacterial SAs act as competitive inhibitors of the dihydropteroate synthase (DHPS), enzyme which involves in folate synthesis. Microorganism is death by decreasing folate level, so SAs can prevent the growth of bacteria and strengthen the body's immune system [1, 2]. SAs have a wide range of antimicrobial activity against both gram-positive and gram-negative bacterias [3, 4]. Nowadays, SAs are also used in combination with trimethoprim to increase efficiency for treatment or prevention of several diseases. Sulfonamide structures consist of benzene ring with a two functional groups including amine group at C4 position and sulfonic acid with different alkyl group as shown in Figure1.1. Furthermore, SAs are widely used as additives in animal feed to prevent bacterial contamination; however, they are often overused because they are inexpensive and readily available [5, 6]. Therefore, SAs can be contaminated in animal meat product. The presence of sulfonamide residue in food is toxic and harmful to human health and they may lead to allergic hypersensitivity. To ensure the safety of food for human consumption, the European Union (EU) has established the maximum residue limits (MRLs) for SAs in animal at  $0.1 \mu\text{g mL}^{-1}$  (animal meat) [3, 7, 8]. The detection of SAs is extremely important.

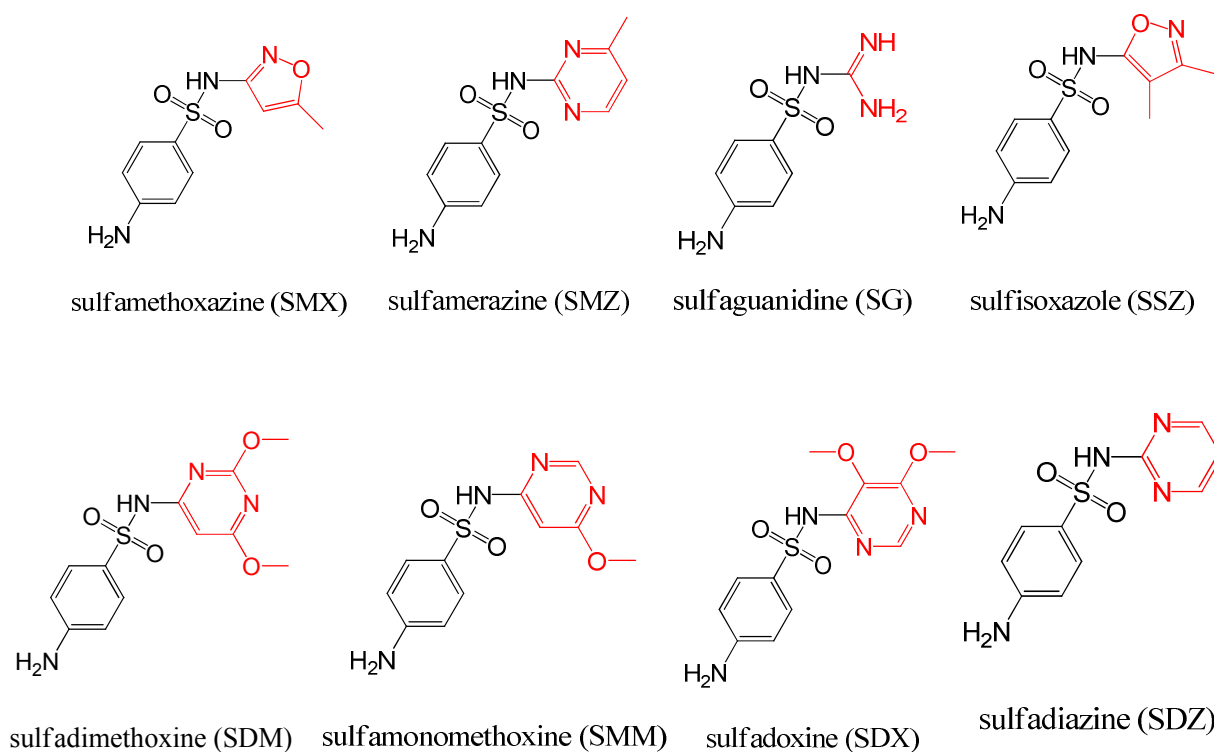


**Figure1.1** Structure of eight SAs in this work

Due to their toxicity, several analytical methods have been developed for SAs determination. These methods were mainly based on bioassay such as Thin-layer chromatography (TLC) [9, 10] screening method using derivatization of SAs with fluorescamine. This method is rather selective and sensitive but it is unreproducible. Enzyme-linked immunoassay (ELISA) [8, 11, 12], which is capable of detecting low concentration of residues in many samples in a short time. In general, the monitoring of SAs is carried out by using chromatographic methods. Commonly, gas chromatography (GC) [13, 14] has been used for determination of SAs in various meats because it provides high reliability and sensitivity; however derivatization of polar SAs is required. High performance liquid chromatography (HPLC) [15-18] with photodiode array (PDA) detector has been applied to determine SA residues in animal origin because this method is very simple and useful for simultaneous determination of SAs.

In recent year, ultra fast liquid chromatography (UFLC) [19-22] that have been developed from HPLC is a new technique for chromatographic methods. It offers several advantages such as high resolution, high sensitivity and allowing for high throughput analysis. To provide the specificity in analysis, UFLC coupled with detection technique has become an attention for sulfonamide determination. The common coupling techniques such as HPLC coupled with ultraviolet (UV) [23, 24] or fluorescent detector [25, 26], which exhibited high sensitivity but it was provided a high detection limit and required derivatization to improve the fluorescence sensitivity. Moreover, UFLC coupled with mass spectrometry has become an interesting tool because of its high specificity, high sensitivity. Nonetheless, the operation cost is very high and it requires the specialist for operation [16-18, 27-30].

Electrochemical detection [31-34] is another promising technique that can provide simple and fast analysis with low operating cost. In order to improve the electrochemical sensitivity, design and modification of working electrode become an interesting issue for ongoing research. Various types of working electrode have been applied for SAs measurement such as boron-doped diamond [33, 36] which showed the excellent sensitivity but the cost of material is very high and it is difficult to produce. Recently, it has been reported that modification of working electrode with nanomaterials such as metallic, nanoparticles, SWCNT, and MWCNT can increase both surface area and conductivity [37, 38]. Until now, graphene [39-42], a two dimensional sheet of  $sp^2$  carbon atom, has become an attractive materials in electrochemistry due to its high electrical conductivity, high mechanical strength and low manufacturing cost. Fabrication of graphene on electrode surface is difficult due to the agglomeration. Therefore, graphene/polyaniline (G/PANI) composite was selected for electrode modification. PANI [43-45] is an interesting conducting polymer material for electrode modification. PANI is unique among conducting polymers because of their stability in both air and aqueous medium. It also has a great variety of potential applications including anticorrosion coatings, batteries, sensors, separation membranes, and antistatic coatings [46]. The structure of PANI consists of phenyl rings in the benzenoid and quinoidform, and nitrogen heteroatoms in either amine ( $-NH-$ ) or imine ( $-N=$ ) form. Due to their excellent electrical properties, PANI can



be easily applied in electrochemical biomolecular application. Moreover, this polymer can improve the distribution of graphene on the electrode surface and also prevent the agglomeration of graphene.

In this work, G/PANI nanocomposite is selected for electrode modification onto screen-printed carbon electrode as working electrode in electrochemical detection for determination of eight SAs (SMM, SDM, SG, SDX, SMX, SSZ, SDZ and SMZ) along with UFLC system. Overall, this novel system UFLC coupled with electrochemical detection will be applied for determination of SAs in shrimp sample.

## **1.2 Objective of Research**

The target of this research is to develop a novel system of UFLC coupling with electrochemical detection by using G/PANI modified screen printed electrode as a new working electrode for simultaneous determination of eight SAs. After that, this proposed system will be applied for determination of SAs in shrimp sample.

## **1.3 Scope of Research**

G/PANI modified screen printed electrode was firstly investigated by using cyclic voltammetry and also compared the sensitivity for determination of eight SAs with unmodified electrode and boron-doped diamond electrode. The novel system of UFLC coupling with amperometric detection by using G/PANI modified screen-printed electrode as a working electrode was used for sensitive separation and selective detection of eight SAs. The optimal conditions pH, flow rate of the mobile phase, detection potential, linearity of calibration curve, limit of detection and limit of quantitation were experimentally studied in detail.

## CHAPTER II

### THEORY

#### 2.1 Sulfonamide [47, 48]

Sulfonamide also known as sulfa drug is one class of antibiotic drug that has been discovered for several years. Sulfonamides can inhibit gram-positive and gram-negative bacteria, nocardia, chlamydia trachomatis and some protozoas. Nowadays, sulfa drugs are commonly used for various treatments of bacterial infections in several diseases such as Stevens-Johnson syndrome. Sulfonamide structures consist of benzene ring with two types of functional groups including amine group at C4 position and sulfonyl with different kind of alkyl group as shown in Figure 2.1.

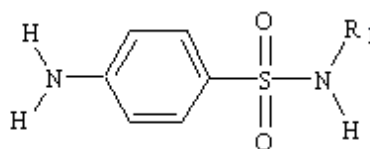


**Figure 2.1** Sulfonamide structure

The action of sulfonamides indicates the difference of selective toxicity between mammal cells and bacterial cells because these cells require folic acid for growth. Folic acid (as a vitamin in food) can diffuse into human cells and cannot cross bacterial cell walls by diffusion or active transport. For this reason, bacteria must synthesize folic acid from para-aminobenzoic acid (PABA). The structural features of PABA are the benzene ring with two substituents para to each other; an amine group at C4 and the singly substituted 1-sulfonamide group as shown in Figure 2.2

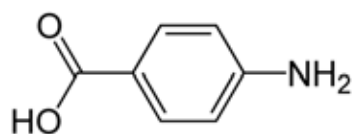


**Figure 2.2** Para-aminobenzoic acid (PABA) structure

Sulfonamide can bind and inhibit a specific enzyme called DHPS. This enzyme is used for the synthesis of folic acid, which is essential nutrient in bacteria. To stop growth of bacteria, reaction of folic acid synthesis need to be inhibited. The diagram of mechanism is shown in Figure 2.3.

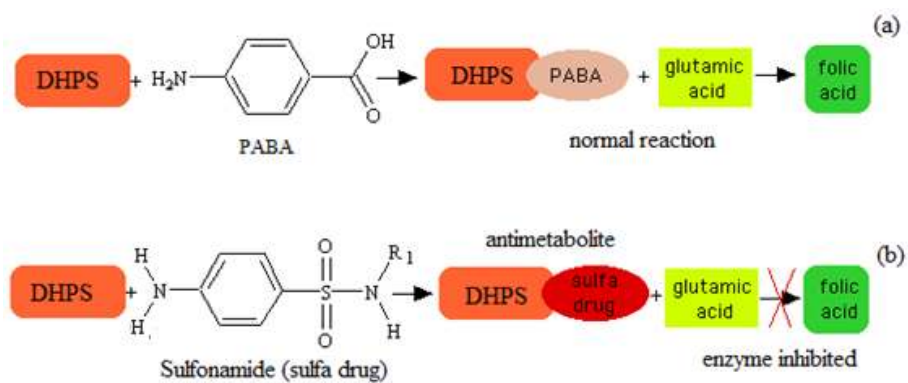


**Figure 2.3** Diagram of mechanism reaction (a) normal reaction of folic acid synthesis (b) antimetabolite of folic acid synthesis. [47]

## 2.2 Principle of chromatography [49-51]

Chromatography is the separation technique, which is employed for separation of multiple analytes. Chromatographic technique was first used for purification of interested analytes from highly matrix sample. Although originally chromatographic technique was innovated for particularly purifying analytes from high matrix sample, these techniques have been currently applied for separation and quantitation of analytes. Chromatography is the highly powerful and popular technique commonly used in the modern analysis. This chromatographic technique was invented by Tswett during his research on separation of plant pigments. Plant extract was performed by petroleum ether through a column consisting of a glass tube packed with calcium carbonate powder. A number of dyes was successfully identified as shown in Figure 2.4.

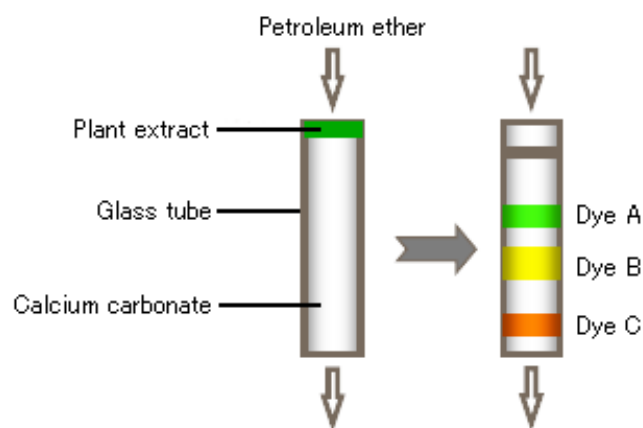


**Figure 2.4** Diagram display of Tswett's experiment [50]

### **2.2.1 The principle of liquid chromatographic methods [52-55]**

Liquid chromatography is a technique used for separation mixture of analytes. The principle of this separation is based on the interactions of the sample with the mobile phase and the stationary phase. Chromatographic techniques are classified into four basic LC methods because of several of stationary phase and mobile phase including liquid-liquid chromatography, liquid-solid chromatography, ion-exchange chromatography and size exclusion chromatography.

#### **2.2.1.1 Liquid-liquid chromatography (LLC)**

Liquid-liquid or partition chromatography concerns about liquid stationary phase which composition is different from that of the moving liquid phase. The solute molecules are distributed between two immiscible liquids due to their relative solubility. One liquid is a mobile phase or carrier while the other liquid perform as stationary phase which is a thin-film formed on the inert surface of solid support. In conventional liquid-liquid chromatography, the stationary phase is a bulk liquid, mechanically held by adsorption on the support. It is popular in recent year using organic phase chemically bounded to the support. The principle of liquid-liquid chromatography is similar to simple extraction and counter-current extraction. Common extraction consists of immiscible liquid in a separatory funnel, and a successive series of extractions is achieved by counter-current extraction. However, liquid-liquid chromatography uses less operation time and is more efficient than counter-current extraction. The partition of various solutes between two liquid phases the separation of analytes. Liquid-liquid chromatography offers unique selectivity for the determination of various analytes because a variety of liquid phase can be selected for the stationary phase. Liquid-liquid chromatography can be classified into two types including normal phase and reverse phase. In normal phase, the support is coated with a polar stationary phase, whereas a relative nonpolar solvent is used as the mobile phase. On the other hand, in reverses phase, the stationary phase is coated with less polar liquid while the polar liquid is the mobile phase. As a result, the elution order of solutes is reversed from the results observed in normal phase.

### **2.2.1.2 Liquid-solid chromatography (LSC)**

Liquid-solid or adsorption chromatography is the oldest type of the liquid chromatography. The mechanism of the separation depends on the adsorption of solutes on the stationary phase involving high-surface-area particles. The term “adsorption” means a physical attachment between the analyte compounds and the particles of stationary phase, which is a solid particle such as silica or alumina. Nowadays, the most system is developed by using the small-particle for increasing the efficiency of the separation. The retention of analyte molecules occurs by adsorption on the surface of particles of stationary phase. Polar compounds adsorb with stronger or greater interaction to the polar stationary phase while non-polar compounds adsorb better to the non-polar stationary phase. Therefore, liquid-solid or adsorption chromatography is a separation process of components in a mixture based on the relative differences in adsorption of components on the stationary phase.

### **2.2.1.3 Ion-exchange chromatography (IEC)**

Ion-exchange chromatography is common technique for the separation of ions and polar molecules. Ion exchange is often used for the separation and purification of proteins, polypeptides, nucleic acids, polynucleotides, and other charged biomolecules. In ion-exchange chromatographic system, the stationary phase contains fixed ionic groups, along with counter ions of opposite charge so the separation in ion exchange chromatography depends upon the reversible adsorption of charged solute molecules to opposite charge molecules immobilized ion exchange groups. This technique can be classified into two modes with different ion-exchange type including anion exchangers (resin with positive functional groups) and cation exchangers (resin with negative functional groups). These functional groups are covalently attached to the support beads. Selection of ion exchanger depends on the charge of the analyte of interest. Separation using ion exchanger is performed in five steps, illustrated schematically in Figure 2.5

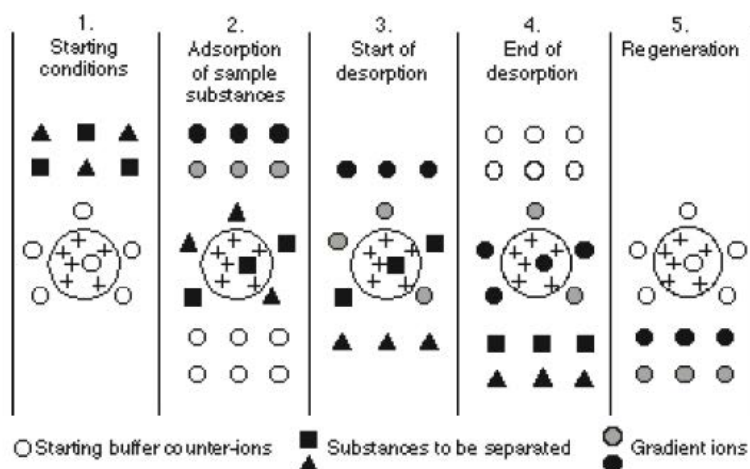


**Figure 2.5** Diagram of ion-exchange mechanism [54]

The first step is equilibration. The ion exchanger is brought to a starting state, in terms of pH and ionic strength, which allows the binding of the desired solute molecules. At this time, the exchanger groups are associated with counter ions using simple anions or cations, such as chloride or sodium. The second step is sample application and adsorption, in which solute molecules carrying the appropriate counter ions. These counter ions bind reversibly to functional group on the resin. Unbound substances can be washed out from the exchanger bed using starting buffer. In the third step, substances are removed from the column by changing elution conditions. This condition normally involves increasing the ionic strength of the eluting buffer or changing its pH. Desorption shown in figure 2.5 is achieved by the introduction of an increasing salt concentration gradient. Solute molecules are released from the column in order to increase their strengths of binding, so the most weakly bound substances are firstly eluted. The fourth and fifth steps are the removal of substances from the column without eluting under the previous experimental conditions and re-equilibration at the starting conditions for the next purification.

#### **2.2.1.4 Size exclusion chromatography (SEC)**

Size exclusion chromatography, also known as gel chromatography is the separation technique based on the molecular size of the components. This technique is the easiest method of the liquid chromatography to understand due to its simplicity. Therefore, this powerful technique has been applied to a board variety of analytes. The column packing is a porous material with pores of a certain size. Usually, separation in size exclusion chromatography is determined strictly by molecular size. Molecules of different sizes can be separated by this technique because of the different time spent inside a solid phase particle, divided into three classes as follows; (i) excluding entrance of relatively larger molecules, (ii) allowing some entrance of medium-sized molecules, and (iii) allowing free accessibility of the smallest molecules. The particles size of analytes can be control by the size of pore. Smaller molecules can easily enter to the tunnel of porous material. On the other hand, large molecule is harder to enter to the tunnel than small molecule. Therefore, smaller molecules elute last and larger molecules elute first in size exclusion chromatography. Figure 2.5 illustrates the separation of three analyte molecules by using size exclusion technique.



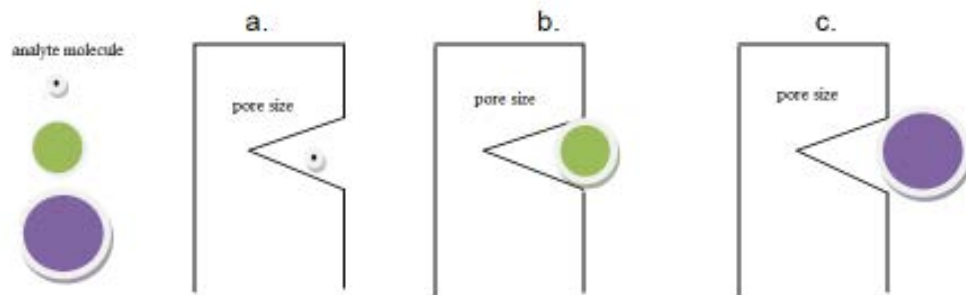


**Figure 2.6** Diagram of the separation of three molecules by Size Exclusion Chromatography (a) Size of black molecule is much smaller compared to the pore size of the solid particle and has total access to the pores (not excluded). (b) The size of green molecule is somewhat smaller compared to the pore size of the solid particle and has some access to the pores (partially excluded). (c) The size of purple molecule is larger than the pore size of the solid particle and does not have any access to the pores (totally excluded).

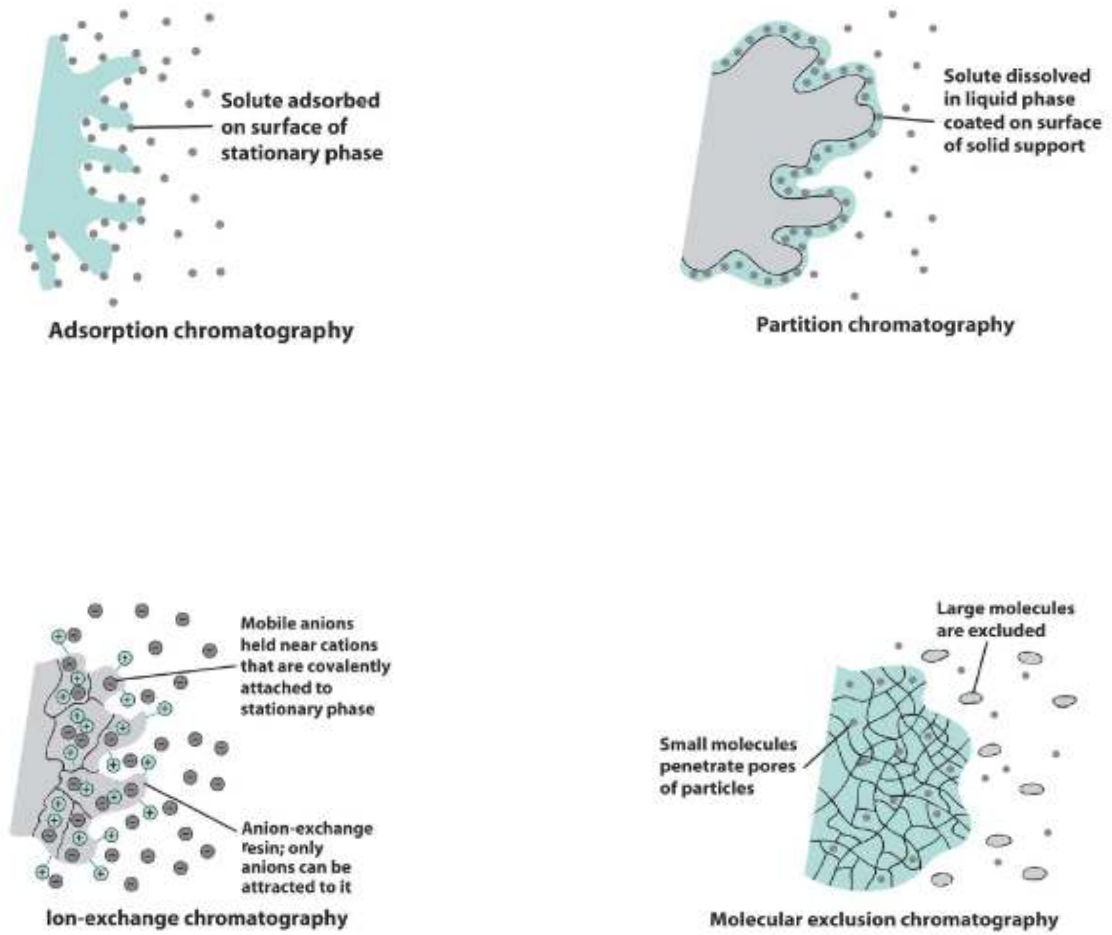


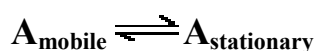
**Figure 2.7** Schematic of the four basic modes of liquid chromatography. [53]

## 2.2.2 Basic factors in liquid chromatography [56-59]

In chromatographic experiments, the separation process requires the suitable combination of operating conditions such as the type of column packing, the length and diameter of the column, type of mobile phase, etc. Selecting the best conditions requires a basic understanding of the basic factors that control separation.

### 2.2.2.1 Retention time ( $t_R$ )

The distribution of analytes between phases can often be described easily. An analyte is in equilibrium between the two phases;



The equilibrium constant (K) is termed the partition coefficient; defined as the molar concentration of analyte in the stationary phase [57]. The time between sample injection and an analyte peak reaching a detector at the end of the column is termed the retention time ( $t_R$ ). Each analyte in a sample will have a different retention time. The time taken for the mobile phase to pass through the column is called  $t_M$ . [57]

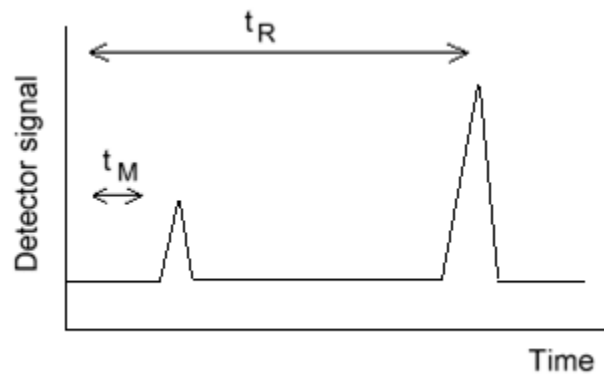


**Figure 2.8** Identification of analytes by retention time ( $t_R$ ).

The migration rate of an analyte on a column can be represented in a term called the retention factor ( $k'$ ). It is also called the capacity factor. The retention factor for an analyte is defined as; [57]

$$k'_A = \frac{t_R - t_M}{t_M}$$

$t_R$  and  $t_M$  are easily obtained from a chromatogram. When  $k'$  of an analyte factor is less than one, resulting in very rapid elution. High  $k'$  (greater than 20) means that elution takes a very long time. [58]

### 2.2.2.2 Resolution

The separation of two species on the column can be describe in the term called selectivity factor ( $\alpha$ ) [58]

$$\alpha = k'_B / k'_A$$

The selectivity factor should be greater than one. Although the selectivity factor ( $\alpha$ ) describes the separation of band centers, peak widths do not take into account. Another factor indicating the performance in the separation is provided by measurement of the resolution. The resolution of two species, A and B, is defined in equation 1:

$$R = 2 [(t_R)_B - (t_R)_A] / (W_A + W_B) \dots \dots \dots (1)$$

Baseline resolution is achieved when  $R = 1.5$ . It is useful to relate the resolution to the number of plates ( $N$ ) in the column, the selectivity factor ( $\alpha$ ) and the retention factors ( $k'$ ) of the two solutes as shown in equation 2;

$$R = \sqrt{N} / 4 [(\alpha - 1) / \alpha] [(1 + k'_B) / k'_B] \dots \dots \dots (2)$$

To obtain high resolution, three terms must be maximized. The number of theoretical plates ( $N$ ), can be lengthening the column leading to increase in retention time band broadening which may not be desirable. Instead of increasing the number of plates, the height equivalent to a theoretical plate should be reduced by reducing the size of

the stationary phase particles. It is often found that separations can be greatly improved by  $k'$ . This can be achieved by changing the temperature or the composition of the mobile phase.

### 2.3 Ultra-fast liquid chromatography (UFLC) [60-62]

It is also known that high performance liquid chromatography (HPLC) is an analysis method yielding high performance and high speed compared with traditional chromatography method. Recently, ultra fast analysis using a high-pressure resistant apparatus has been attracting attention. The principle of UPLC is the same as HPLC. However, the underlying principles of this evolution are governed by the van Deemter equation. The van Deemter equation is an empirical formula that shows the relationship between linear velocity (flow rate), and plate height (column efficiency). Since particle of stationary phase material size is one of the variables of the van Deemter equation, the curve in Figure 2.8 generated can be used to investigate chromatographic performance. As the particle size decreases to less than  $2.5\ \mu\text{m}$ , UFLC is a significant gain in efficiency even when flow rates are increased or linear velocities are increased.

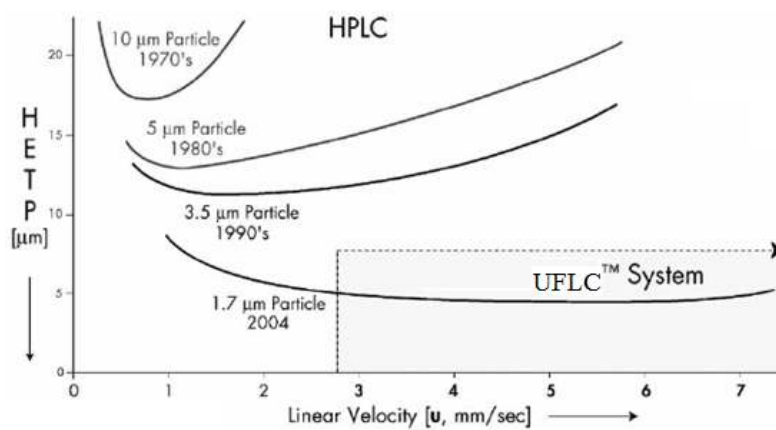


**Figure 2.9** Diagram illustrating the van Deemter plot. [61]

In general, increasing the efficiency of a separation will also increase its resolution. Since both efficiency and optimum flow rate are inversely proportional to particle size, a decrease in the particle size will also increase efficiency and speed up the flow rate. UFLC provides shorter analysis time, higher resolution and sample throughput than conventional LC.

## 2.4 Ultra fast liquid chromatography configuration [62]

Basic UFLC configuration is not different to HPLC system. UFLC system consists of a pumping, sample-injection, separation, detection, and data-processing units. Each unit is essential for performing the analysis as shown in Figure 2.9.

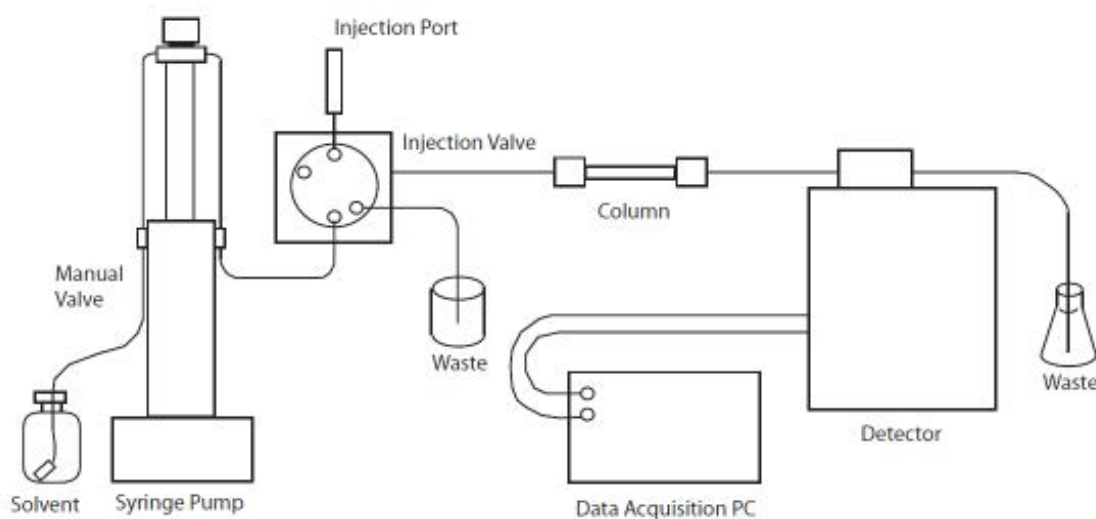


**Figure 2.10** Basic configuration of UFLC system. [62]

### 2.4.1 Pumping unit and Solvent Delivery Unit [63]

The UFLC pump can be employed at higher pressure than conventional HPLC pump. Therefore, the most important advantages of UFLC pumps are higher resolution, less time analysis and increased sample load capacity. There are two modes of pump module in UFLC system; isocratic pump and gradient pump used in UFLC system. Isocratic pump delivers constant mobile phase composition while gradient pump delivers variable mobile phase composition. The selection of pump mode depends on the purpose of the each analysis. The parallel double-plunger model in UPLC pump provides superior pressure capacity and stable solvent delivery. An automatic rinsing kit can be used for standard method to ensure improved plunger seal life under high-pressure delivery conditions. Flow rate is in the range of 0.0001 to 3 mL/min (at 1.0 to 66 MPa) and 3.0001 to 5 mL/min (at 1.0 to 44 MPa). The solvent deliver units of Shimadzu LC-20ADXR UFLC as shown in Figure 2.11.



**Figure 2.11** Solvent deliver unit (Shimadzu LC-20ADXR UFLC)



### 2.4.2 Sample-injection unit [63]

In UFLC system, the simple-injection unit is achieved by a manual injector or an autosampler. Each type is connected with six-port valves, so that a sample can be injected into the flow path at continuous pressure. For the manual injector, the knob is manually operated to deliver the sample to the column as shown in Figure 2.12. Step one, the knob is set at the "LOAD" position for sample injection, as shown in the left image. Using a microsyringe, the sample can be injected into the sample loop, which is separated from the flow path. Step two, the knob is turned to the "INJECT" position. The eluent travels through the loop from the pump then delivers the sample to the column. The autosampler can perform similar work automatically, enabling unmanned continuous operation.

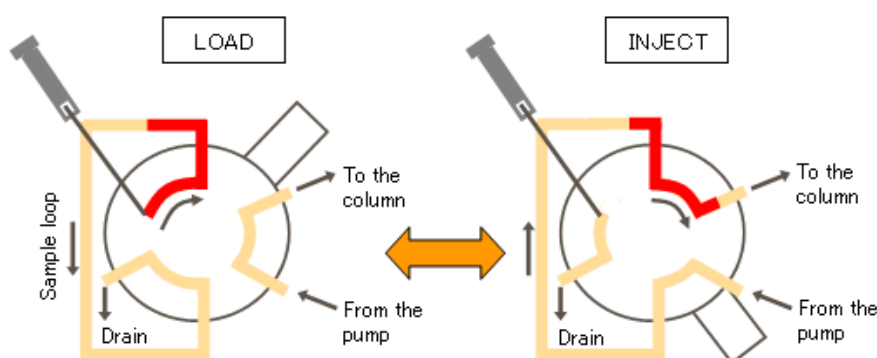


**Figure 2.12** Flow path of manual injector [63]

Most of UFLC systems are carried out with an autosampler injection to achieve the efficiency of analysis results. The autosampler injection (SIL-20AD XR) in Figure 2.13 is a total volume injection type autosampler. In addition to a high-speed injection function and high-precision function for injecting trace quantities, the autosampler features an improved high-pressure valve that increases the pressure resistance (max. allowable pressure: 66 MPa). The internal volume of the high-

pressure valve was reduced to suppress sample diffusion, which is especially suited to high separation analysis.



**Figure 2.13** Autosampler unit (Shimadzu LC-20ADXR UFLC)

#### **2.4.3 Separation unit [50-52, 64]**

The separation unit was performed by using column. The efficiency of a column is measured by theoretical plates and can be normalized with the length of the column to give the height equivalent theoretical plate, called HETP or H. The Van Deemter equation describes the various factors influencing H and is divided into eddy diffusion, longitudinal diffusion, and mass transfer terms. The relative importance of these factors varies with mobile phase velocity. Particle size and morphology of stationary phase material contribute to H, along with a variety of other factors. Therefore, there are two related terms used for describing column efficiency or number of theoretical plates (N) and height equivalent to a theoretical plate (H)

### 2.4.3.1 Number of Theoretical Plates (N)

The column efficiency related to the number of theoretical plates is a mathematical concept and can be calculated using the equation 3.

$$N = 5.545 (t_R / W_h)^2 \dots\dots\dots(3)$$

Where;

N = number of theoretical plates

$t_R$  = Retention time

$W_h$  = Peak width at half height (in units of time)

Due to theoretical plate, columns with high plate numbers are considered to be greater performance, that is, have higher column efficiency, than columns with a lower plate count. A column with a high number of theoretical plates will have a narrower peak at a given retention time than a column with a lower N number. High column efficiency is beneficial since less peak separation (meaning lower alpha,  $\alpha$ ) is required to completely resolve narrow peaks. On stationary phases where the alphas ( $\alpha$ ) are small, more efficient columns are needed. Column efficiency is a function of the column dimensions (diameter, length and film thickness), the type of carrier gas and its flow rate or average linear velocity, and the compound and its retention. For column comparison purposes, the number of theoretical plates per meter (N/m) is used.

### 2.4.3.2 Height Equivalent to a Theoretical Plate (H) [51]

Another evaluation of column efficiency is the height equivalent to a theoretical plate denoted as H. It is calculated using equation 4. Length of column usually was reported in millimeters.

$$H = L/N \dots \dots \dots (4)$$

Where;

L= length of column (mm)

N= number of theoretical plates

In the case of the shorter theoretical plate, the more plates are contained in any length of column. This imply to more plates per meter and higher column efficiency. The equation 5 relating plate height to fluid velocity was called van Deemter equation.

$$HETP = A + B/u + C.u \dots \dots \dots (5)$$

Where;

HETP = height equivalent to a theoretical plate

A = eddy diffusion parameter

B = longitudinal diffusioncoefficient

C = resistance to mass transfer coefficient

$u$  = linear velocity ( $m s^{-1}$ )

From this equation, the parameters that influence the overall peak widths are expressed in three terms:

- **A-term: eddy diffusion:**

The A-term in the Van Deemter equation describes the peak broadening due to the presence of stationary phase particles in the column. The column packing consists of stationary phase in the flow channels. Due to the difference in packing and particle shape, the speed of the mobile phase in various flow channels differs and, analyte molecules travel along different flow paths through the channels.

- **B-term: longitudinal diffusion:**

The B-term in the van Deemter equation, also known as longitudinal diffusion, refers to the diffusion of individual analyte molecules in the mobile phase along the longitudinal direction of a column. Longitudinal diffusion contributes to peak broadening only at very low flow rates below the minimum (optimum) plate height.

**C-term: resistance against mass transfer.**

The C-term in the van Deemter equation relates to the mass transfer of sample components between the stationary phase and the mobile phase during separation, which chromatographic system is in dynamic equilibrium. As the mobile phase is moving continuously, the system has to restore this equilibrium as well. It takes time to restore equilibrium (resistance to mass transfer); therefore, the concentration profiles of sample components between mobile and stationary phase are slightly shifted. This results show in additional peak broadening.

#### 2.4.4 Detection unit

The detection unit is used for monitoring the data eluted from the column. The detection data is usually converted to be an electrical signal. Several detection techniques are selected to suit the sample. The general detectors in the chromatographic system are shown below:

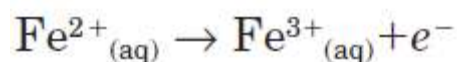
1. Ultraviolet (UV) detector; this detector is normally used to detect components absorbing wavelength of 400 nm or less in the ultraviolet region. The common light source is a D2 lamp.
2. Ultraviolet -Visible (UV-VIS) detector; this detector is useful for the detection of coloring compounds such as dyes and stains due to coverage of the visible light region in the range of 200-800 nm. The common light sources consist of D2 lamp and W lamp.
3. Diode array detector (DAD); this detector provides an information covering a broad range of wavelengths simultaneously. Data on the spectrum from the ultraviolet and visible light range is also recorded.
4. Fluorescence (FL) detector; this detector can specifically detect fluorescent substances with high sensitivity.
5. Differential refractive index (RI) detector; the principle of the detector involves monitoring the change in the refractive index. Components without absorbing ultraviolet light can also be detected despite low sensitivity.
6. Conductivity detector; mainly inorganic ions are detected by measuring the conductivity.
7. Electrochemical (EC) detector; the electrochemical detector is also a well-known detector. It has been coupled with the chromatographic system because of its high selectivity and sensitivity for electroactive compounds.

## 2.5 Principle of Electrochemistry [65, 66]

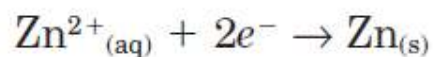
Electrochemistry is one subject of chemistry studying about chemical interactions relating to electron transfer. Normally, these interactions involve electron transfer between the electrode surface and electroactive species in solution. To approach relationships in electrochemical reactions, it is necessary to understand terms and basic principles of electricity. The electrochemical reactions are chemical reactions where the electrons are transferred from one atom or molecule to another. There are two different types of electrochemical reactions that are distinguished by the changes of oxidation state including oxidation and reduction reactions. The term of redox is an abbreviation for both reactions between oxidation and reduction reactions.

In the oxidation reaction, electrons are donated from atoms of the elements involved in the reaction. The charge of atoms must then become more positive.

### Example



On the other hand, the reduction reaction is an opposite of the oxidation reaction. Electrons are gained by atoms of the elements involved in the reaction.

**Example**

A redox reaction is a kind of electrochemical reaction where both reduction and oxidation reactions happen. The electrons lost in the oxidation component are gained in a reduction component.

**2.5.1 Electrochemical cells**

Commonly, oxidation-reduction or redox reactions occurred in electrochemical cells. There are two types of electrochemical cells; galvanic cells and electrolytic cells. Spontaneous reactions usually occur in galvanic while nonspontaneous reactions occur in electrolytic cells. Both types of cells contain electrodes where the oxidation and reduction reactions occur. Oxidation is obtained at the electrode termed the anode, and reduction is observed at the electrode called the cathode.



### 2.5.1.1 Galvanic cell

The spontaneous reaction is redox reaction in a galvanic cell. Galvanic cells are commonly used as batteries or others energy storage. Galvanic cell reactions supply energy which is controlled by the oxidation and reduction reactions. The redox reactions occur in containers connected by salt bridge for permitting electrons to flow. The common galvanic cell as shown in Figure 2.14 is the Daniell cell.

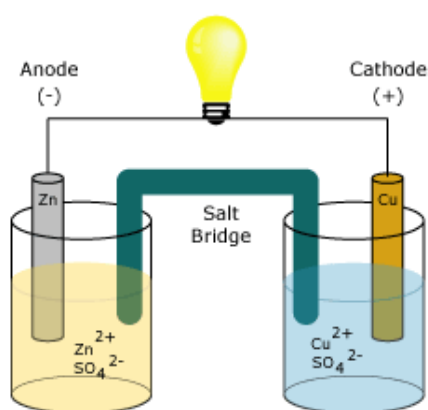


**Figure 2.14** Diagram of galvanic cell [65]

### 2.5.1.2 Electrolytic Cells

The nonspontaneous redox reaction in an electrolytic cell. Electrical energy is needed to promote the electrolysis reaction. An example of an electrolytic cell is shown below. Molten NaCl is electrolyzed to produce liquid sodium and chlorine gas. The sodium ions migrate toward the cathode, where they are reduced to sodium metal. Chloride ions migrate to the anode to oxidize to form chlorine gas. The chlorine gas can be collected surrounding the cell. The sodium metal is less dense than the molten salt. Therefore, the sodium metal is removed by floating to the top of the reaction container.

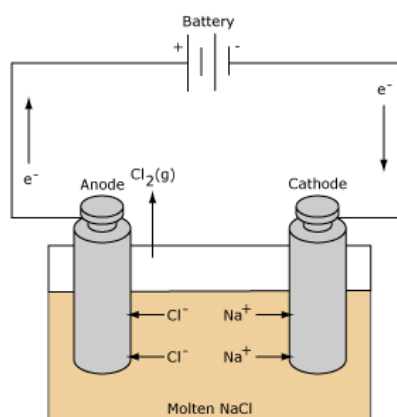


**Figure 2.15** Diagram of electrolytic cell [66]

### 2.5.2 Mass transport process in electrochemical system [67]

It is already known that a typical electrolysis reaction involves the charge transfer between an electrode and species in solution. This whole process occurs at the interface between the electrode and the electrolyte. There are three forms of mass transport which can influence an electrolysis reaction including Diffusion, Convection, and Migration.

### 2.5.2.1 Diffusion

Diffusion occurs in all solutions and arises from local uneven concentrations of reagents. Diffusion is particularly significant in an electrolysis experiment since electron transfer from electrochemical reaction only occurs at the electrode surface. Consequently, there will be a lower reactant concentration at the electrode than in bulk solution. Similarly, the higher concentration of product will exist near the electrode than far away in solution. The rate of movement of material by diffusion can be predicted mathematically, and Fick's law propose two laws to quantify the processes. The equation of first law is shown in equation 6.

$$J_o = - D_o(\partial C_o / \partial X) \dots \dots \dots (6)$$

Fick's first law relates to the diffusional flux,  $J_o$  (the rate of movement of material by diffusion), to the concentration gradient and the diffusion coefficient,  $D_o$ . The negative sign simply indicate that material moves down a concentration gradient from regions of high to low concentration. However, in many measurements, the concentration of material varied as a function of time can be predicted from the first law in equation 7.

$$\partial C_o / \partial t = D_o(\partial^2 C_o / \partial X^2) \dots \dots \dots (7)$$

Fick's second law is an important relationship since it allows the prediction of the variation of concentration of redox species as a function of time within the electrochemical cell. To solve these expressions, analytical or computational models are usually used.

### 2.5.2.2 Convection

Convection obtains from the action of a force in the solution. This can be a pump, a flow of gas or even gravity. There are two forms of convection the first is called natural convection being in any solution. This natural convection is produced by small thermal or density differences. The convection acts to mix the solution in a random and consequently unpredictable manner. It is possible to remove out the natural convection effects from an electrochemical experiment by intentionally introducing convection into the cell. Forced convection is another form of convection. It is commonly a number of orders of magnitude greater than any natural convection effects. Therefore, force convection can effectively remove the random convection from the experimental measurements. This is only true if the force convection is introduced in a well-defined and quantitative manner.

### 2.5.2.3 Migration

Migration is essentially an electrostatic effect arising due to the application of a potential on the electrodes. Migration can effectively generate a charged interface (the electrodes). Electrostatic forces can attract or repel charged species near the interface. The migratory flux can be express mathematically in the equation 8.

$$\partial C_o / \partial t = -u C_o (\partial \Phi / \partial X) \dots \dots \dots (8)$$

Because of ion solvation effects and diffuse layer interactions in solution, migration is notoriously difficult to calculate accurately for real solutions. Therefore, most voltammetric measurements are carry out in solutions which contain a background electrolyte - this compound is a salt (eg. KCl), which does not undergo electrolysis itself but helps to protect the reactants from migratory effects. By adding a large quantity of the electrolyte, the electrolysis reaction is not significantly effected by

migration. The purpose of adding a background electrolyte into a solution is not however only to get rid of migration effects as it also acts as a conductor to help the passage of current through the solution.

### 2.5.3 Voltammetric technique

Voltammetric technique, the effects of the applied potential and the behavior of the redox current are described by the Nernst or Butler–Volmer equations. The applied potential controls the concentrations of the redox species at the electrode surface ( $C_O^0$  and  $C_R^0$ ) and the rate of the reaction ( $k^0$ ), are described by equation mentioned above. In the cases where diffusion plays an important role for controlled process, the current obtaining from the redox process (known as the faradaic current) is related to the material flux at the electrode–solution interface. The relationship between these processes is in charge for the characteristic features observed in the voltammograms of the various electrodes.

For a reversible electrochemical reaction, which can be described by  $O + ne \rightleftharpoons R$ , the application of potential  $E$  forces the respective concentrations of  $O$  and  $R$  at the surface of the electrode (that is,  $C_O^0$  and  $C_R^0$ ) to a ratio following the Nernst equation 9.

$$E = E^0 - [(RT/nF) (\ln C_R^0/C_O^0)] \dots \dots \dots (9)$$

Where;

$R$  = the molar gas constant ( $8.3144 \text{ J}\cdot\text{mol}^{-1}\text{K}^{-1}$ )

$T$  = the absolute temperature (K)

$n$  = the number of electrons transferred

$F$  = faraday constant ( $96,485 \text{ C/equiv}$ )

$E^0$  = the standard reduction potential for the redox couple

$C_{\text{O}}^0$  = concentrations of O at the electrode surface

$C_{\text{R}}^0$  = concentrations of R at the electrode surface

If the potential applied to the electrode is changed, the ratio of  $C_{\text{O}}^0$  and  $C_{\text{R}}^0$  at the surface will also change to satisfy in equation above. If the potential is made more negative, the ratio becomes larger (that is, O is reduced). Conversely, if the potential is made more positive, the ratio is smaller (that is, R is oxidized). It is useful for some techniques to use the relationship known as the Butler–Volmer equation (10) relate the variables for current, potential, and concentration:

$$i/nFA = K^0 \{C_{\text{O}}^0 \exp[-\alpha\Theta] - C_{\text{R}}^0 \exp[(1-\alpha)\Theta]\} \dots\dots\dots(10)$$

Where;

$\Theta = nF(E - E^0)/RT$

$k^0$  = the heterogeneous rate constant

$\alpha$  = transfer coefficient

$A$  = the area of the electrode

Various voltammetric methods have their own exceptional laws and theoretical relationships that explain and predict in details with the variety of aspects of the  $i-E$  behavior (such as curve shape, peak height, width, and position). In this research,

cyclic voltammetry and amperometry were used for investigating the electrochemical behavior and determination of the analytes.

### **2.5.3.1 Cyclic voltammetry [68]**

Cyclic voltammetry is a method for studying the electrochemical behavior of a system. In this technique, current flowing between the electrode of interest (whose potential is monitored with respect to a reference electrode) and a counter electrode is measured under the control of a potentiostat. The voltammogram shows the possibility of different electrochemical processes to occur. A triangular potential scan is provided to the working electrode, whereby the potential rises from a start value to a final value then returns back to the start potential at a constant potential scan rate. The scan rate can be applied from a few millivolts per second to a hundred volts per second. The current measured during this process is often normalized to the electrode surface area and referred to as the current density. A cyclic voltammogram is obtained from the plot of current density against the applied potential. A peak in the measured current is seen at a potential that is characteristic of any electrode reaction taking place. The peak width and height for a particular process depends on the scan rate, electrolyte concentration and the electrode material. A schematic cyclic voltammogram of a reversible redox process is shown in Figure 2.16.

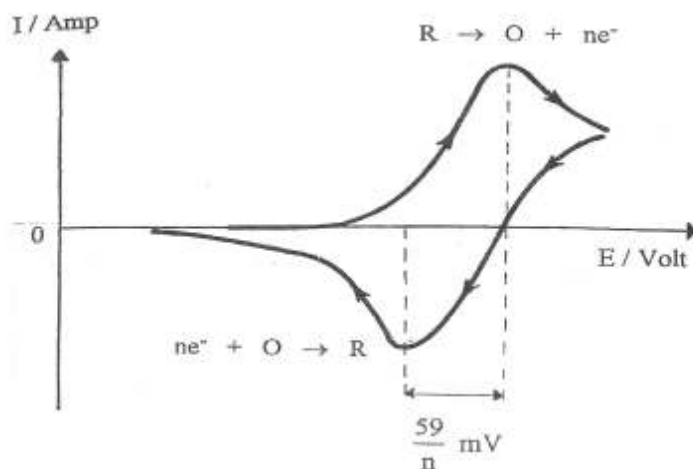


**Figure 2.16** A schematic cyclic voltammogram [68]

### 2.5.3.2 Amperometric detection

Amperometric detector is commonly used in electrochemical detection. The amperometric technique was performed by maintaining a constant potential at working electrode with respect to a reference electrode. The resulting current is directly correlated to the bulk concentration of the electroactive compound. Amperometric detection in which the measuring principle based on amperometry was used as detection technique for Ultra Fast Liquid Chromatography (UFLC) in this research. The thin layer flow cell in this research consist of three-electrode types; working electrode, reference electrode and counter electrode. Figure 2.17 shows the schematic of a commercial thin layer flow cell.





**Figure 2.17** A schematic thin layer flow cell (GL science)

#### **2.5.4 Instrumentation in electrochemistry [65,66]**

Most electrochemical work is accomplished by employing a potentiostat. A potentiostat is an electronic device controlling the voltage difference between a working electrode and a reference electrode. Both electrodes are in an electrochemical cell. The potentiostat monitors the current flow between the working and auxiliary electrodes. The controlled variable in a potentiostat is the cell potential, and the monitored variable is the current. A potentiostat generally functions with an electrochemical cell containing three electrodes. Figure 2.18 shows the schematic of potentiostat linked to an electrochemical cell.

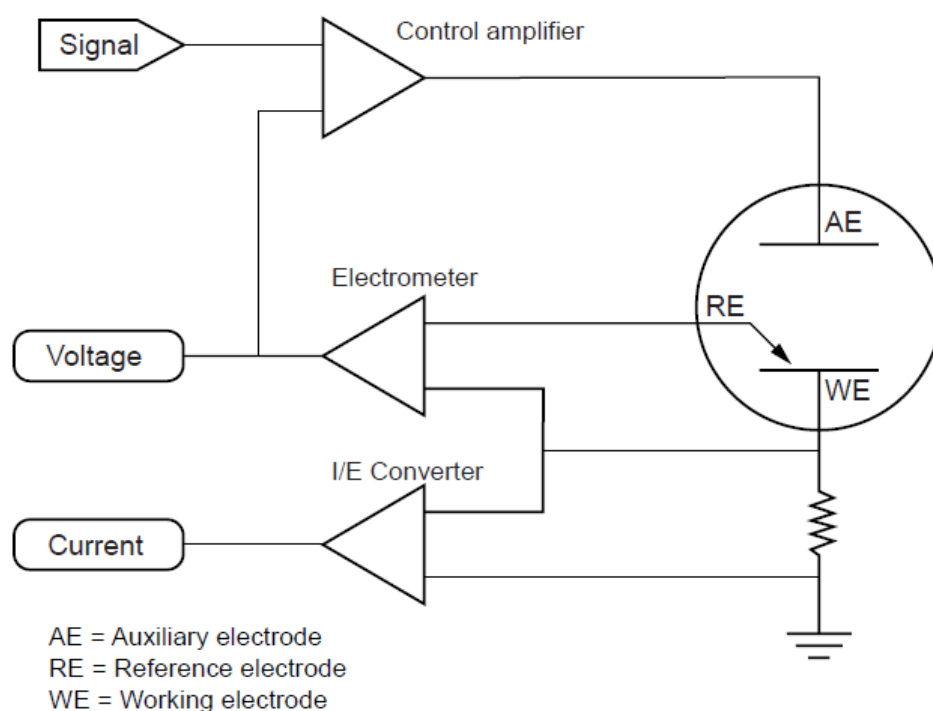


**Figure 2.18** Schematic of potentiostat linked to an electrochemical cell. [65]

#### 2.5.4.1 Working electrode

The working electrode is the electrode, which the analyte is oxidized or reduced. The active potential of the working electrode is measured against a standard reference electrode. The reference electrode is essential to accurately measure the potential of the working electrode. The electrode system includes counter electrode, which is complimentary to the working electrode. The driving potential is applied to activate the electrochemical reaction to obtain the required oxidation or reduction. Nowadays, there are many kind of working electrodes. The working electrode materials for electrochemical detection have been reported as follows.

- Boron-doped diamond (BDD)

Boron-doped diamond is an excellent electrode material providing a large potential window in aqueous solution and low background current. The wider potential window and lower background currents make the BDD material very attractive for electrochemical analysis. Reactions occurring in potential ranges from about -0.5 V to -1.2 V and about +1.8 V to 2.5 V, which could not be analyzed on traditional electrode surfaces such as Au and Pt, can now be analyzed. The lower background current allows the higher sensitivity and the lower detection limits.

- Graphene (G)

G is a flat monolayer of carbon atoms strongly packed into a two-dimensional (2D) honeycomb lattice. A platform building block of other graphitic allotropes includes three-dimensional graphite, one-dimensional carbon nanotubes and zero-dimensional fullerenes. Graphene was discovered in 2004 by Geim and Novoselvo, who succeeded in isolation of thin carbon film and ultimately monolayer graphene by simply using scotch tape. Graphene is an excellent conductor material and thus, graphene modified electrodes exhibit well electrochemical response.

#### **2.5.4.2 Reference electrode [66]**

A reference electrode is used in measuring the working electrode potential. A reference electrode should have a constant electrochemical potential as long as no current flows through it. The most common laboratory reference electrodes are the saturated calomel electrode (SCE) and the silver/silver chloride (Ag/AgCl) electrodes.

#### **2.5.4.3 Counter electrode [66]**

The counter electrode (auxiliary electrode) is a conductor that completes the cell circuit. The counter (auxiliary) electrode in lab cells is generally an inert conductor like platinum or graphite. The current flowing into the solution to the working electrode leaves the solution to the counter electrode.

### **2.6 Solid phase extraction techniques [69, 70]**

Solid phase extraction (SPE) is a sample preparation method used in analytical system for the extraction of analytes from a complicated matrix. This sample preparation method facilitates the extraction, cleanup and concentration of analytes prior to their quantification. Solid phase extraction avoids most problems occurring in liquid-liquid extraction and improves quantitative recovery yields. This technique is less time of analysis, simple to perform and can be automated.

The principles of solid phase extraction are very similar to those of liquid chromatography. In liquid chromatography, an appropriate mobile phase is chosen to permit the sample components to continuously interact with the packing bed as they pass through the column. The extent to which the sample components interact with the packing varies due to structural and functional group differences, causing them to exit the column at different times.

### 2.6.1 SPE procedure [70]

The principle of Solid phase extraction is using the difference of affinity between an analyte and interferences, presenting in a liquid matrix, for a solid phase (sorbent). This affinity allows the separation of the target analyte from the interferences. There are four steps for typical solid phase extraction as shown in Figure 2.19:

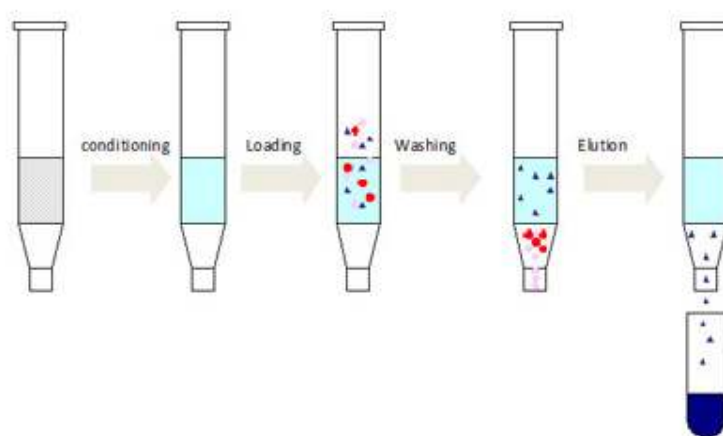


**Figure 2.19** Schematic representation of SPE procedure [70]

First, the cartridge is equilibrated or conditioned with a solvent to wet the sorbent. Then the loading solution containing the analyte is percolated through the solid phase. Ideally, the analyte and some impurities are retained on the sorbent. Then, the sorbent is washed to remove impurities. Finally, the analyte is collected during this elution step.

## 2.7 Literature reviews

Recently, there are many techniques have been developed for sulfonamide determination such as thin-layer chromatography (TLC), enzyme-linked immunoassay (ELISA), gas chromatography (GC), capillary electrophoresis (CE), high performance liquid chromatography (HPLC) and ultra-fast liquid chromatography (UFLC). Furthermore, the coupling detections have been also used for SAs analyte such as ultraviolet (UV), fluorescent detector and mass spectrometric detection.

In 1997, Barbara et al. [13] reported the analysis of nine sulfonamides by using gas chromatography coupled with atomic emission detection. Atomic emission detection has been used to simultaneous quantify and identify the N<sup>1</sup>-methylated compound, which are sulfonamides derivatives. The evaluation of elemental ratios of carbon, nitrogen and sulfur content showed a significantly extended linear dynamic range. Excellent linearity of sulfonamides in methanol is obtained between 3-80 ng  $\mu\text{l}^{-1}$ .

In 2001, Ming-Ren et al. [15] developed liquid chromatography–electrospray-mass spectrometry (LC–ES-MS) for the quantitative determination of nine sulfonamides [sulfadiazine (SDZ), sulfapyridine (SPY), sulfamerazine (SMZ), sulfamethazine (SMT), sulfamonomethoxine (SMX), sulfisoxazole (SSZ), sulfadimethoxine (SDM), sulfaquinoxaline (SQ) and sulfaphenazole (SP)] in meat. Selective ion monitoring was performed for quantitative determination. Results showed the linearity of 0.1–10  $\mu\text{g mL}^{-1}$ . Blank meat samples were fortified at levels between 50 and 500  $\mu\text{g kg}^{-1}$ . The limits of detection were found to be 10  $\mu\text{g kg}^{-1}$ . This newly method was used to detect sulfonamides in various beef, pork and chicken samples from local markets.

In 2002, Titus et al. [71] reported the detection of sulfonamide compounds in a mixture of standards at a poly (3-methylthiophene) coated on glassy carbon (GC) electrode. Square wave voltammetry (SWV) with cathodic reduction (0 to - 4.0 V) was used for the detection of seven sulfonamide compounds in a mixture. The oxidation potentials ( $E_{pa}$ ) of the compounds were between + 0.788 to + 1.158 V. The poly (3-methylthiophene) film provided better sensitivity for determination of sulfonamides in a mixture, compared to the GC electrode.

In 2003, Ming-Ren et al.[72] described a newly developed capillary electrophoresis (CE) with solid-phase extraction (SPE) method for the quantitative determination of eight sulfonamides (sulfamethazine (SMZ), sulfamerazine (SMR), sulfadiazine (SDZ), sulfadimethoxine (SDM), sulfamonomethoxine (SMM), sulfaphenazole (SPA), sulfaquinoaline (SQF) and sulfisoxazole (SIA) in meat. The conditions of 35 mM  $\text{Na}_3\text{PO}_4 - \text{H}_3\text{PO}_4$  buffer (pH 6.5) at an applied voltage of 25 kV was used for complete separation of eight sulfonamides. The linearity was 0.5–50  $\mu\text{g mL}^{-1}$  of each compound. The recovery of SPE method was 80 to 97% and the detection limits of each sulfonamide approximately ranged from 5 to 10  $\mu\text{g kg}^{-1}$ . The detection and quantification limits for this newly developed method are below the permissible MRL and low enough to determine residues of these drugs in meat.

In 2004, Chuan-Feng et al. [25] reported that a new fluorescent chemosensor based on an acyclic tetra-sulfonamide derivative linked to two dansyl groups was synthesized. This chemosensor provided selective binding ability to fluoride ions over other halide ions in fluorescence detection. The  $^1\text{H}$  NMR spectra of the 9-position of 9,10-dihydroanthracene moiety in receptor 1 showed that the fluoride ion had the strong hydrogen binding interaction with the protons of sulfonamide and also with the methylene protons at the 9-position of 9,10-dihydroanthracene moiety. Therefore, a new fluorescent chemosensor based on an acyclic tetra-sulfonamide derivative linked to two dansyl groups was successfully high selective on analyte target.

In 2005, Jorge et al. [73] developed the determination of seven sulfonamides by means of HPLC with chemiluminescence detection. The analytes are derivatized

with fluorescamine. They were then separated and subsequently participated in the post-column chemiluminescence (CL) in peroxyoxalate system (PO) using imidazole as a catalyst. The method exhibits the resolution of seven sulfonamides less than 12 min, providing the advantage of the very sensitive CL detection. The determination of sulfonamides in milk was found to be very low in  $\mu\text{g L}^{-1}$  range. Moreover, the time of analysis is shorter than those reported by other chromatographic methods.

In 2006, Anchana et al. [34] presented electroanalysis of sulfonamides by two approaches including flow injection system and high-performance liquid chromatography. Cyclic voltammetry at a boron-doped diamond (BDD) electrode compared with that at glassy carbon electrode was investigated. The BDD electrode provided well-resolved oxidation, irreversible cyclic voltammograms and higher current signals than glassy carbon electrode in 0.1M phosphate solution (pH 3). The measurements by FIA using the BDD electrode as an amperometric sensor were performed in a 0.1 M phosphate solution (pH 3) at an applied potential of 1100 mV versus Ag/AgCl. HPLC system consisted of a Water Model 510 solvent delivery system, with a flow rate of  $1.0 \text{ mL min}^{-1}$ . 0.1 M sodium dihydrogen phosphate (pH 3), acetonitrile (80:20; v/v), was used as the mobile phase for FIA experiments, and eluent in the liquid chromatographic experiments. The linearity range was found to be in the range of  $0.05 - 100 \mu\text{g mL}^{-1}$ . The detection limit (DL) and quantitative limit (QL) for the four SAs was found in the range of  $0.011 - 0.107 \mu\text{g mL}^{-1}$ , respectively. This method was also used for determination of sulfonamides in egg samples with high recoveries between 90.0 and 107.7 %.

In 2008, Cristine et al. [74] developed electroanalytical determination of sulfadiazine and sulfamethoxazole in pharmaceuticals using a boron-doped diamond electrode. The square-wave voltammetry (SWV) technique was used for detection of sulfadiazine and sulfamethoxazole determination. The electroanalytical determination of sulfadiazine was performed in ethanol +  $0.5 \text{ molL}^{-1} \text{ H}_2\text{SO}_4$  50/50 (v/v), and sulfamethoxazole in ethanol: phosphate buffer 50:50 (v/v) solutions. The two analytes showed irreversible oxidation peak at around +1.1 V. Calibration curves were obtained in the concentration ranges of  $8.01 \times 10^{-6}$  to  $1.19 \times 10^{-4} \text{ mol L}^{-1}$  for



sulfadiazine and  $6.10 \times 10^{-6}$  to  $6.01 \times 10^{-5}$  mol L<sup>-1</sup> for sulfamethoxazole and the detection limits was found to be in the range of  $2.19 \times 10^{-6}$  and  $1.15 \times 10^{-6}$  mol L<sup>-1</sup>, respectively. For both sulfonamides, recovery values were in the range of 95–104%, indicating no matrix interference effects on the analytical results.

In 2010, Wenjun et al. [75] studied the analysis of seven sulfonamides in milk by cloud point extraction and high performance liquid chromatography. An efficient and environmentally friendly analytical methodology is proposed for extracting and preconcentrations even sulfonamides from milk prior to high performance liquid chromatography with ultraviolet detection (HPLC–UV). The linear range of quantitation for all analytes was approximately 0.05–2.0 mg L<sup>-1</sup>, and the correlation coefficients of the calibration curves were  $\geq 0.9999$ . The limits of detection (LOD) of the sulfonamides ranged from 2.23 to 9.79  $\mu\text{g L}^{-1}$ . The average recoveries and relative standard deviations were in the range of 67.0–105.7% and 0.93–8.31%, respectively. The proposed method based on CPE prior to HPLC–UV for the determination of SAs in milk was found to be high sensitivity, low-cost environmentally friendly user.

In 2011, Silvia et al. [4] reported two analytical methodologies for the simultaneous analysis of eight sulfonamide antibiotics in animal feeds. The determination was studied by high-performance liquid chromatography using fluorometric detection with precolumnderivatization. The separation of the derivatized compounds was performed using two different chromatographic columns: a conventional C18 column and a recently available core-shell particle Kinetex C18 column. The experiments showed that the method using the Kinetex column was superior with regard to speed of analysis and precision, both under repeatability and intermediate reproducibility conditions. The limits of detection and quantification were also greatly improved, below 0.10 and 0.34  $\mu\text{g g}^{-1}$ , respectively. Analytes were extracted in a simple and rapid procedure by manual shaking with mean recoveries ranging from 72.7% to 99.4% with relative standard deviations below 9 %. This new analytical methodology is considered to be suitable for the determination of SAs in animal feeds.

In 2011, Chang et al. [76] studied the method for monitoring of 14 sulfonamide antibiotic residues in marine products using HPLC-PDA and LC-MS/MS technique. In analyzing step, the residues of 14 sulfonamides (SAs) were determined by high-performance liquid chromatography (HPLC) with photodiode array detector. In confirmatory step, ultra-performance liquid chromatography-tandem mass spectroscopy (UPLC-MS/MS) was used for unequivocal identification of target compounds. The result showed that no sulfonamide antimicrobial was found in more than 99% of the samples analyzed in this study.

Later In 2011, Yan-Bo et al. [77] presented new technique of retrieving graphene from aqueous dispersion. The new method was established based on large surface area and two-dimensional planar structure of graphene. The  $\text{Fe}_3\text{O}_4@\text{SiO}_2$  and graphene were used as an adsorbent to extract six sulfonamide antibiotics (SAs) from water samples. Under the optimal conditions, a rapid and effective determination of SAs in environmental water samples was achieved. The limits of detection for six SAs ranged from 0.09 - 0.16 ng mL<sup>-1</sup>. Good reproducibility was obtained. The relative standard deviations of intra- and inter-day analysis were found to be less than 10.7% and 9.8%, respectively. The study demonstrates that the proposed material is effective and efficient for sample preparation.

## CHAPTER III

### EXPERIMENTAL

All chemicals, reagents, instruments, apparatus, procedure of the experiment, method for preparation and modification of the electrode are illustrated in the detail in this chapter.

#### 3.1 Chemicals and reagents

All chemicals and their suppliers are shown in Table 3.1

**Table 3.1** List of all chemicals and reagents and their suppliers

Chemicals/ Reagents	Suppliers
Sulfadiazine (SDZ)	Sigma-Aldrich (USA)
Sulfamerazine (SMZ)	Sigma-Aldrich (USA)
Sulfaguanidine (SG)	Sigma-Aldrich (USA)
Sulfisoxazole (SSZ)	Sigma-Aldrich (USA)
Sulfadimethoxine (SDM)	Sigma-Aldrich (USA)
Sulfamonomethoxine (SMM)	Sigma-Aldrich (USA)
Sulfadoxine (SDX)	Sigma-Aldrich (USA)
Sulfamethoxazole (SMX)	Sigma-Aldrich (USA)

Ethylenediaminetetraaceticacid disodium salt dehydrate (EDTA)	Sigma-Aldrich (USA)
Carbon powder (particle size < 20 µm)	Sigma-Aldrich (USA)
Potassium ferricyanide ( $K_3[Fe(CN)_3]$ )	Sigma-Aldrich (USA)
Potassium ferrocyanidetrihydrate ( $K_4[Fe(CN)_3].3H_2O$ )	A.C.S (USA)
Potassium chloride (KCl)	Ajax Finechem (New Zealand)
Graphene (G)	A.C.S (USA)
Disodium hydrogen phosphate dehydrate ( $Na_2HPO_4$ )	Merck (Germany)
Acetic acid ( $CH_3COOH$ )	Merck (Germany)
Ortho-phosphoric acid 85% ( $H_3PO_4$ )	Merck (Germany)
Sodium hydroxide (NaOH)	Merck (Germany)
Ethanol (HPLC grade)	Merck (Germany)
Acetonitrile (HPLC grade)	Merck (Germany)
2-Propanol	Merck (Germany)
Nitric acid ( $HNO_3$ )	Merck (Germany)

### 3.2 Instruments and apparatus

All instruments and apparatus are shown in Table 3.2

**Table 3.2** List of all instruments and apparatus

<b>Instruments and equipment</b>	<b>Suppliers</b>
UPLC LC-20AD XR pump	Shimadzu (Japan)
UPLC SIL-20A XR autosampler	Shimadzu (Japan)
UPLC CTO-20AC column oven	Shimadzu (Japan)
CHI1232A	CH Instrument (USA)
Inertsil C4 (GL science, 150mm × 4.6mm i.d.; particle size, 5µm)	GL science (USA)
Electrochemical flow cell	Bioanalytical System (USA)
Teflon cell gasket	Bioanalytical System (USA)
PEEK tubing (0.25 mm. i.d.)	Upchurch (USA)
Teflon tubing (1/10 inch i.d.)	Upchurch (USA)
Silver/silver chloride electrode (Ag/AgCl)	Bioanalytical System (Japan)
Boron-doped diamond electrode (BDD)	Toyo Kohan Co., Ltd. (Japan)
Stainless steel electrode	Bioanalytical System (USA)
Platinum wire	Bioanalytical System (USA)
Bioanalytical System	Bioanalytical System (USA)

pH meter	Metrohm (USA)
Milli Q water system $R \geq 18.2 \text{ M}\Omega\text{cm}$	Millipore (USA)
Centrifuge	Cole parmer (USA)
Analytical balance	Mettler Toledo (Switzerland)
Vortex mixer VTX-3000L	Mixer Uzusio LMS (Japan)
Autopipette	Eppendorf (Germany)
Filter membrane (0.20 $\mu\text{m}$ )	National scientific (USA)
Nylon syringe filters (0.20 $\mu\text{m}$ )	ChroMex (USA)
Ultrasonic bath	ULTRASONIK 28H, ESP Chemicals, Inc., (USA)
Vacuum pump	GAST (USA)
12 position vacuum manifold system	Phenomenex (USA)
Microcolumn VertiPak™ HCP	Vertical chromatography (USA)

### **3.3 Preparation of chemicals and reagents solution**

#### **3.3.1 Preparation of solution for cyclic voltammetry**

##### **3.3.1.1 Preparation of 0.1 M KCl solution**

The solution of 0.1 M KCl was used as supporting electrolyte for investigation of the G/PANI modified electrode. The solution was prepared simply by dissolving 1.86 g of KCl with Milli-Q water and after that adjusting to final volume of 250 mL in volumetric flask. This solution can be kept for month by storage at 4 °C in refrigerator.

##### **3.3.1.2 Preparation of $K_3Fe(CN)_6$ and $K_4Fe(CN)_6$ solution**

The solution of  $K_3Fe(CN)_6$  and  $K_4Fe(CN)_6$  at 1 mM was used for characterization of the G/PANI modified electrode. The mixture solution was prepared by weighing 8.23 mg of  $K_3Fe(CN)_6$  and 10.00 mg of  $K_4Fe(CN)_6 \cdot 3H_2O$  and dissolving in supporting electrolyte 0.1 KCl to final volume of 25 mL in volumetric flask.

##### **3.3.1.3 Supporting electrolyte solution**

The potassium hydrogen phosphate solution 0.05 M at pH 3 was used as supporting electrolyte for cyclic voltammetric investigation of eight SAs. The supporting electrolyte was prepared daily by dissolving potassium dihydrogen phosphate 6.805 g in Milli-Q water and transferring the homogeneous solution into 1000 mL volumetric flask. Before adjusting to the final volume, potassium hydrogen phosphate solution was added with phosphoric acid to make pH as 3.

#### **3.3.1.4 Stock standard solution**

The stock standard solution of eight SAs at  $1000 \mu\text{g mL}^{-1}$  was prepared by dissolving 10 mg of each compound in acetonitrile: Milli-Q water (50:50; v/v) to final volume of 10 mL in volumetric flask and then stored the stock standard solution into opaque bottles at  $4 \text{ }^\circ\text{C}$ . To prepare working standard solution, the stock standard solution was diluted to suitable proportions with an acetonitrile: Milli-Q water (50:50; v/v) solution.

#### **3.3.1.5 Working standard solution**

The working standard solution for cyclic voltammetric experiment was performed by dilution of stock standard solution to suitable proportions into 3 mL electrochemical cell. The working standard solution of each sulfonamides  $50 \mu\text{g mL}^{-1}$  was prepared by pipetting 0.15 mL of each compound into the electrochemical cell and then adjusting to 3 mL with 2.85 mL of supporting electrolyte.

### **3.3.2 Preparation of solution for UFLC-ECD**

#### **3.3.2.1 Mobile phases**

The mixture of 0.05 M phosphate buffer solution (pH 3): acetonitrile: ethanol (70:25:5; v/v/v) was used as mobile phase of UFLC-ECD system. To study the effect of pH, phosphate buffer solution were prepared with the different pH by dissolving potassium dihydrogen orthophosphate and disodium hydrogen orthophosphate in Milli-Q water to final volume of 100 mL in volumetric flask. The weight of these compounds in the pH range of 5-8 was shown in Table 3.3.



**Table 3.3** Preparation of phosphate buffer solution (pH 5-8)

pH	Potassium dihydrogen phosphate (g)	Disodium hydrogen phosphate (g)
5	0.6745	0.0071
6	0.6049	0.0987
7	0.2810	0.3524
8	0.0251	0.8570

The phosphate buffer solution at pH 3 and pH 4 were prepared by weighing potassium dihydrogen phosphate 3.4025 g and then dissolved with Milli-Q water to form homogeneous solution after that adjusted pH to 3 and 4 with phosphoric acid, respectively and made up to 500 mL in volumetric flask. The refreshed phosphate buffer solutions were prepared daily and filtered through a 0.22  $\mu\text{m}$  Nylon membrane filter before use into our proposed UFLC-ECD system.

### 3.3.2.2 Stock standard solution

The stock standard solution of eight sulfonamides at  $1000 \mu\text{g mL}^{-1}$  was prepared by dissolving 10 mg of SMM, SDM, SG, SDX, SMX, SSZ, SDZ and SMZ in acetonitrile: Milli-Q water (50:50; v/v) to final volume of 10 mL in volumetric flask and then stored the stock standard solution into bottles at  $4^\circ\text{C}$ .

### **3.3.2.3 Working standard solution**

The working standard solution for UFLC-ECD system was prepared by pipetting 0.1 mL (100  $\mu$ L) of stock standard solution of SMM, SDM, SG, SDX, SMX, SSZ, SDZ and SMZ into 10 mL of acetonitrile: Milli Q water (50: 50; v/v). Prior to use, working standard solution was filtered through a 0.22  $\mu$ m Nylon membrane filter.

### **3.3.3 Preparation of solution for sample preparation**

#### **3.3.3.1 Na<sub>2</sub>EDTA-Mallvaine's Buffer solution**

Solid phase extraction was applied for sample preparation. Microcolumn Vertipak<sup>TM</sup> HCP was selected for sample clean up and extraction of SAs from shrimp sample. Na<sub>2</sub>EDTA-Mallvaine's buffer at pH 4 was used as extraction solution for elution of SAs. The solution of Na<sub>2</sub>EDTA-Mallvaine's buffer pH 4 was prepared by dissolving 0.651 g of disodium hydrogen phosphate dehydrate, 0.676 g of citric acid and 0.186 g of Na<sub>2</sub>EDTA in 50 mL volumetric flask by using Milli-Q water for dissolution. After that, the extraction solution was adjusted to pH 4 with phosphoric acid or sodium hydroxide for made up the solution at pH 4.

#### **3.3.3.2 Sample preparation of shrimp**

Shrimp sample was acquired from a local market in Thailand. First, 2 g of homogeneous shrimp sample and 10 mL of Na<sub>2</sub>EDTA-McIlvaine's buffer were added into centrifuge tube and mixed on a vortex mixer with high speed rate for 5 min. The mixture was placed in an ultrasonic bath for providing complete distribution of SAs from shrimp to supernatant. Supernatant containing SAs was obtained from centrifugation at 3500 rpm for 10 min. Next, supernatant was extracted and cleaned up with solid-phase extraction (SPE) column connected to a 12-position vacuum manifold system as the following steps. SPE tube was firstly condition with 5 mL of methanol and equilibrated with 5 mL of Milli-Q water and 5 mL of Na<sub>2</sub>EDTA-

McIlvaine's buffer, respectively. Next, supernatant was loaded into the SPE tube. During this step, the SAs compounds are retained on the SPE tube. 7 mL of methanol was used for elution of the eluent. Finally, the extracted solution was filtered through a 0.20  $\mu\text{m}$  nylon membrane filter before direct injection into our proposed UPLC-ECD system.

### **3.4 Electrode preparation**

#### **3.4.1 Preparation of solution for G/PANI modified electrode**

##### **3.4.1.1 Graphene suspension**

Graphene solution was prepared by dispersing graphene powder 20 mg into DMF 10 mL. The graphene solution was sonicated by ultrasonic bath and left over night to dissolve graphene to form homogeneous solution as shown in Figure 3.1



**Figure 3.1** Homogeneous graphene (G) solution

### 3.4.1.2 Polyaniline solution

To prepare polyaniline solution, sulfonic acid was used as doping agents for achieving conductivity of polyaniline. Polyaniline solution was simply prepared by mixing 100 mg of polyaniline and 129 mg of sulfonic acid by using mortar and pestle and after that transferred the mixture into 15 mL of chloroform solution. Then, the solution was stirred with magnetic bar for 2 hour. Finally, polyaniline solution was filtered through a 0.45  $\mu\text{m}$  Nylon membrane filter. The solution of polyaniline showed a dark green color as presented in Figure 3.2



**Figure 3.2** Homogeneous polyaniline (PANI) solution

### **3.4.1.3 Preparation of G/PANI solution**

The solution with ratio of 1:1 between graphene and polyaniline composites was used for modified solution. G/PANI solution was prepared by pipetting 0.5 mL (500  $\mu$ L) of graphene solution and 0.5 mL (500  $\mu$ L) of polyaniline solution in appropriate portion of the ratio of 1:1, after that the G/PANI solution was sprayed on screen-printed carbon electrode by using electrospray technique.

### **3.4.2 Preparation of screen-printed carbon electrode**

A screen-printed carbon electrode was prepared by in-house screen-printing technique. Firstly, 2 g of silver/silver chloride ink was printed onto the PVC substrate to create the conducting part on the electrode, and the electrode was then dried in an oven at 55°C for 1 hour. Next, 2 g of carbon ink was dissolved in binder solution 3 mL to form suitable portion of carbon ink for screening step. After that, carbon ink was printed over some parts of conducting silver/silver chloride to achieve the screen-printed carbon electrode. Finally, the electrode was dried in an oven at 55°C for 1 hour. The procedure steps for screen-printed electrode preparation are shown schematically in Figure 3.3 and 3.4, respectively.

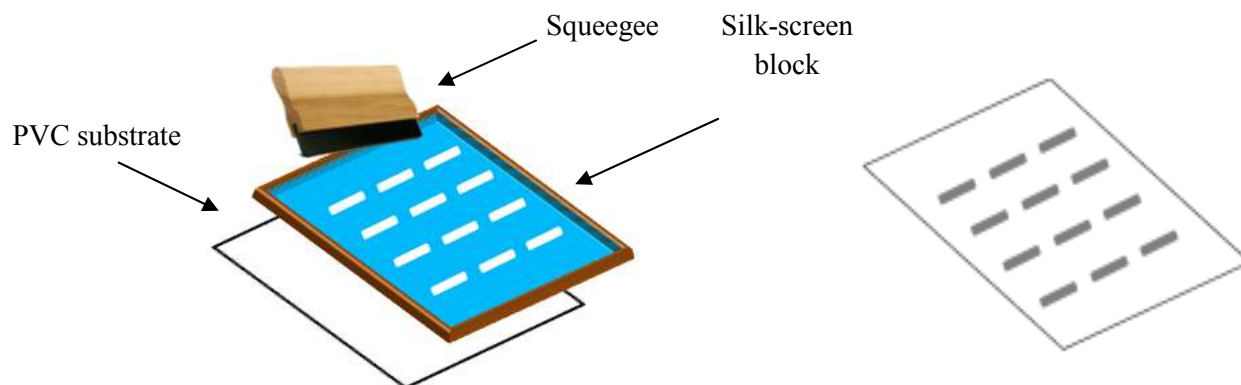


**Figure 3.3** (Step I) In-house screen-printing technique for conductive pad

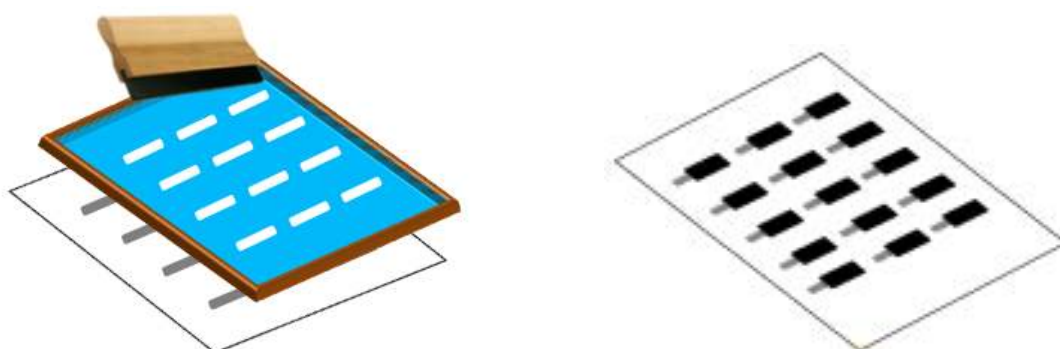


**Figure 3.4** (Step II) In-house screen-printing technique for screen-printing carbon electrode

### 3.4.3 Preparation of G/PANI-modified electrode

G/PANI modified electrode was fabricated by using electrospray technique as shown in Figure 3.5. The solution of G/PANI (1:1) nanocomposites was sprayed with high voltage on the screen-printed carbon electrode. First, the homogeneous solution between of graphene and polyaniline was filled into the needle with a diameter of 0.45 mm. Next, placed the screen-printed carbon electrode to the ground collector with distance between the needle and ground collector is 5 cm. The spraying time at 5 minute and applied voltage at 10 KV were used for sprayed the G/PANI (1:1) solution onto the screen-printed carbon electrode surface. Finally, the surface morphology of G/PANI modified electrode was characterized by scanning electron microscope (SEM).

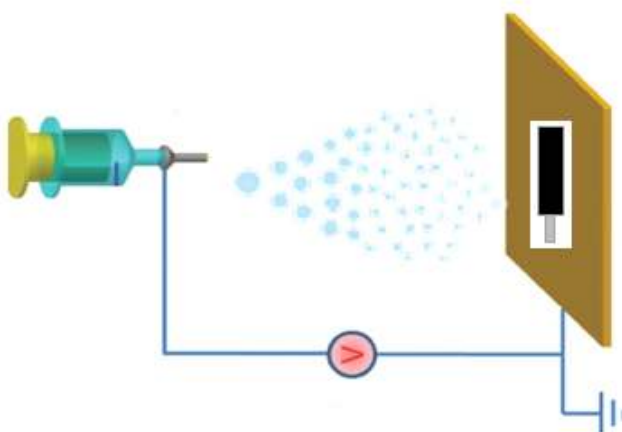


**Figure 3.5** Schematic diagram of electrospray technique for preparation of G/PANI modified electrode

### **3.5 Procedure**

#### **3.5.1 Cyclic voltammetry study**

To characterize of the electrode, the electrochemical behavior of the electrode was investigated by using Autolab Potentiostat100. The single compartment electrode glass cell consists of three electrodes with the volume of 3 mL. The working electrode was pressed against a smooth ground joint at the bottom of the cell and isolated by placing the backside of the substrate onto a brass plate. Ag/AgCl electrode with salt bridge was used as reference electrode, and counter electrode was a platinum wire. The electrochemical equipment was housed in a faradaic cage to reduce electronic noise.

##### **3.5.1.1 Electrochemical investigation of G/PANI modified electrode**

To study the electrochemical behavior of G/PANI-modified electrode, the mixture solution of 1 mM  $K_3Fe(CN)_6$  and  $K_4Fe(CN)_6$  was used for first investigation. The solution of 0.1 M KCl was used as supporting electrolyte, and the scan rate was  $100 \text{ mV s}^{-1}$ . The results obtained from cyclic voltammograms of G/PANI modified electrode as working electrode.

##### **3.5.1.2 Study the mass transfer process of G/PANI modified electrode**

To study the mass transfer process of G/PANI modified electrode, the square root of scan rate and the current were plotted. The effect of the scan rate on the electrochemical behavior of  $K_3Fe(CN)_6$  and  $K_4Fe(CN)_6$  was investigated by variation of scan rate using cyclic voltammetry. The solution of 0.1 M KCl was used as supporting electrolyte. The potential was scan in the range of -0.5 to 1.0 V at the scan rate of 10, 20, 50, 100 and  $200 \text{ mV s}^{-1}$ , respectively.



### **3.5.1.3 Comparison between G/PANI-modified electrode and unmodified electrode**

In order to test the electrochemical potential of the modified electrode, the electrochemical behavior of G/PANI-modified electrode was characterized by cyclic voltammetry of  $50 \mu\text{g mL}^{-1}$  eight SAs compared to an unmodified carbon electrode by using 0.05 M phosphate buffer solution (pH 3) as supporting electrolyte. The scan rate was  $100 \text{ mV s}^{-1}$  at the potential range was 0.7 to 1.5 V.

### **3.5.1.4 Comparison between G/PANI modified electrode and BDD electrode**

The boron doped diamond (BDD) electrode was used for determination of sulfonamide previously because this electrode performed an excellent sensitivity for sulfonamides detection, but the cost of material was very expensive. To examine the performance of the G/PANI modified electrode, BDD was also used as working electrode for characterization of eight SAs at same condition as unmodified electrodes. The results from cyclic voltammograms of eight SAs at the concentration of  $50 \mu\text{g mL}^{-1}$  used as testing solution for both electrodes were compared.

### **3.5.2 Ultra-fast liquid chromatography coupled with electrochemical detection**

#### **3.5.2.1 The effect of detection potential**

Hydrodynamic voltammetry was applied to obtain the optimal potential in amperometric detection. The mixture of SG, SDZ, SMZ, SMM, SDX, SMX, SSZ and SDM at the concentration  $10 \mu\text{g mL}^{-1}$  was prepared for study the effect of detection potential in amperometric detection of UFLC-ECD system with flow rate of  $1.5 \text{ mL min}^{-1}$ . The effect of detection potential for all eight SAs was obtained by changing the detection potential in the range of 1.1 V to 1.5 V vs. Ag/AgCl. The data was obtained by recording the current at each potential.

#### **3.5.2.2 The effect of pH**

In this work mobile phase consisted of phosphate buffer solution, acetonitrile and ethanol. To study the effect of pH on the separation of eight SAs, phosphate buffer solution was prepared at pH 3, 4, 5, 6 and 7, respectively. The mixture of organic solvent between acetonitrile and ethanol was also used as mobile phase to improve retention time of the separation. These experiments were performed to obtain the optimal pH for eight SAs detection.

#### **3.5.2.3 Optimal flow rate of mobile phase**

To study the effect on the separation of eight SAs, the flow rate of the mobile phase for carrying eight SAs to electrochemical flow cell was studied in the range of  $0.5 - 2.0 \text{ mL min}^{-1}$ . The eight SAs were prepared at the concentration of  $10 \mu\text{g mL}^{-1}$ . The retention time of mixture compounds was measured for each flow rate to obtain the suitable flow rate of UFLC-ECD system.

### 3.5.2.4 Optimal condition for UFLC-ECD system

UFLC-ECD using G/PANI-modified screen-printed carbon electrode as a working electrode was performed for determination of eight sulfonamides (SG, SDZ, SMZ, SMM, SDX, SMX, SSZ and SDM). To acquire optimum condition for the separation of these compounds, the suitable conditions as shown in Table 3.4 were applied for separation of  $10 \mu\text{g mL}^{-1}$  eight SAs as standard solution.

**Table 3.4** Conditions parameters of UFLC-ECD system for the detection of eight SAs

Parameters	Optimal conditions
Column	Inertsil C4 (150 x 4.6 mm)
Mobile phase	Potassium hydrogen phosphate (pH3): ACN: EtOH (75:25:5, v/v/v)
Flow rate	$1.5 \text{ mL min}^{-1}$
Injection volume	$25 \mu\text{L}$
Temperature	$25^\circ \text{C}$
Detector	Amperometric detection at 1.4 V vs.Ag/AgCl

### 3.6 Analytical performance

The analytical performance of UFLC-ECD system including linearity, accuracy and precision, limit of detection (LOD) and limit of quantification (LOQ) were studied for assessment the quality of analytical methods.

#### 3.6.1 Linearity

Linearity was established by measuring between current and concentration of eight SAs. The standard solution of eight SAs was prepared in the concentration range of 0.1 – 100  $\mu\text{g mL}^{-1}$  by diluting from stock solution (1000  $\mu\text{g mL}^{-1}$ ). The linearity was obtained from injection of repeated 3 times of each concentration with the optimal conditions. After that, the correlation coefficients of the linearity were investigated by evaluating from the response signal that should be directly proportional to the concentrations of the SAs.

#### 3.6.2 Accuracy and precision

To examine the reliability of the system, precision and accuracy of analytical procedure were investigated. The intra and inter-day recovery of this novel UFLC-ECD system was assessed to obtain the accuracy from calculating the percent recovery (% recovery) between percentage of the measured spiked SAs in matrix sample, relating to the amount of spiked SAs to sample at level of 3, 5 and 9  $\mu\text{g mL}^{-1}$ , respectively.

The equation is showed below,

$$\% \text{ recovery} = \frac{\text{Spike}_{\text{matrix}}}{\text{Spike}_{\text{blank}}} \times 100$$

The inter and intra-day precision is evaluated from calculated relative standard deviation or % RSD. The spiked concentration at 3, 5 and 9  $\mu\text{g mL}^{-1}$  was investigated for estimate repeatability and reproducibility of the proposed method.

The equation is showed below,

$$\%RSD = \frac{\text{standard deviation}}{\text{Mean}} \times 100$$

To accept the precision of this system, %RSD value of the developed method should be less than %RSD of the AOAC International recommended value.

### **3.6.3 Limit of detection (LOD) and Limit of quantification (LOQ)**

The limit of detection (LOD) and limit of quantification (LOQ) were calculated from the equation;  $LOD = 3S_B/b$  and  $LOQ = 10S_B/b$ , when  $S_B$  was the standard deviation of the mean value for 10 signals of the blank, and  $b$  was the slope of the straight line in the linearity curve.

#### **3.6.4 Comparison of the novel system UFLC-ECD and standard method**

To validate the developed method of UFLC-ECD using G/PANI modified electrode, the result from this novel system was compared to standard method which is UFLC coupled with ultraviolet detection. To investigate a reliability of the system, standard addition method was also used to determine the amount of SAs in real sample. A paired t-test at 95% confidence interval was performed on the results obtained from three spiked sample with different concentrations (blank shrimp, spiked shrimp at  $3\mu\text{g mL}^{-1}$  and spiked shrimp at  $5\mu\text{g mL}^{-1}$ ). The  $t_{\text{calculated}}$  was calculated for comparison with  $t_{\text{critical}}$  for data analysis between the two methods.

## **CHAPTER IV**

### **RESULTS AND DISCUSSION**

This chapter demonstrated the results that obtained from method development for the determination of SAs using UFLC-ECD coupled with G/PANI-modified screen-printed carbon electrode. The results were investigated by cyclic voltammetry and UFLC-ECD, respectively. The suitable parameters of the method including potential of amperometric detection, pH of running buffer, flow rate of the mobile phase and condition of the separation were studied. Finally the G/PANI modified screen-printed carbon electrode was applied for the determination of sulfonamide in real sample.

#### **4.1 Characterization of G/PANI modified electrode**

##### **4.1.1 Surface morphology of G/PANI modified electrode**

G/PANI modified screen-printed carbon electrode was fabricated by using electrospray technique. The composite of graphene and polyaniline was used as modified material on a carbon electrode. To prevent agglomeration of graphene, polyaniline was applied for modification of the electrode. Polyaniline was a conducting polymer improving the spreading of graphene sheet on the electrode surface. Under the suitable condition, the solution of G/PANI (1:1) was electrosprayed with high voltage on electrode surface to achieve the electrode modification. To ensure the distribution of graphene and polyaniline on the electrode surface, the surface morphology of modified electrode was characterized by scanning electron microscopy (SEM). The image of SEM shows in Figure 4.1. The results indicated that the modified electrode provided homogeneous and well distribution of graphene and polyaniline as nanocomposite on the electrode surface. Therefore,

electrospraying technique of G/PANI nanocomposite was successfully applied for the modification of electrode surface with ease to set up and low cost operation.

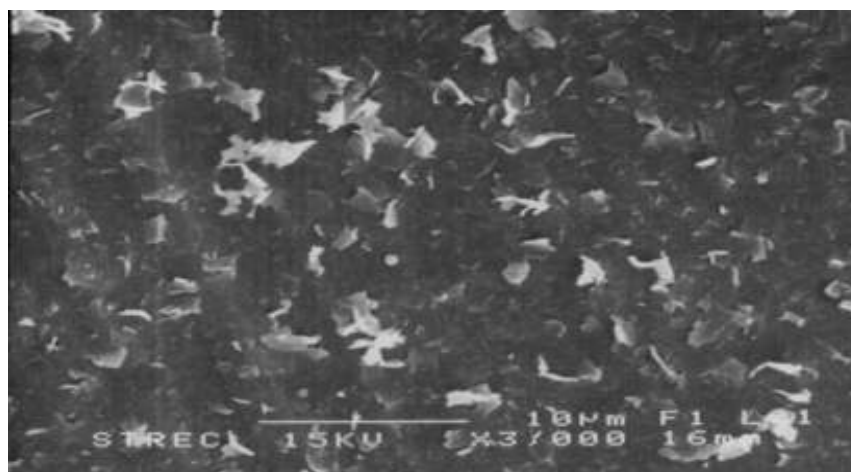


**Figure 4.1** SEM images of G/PANI (1:1) nanocomposite. Condition: No. needle; No.24 ( $\varnothing$  0.45), voltage; 10 kV, time; 5 min



#### 4.1.2 Electrochemical behavior of G/PANI modified electrode

The cyclic voltammetry was used to study the electrochemical behavior of the G/PANI modified screen-printed carbon electrode. The electrochemical redox response of 1mM  $K_3Fe(CN)_6$  and  $K_4Fe(CN)_6$  in 0.1 M KCl solution was firstly investigated. The cyclic voltammogram of  $K_3Fe(CN)_6$  and  $K_4Fe(CN)_6$  at G/PANI modified screen-printed carbon electrode was compared to an unmodified carbon electrode in the potential range of -0.5 to 1.0 V are shown in Figure 4.2. The cyclic voltammogram on G/PANI modified screen-printed carbon electrode exhibited well-defined pair of oxidation-reduction peak, and provided high current response of anodic current ( $i_{pa}$ ) and cathodic current ( $i_{pc}$ ) compared to current obtained from unmodified carbon electrode. The oxidation peaks on the G/PANI modified screen-printed carbon electrode and unmodified electrode were observed at approximately 0.3 and 0.5 V. vs. Ag/AgCl, respectively. While the reduction peaks were observed at approximately 0.2 and 0.0 V. vs. Ag/AgCl, respectively. Moreover, G/PANI modified screen-printed carbon electrode demonstrated small  $\Delta E_p$  compared to  $\Delta E_p$  obtained from unmodified carbon electrode. Therefore, G/PANI modified screen-printed carbon electrode shows an excellent electrochemical redox behavior. For this reason, G/PANI modified screen-printed carbon electrode was chosen as new working electrode for applying to the determination of sulfonamides.

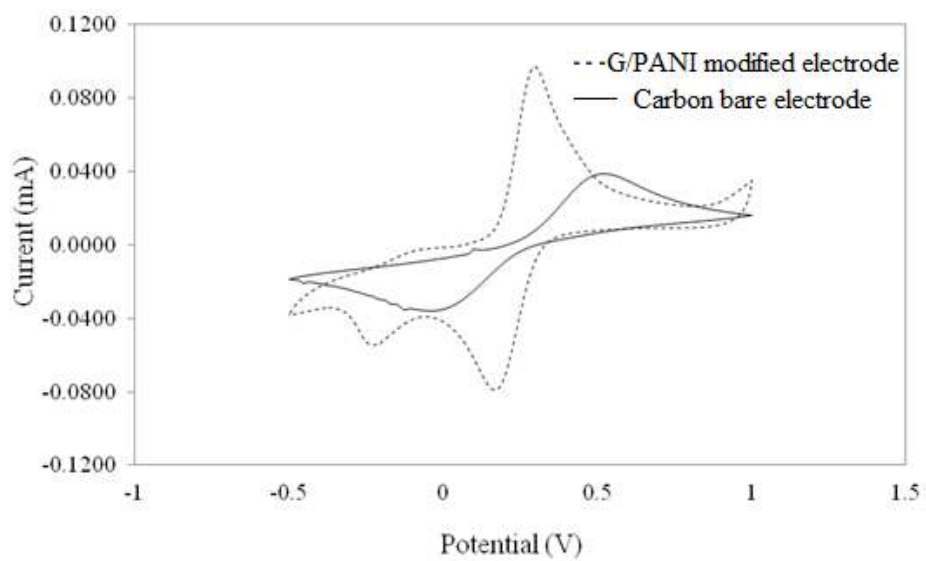


**Figure 4.2** Cyclic voltammograms of 1 mM  $[\text{Fe}(\text{CN})_6]^{3-} / [\text{Fe}(\text{CN})_6]^{4-}$  for (---) G/PANI- modified carbon electrode and (—) carbon bare electrode vs. Ag/AgCl with scan rate of  $100 \text{ mV s}^{-1}$

### 4.1.3 The mass transfer process at G/PANI modified electrode

Cyclic voltammetry was used to study the electron transfer process of 1 mM  $K_3Fe(CN)_6$  and  $K_4Fe(CN)_6$  in 0.1 M KCl solution. The effect of scan rate in the range of 10 to 200  $mV s^{-1}$  on the electrochemical behaviors of  $K_3Fe(CN)_6$  and  $K_4Fe(CN)_6$  was investigated. The cyclic voltammograms of  $K_3Fe(CN)_6$  and  $K_4Fe(CN)_6$  were shown in Figure 4.3. From the Randles-Sevcik equation as shown in the equation below, the peak current was directly proportional to the square root of the scan rate. Current obtained at G/PANI-modified electrode is from diffusion-controlled process following equation 11.

$$I_p(\text{diffusion}) = (2.686 \times 10^5)n^{3/2}ACD^{1/2}\nu^{1/2} \dots\dots\dots(11)$$

Where

$i_p$  = peak current, A

$n$  = electron stoichiometry

$A$  = electrode area,  $cm^2$

$D$  = diffusion coefficient,  $cm^2 s^{-1}$

$C$  = concentration,  $mol/cm^3$

$\nu$  = scan rate,  $V s^{-1}$

In Figure 4.4, the plot between the current and the square root of the scan rates was studied. The linear relationship between the  $i_{pa}$  and the square root of the scan rate was also observed with the correlation coefficient of 0.9947. The linear relationship between the  $i_{pc}$  and the square root of the scan rate was also observed with the correlation coefficient of 0.9942. It can be seen that the current response directly proportional to the square root of the scan rate as mentioned above hence, the diffusion controlled process occurred at the electrode surface.

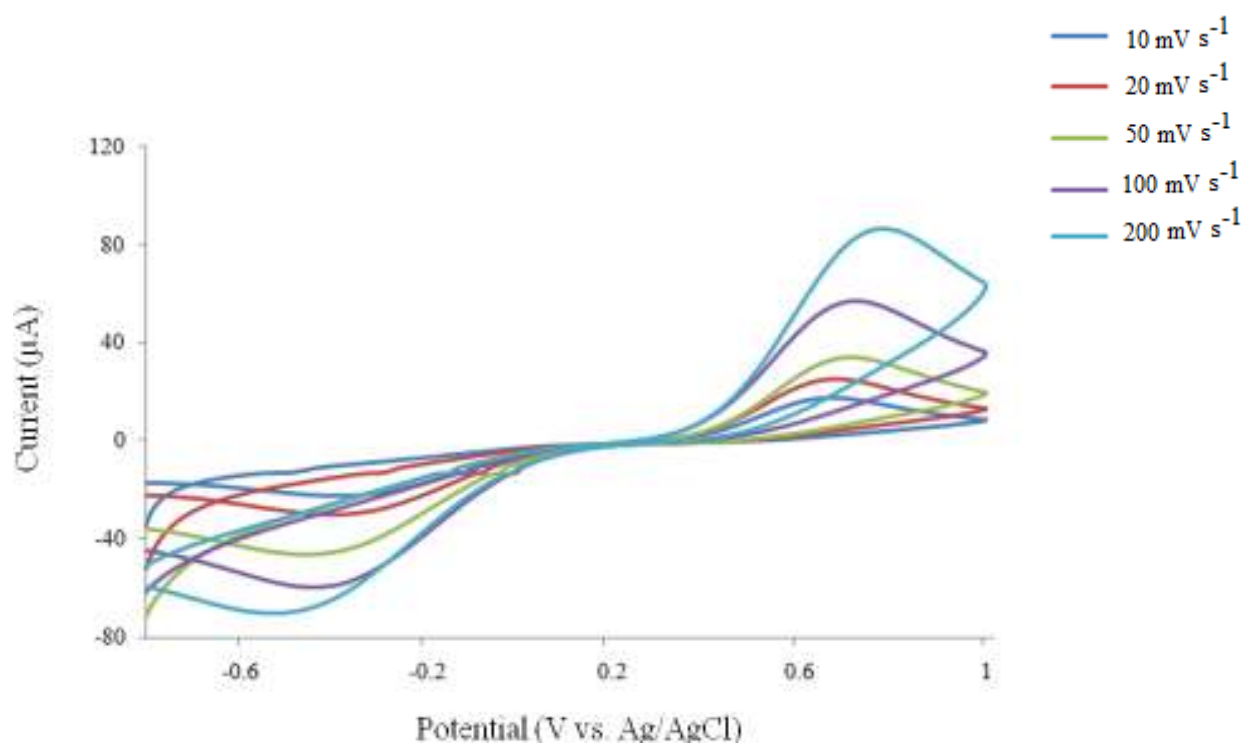


**Figure 4.3** Cyclic voltammograms of 0.1 mM  $[\text{Fe}(\text{CN})_6]^{3-}$  and  $[\text{Fe}(\text{CN})_6]^{4-}$  for G/PANI-modified carbon electrode vs. Ag/AgCl with scan rate of 10, 20, 50, 100 and 200  $\text{mV s}^{-1}$ .

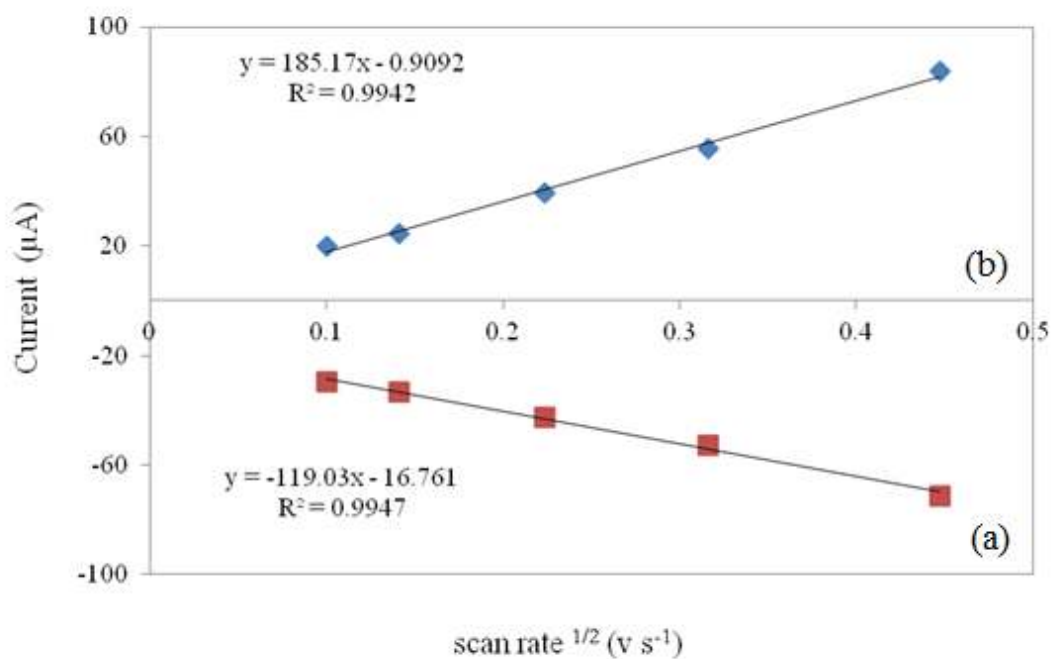


**Figure 4.4** The relationship between anodic current;  $i_{ac}$  (a) and cathodic current;  $i_{pc}$  (b) versus scan rate $^{1/2}$  of 0.1mM  $[Fe(CN)_6]^{3-}/[Fe(CN)_6]^{4-}$  in 0.1 M KCl solution.

## **4.2 Cyclic voltammetry investigated for the determination of eight SAs**

### **4.2.1 Cyclic voltammetry of eight SAs on G/PANI modified electrode compared to unmodified electrode**

Cyclic voltammetry was used to investigate all of eight SAs by using G/PANI modified screen-printed carbon electrode comparing to unmodified electrode. The comparison of the cyclic voltammetric result of  $50 \mu\text{g mL}^{-1}$  SMM, SDM, SG, SDX, SMX, SSZ, SDZ and SMZ are shown in Figure 4.5, 4.6, 4.7, 4.8, 4.9, 4.10, 4.11 and 4.12, respectively.  $i_{\text{pa}}$  of all eight SAs exhibited a well-defined irreversible oxidation peak at 1.2 V vs. Ag/AgCl, approximately. The anodic peak current obtained from G/PANI modified screen-printed carbon electrode is much higher significantly than the one from unmodified electrode for all SAs because the nanocomposites of G/PANI can obviously promotes the sensitivity of electrochemical reaction. Therefore, G/PANI modified screen-printed carbon electrode showed the excellent performance for detecting eight SAs.

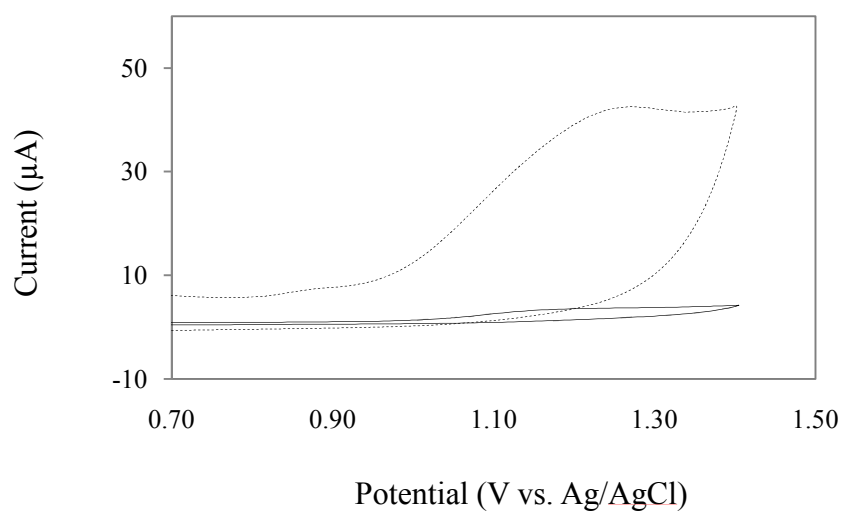


**Figure 4.5** Cyclic voltammograms for (---) G/PANI-modified carbon electrode and (—) bare carbon vs. Ag/AgCl in  $50 \mu\text{g mL}^{-1}$  SMM, 0.1 M phosphate solution pH 3.0 with scan rate  $100 \text{ mV s}^{-1}$ .

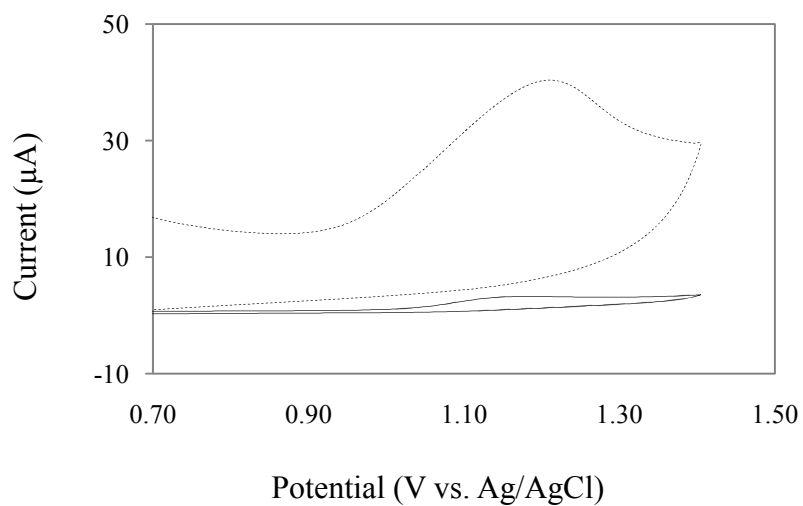


**Figure 4.6** Cyclic voltammograms for (---) G/PANI-modified carbon electrode and (—) bare carbon vs. Ag/AgCl in  $50 \mu\text{g mL}^{-1}$  SDM, 0.1 M phosphate solution pH 3.0 with scan rate  $100 \text{ mV s}^{-1}$ .

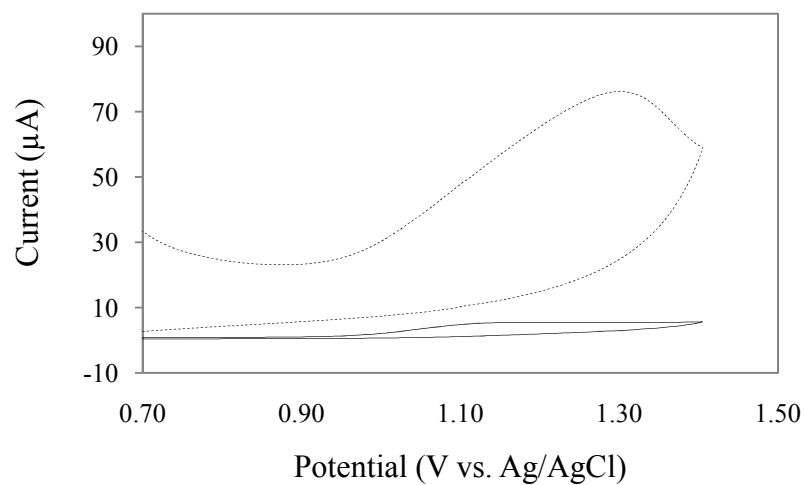


**Figure 4.7** Cyclic voltammograms for (---) G/PANI-modified carbon electrode and (—) bare carbon vs. Ag/AgCl in  $50 \mu\text{g mL}^{-1}$  SG, 0.1 M phosphate solution pH 3.0 with scan rate  $100 \text{ mV s}^{-1}$ .

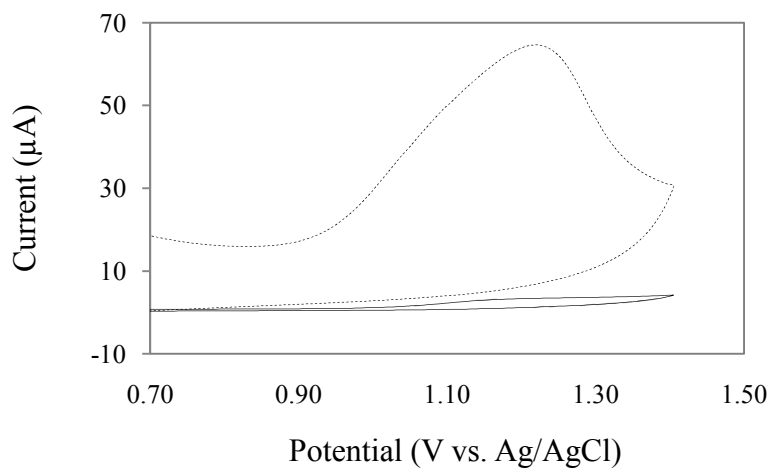


**Figure 4.8** Cyclic voltammograms for (---) G/PANI-modified carbon electrode and (—) bare carbon vs. Ag/AgCl in  $50 \mu\text{g mL}^{-1}$  SDX, 0.1 M phosphate solution pH 3.0 with scan rate  $100 \text{ mV s}^{-1}$ .



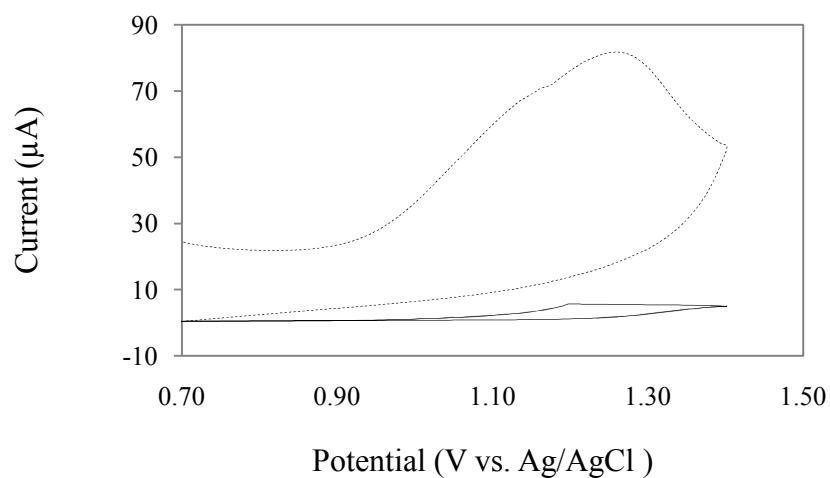


**Figure 4.9** Cyclic voltammograms for (---) G/PANI-modified carbon electrode and (—) bare carbon vs. Ag/AgCl in  $50 \mu\text{g mL}^{-1}$  SMX, 0.1 M phosphate solution pH 3.0 with scan rate  $100 \text{ mV s}^{-1}$ .

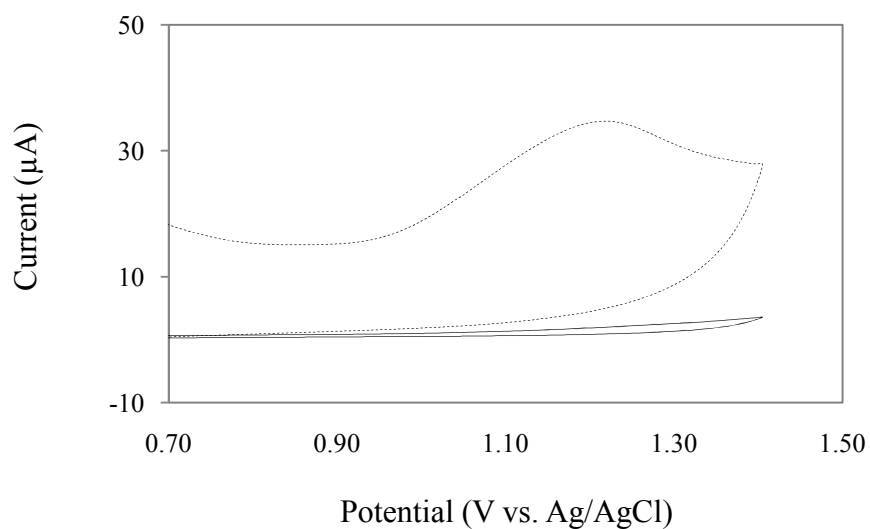


**Figure 4.10** Cyclic voltammograms for (---) G/PANI-modified carbon electrode and (—) bare carbon vs. Ag/AgCl in  $50 \mu\text{g mL}^{-1}$  SSZ, 0.1 M phosphate solution pH 3.0 with scan rate  $100 \text{ mV s}^{-1}$ .

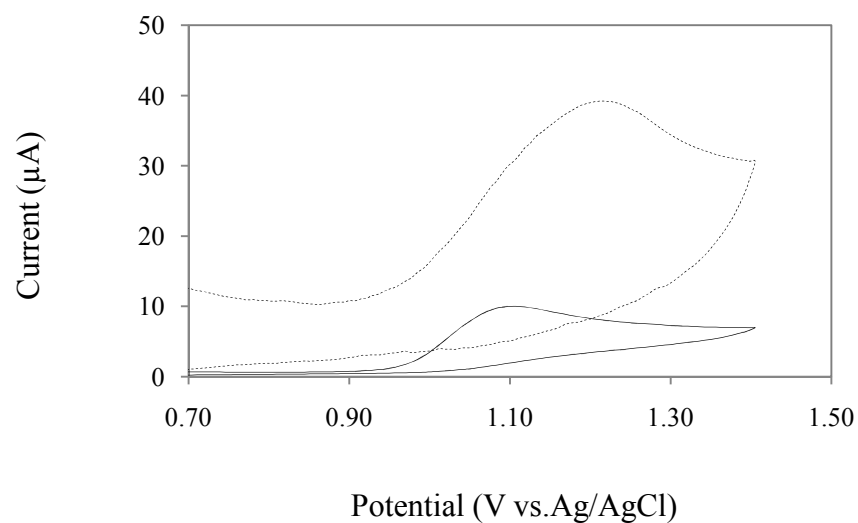


**Figure 4.11** Cyclic voltammograms for (---) G/PANI-modified carbon electrode and (—) bare carbon vs. Ag/AgCl in  $50 \mu\text{g mL}^{-1}$  SDZ, 0.1 M phosphate solution pH 3.0 with scan rate  $100 \text{ mV s}^{-1}$ .

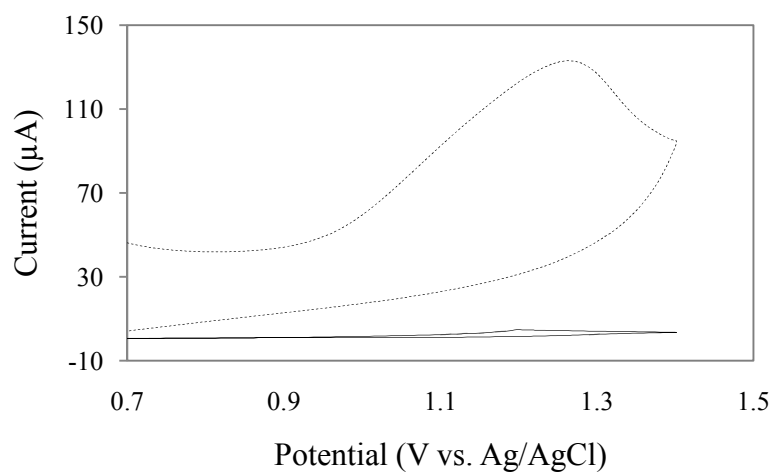


**Figure 4.12** Cyclic voltammograms for (---) G/PANI-modified carbon electrode and (—) bare carbon vs. Ag/AgCl in  $50 \mu\text{g mL}^{-1}$  SMZ, 0.1 M phosphate solution pH 3.0 with scan rate  $100 \text{ mVs}^{-1}$ .

#### **4.2.2 Cyclic voltammetry of eight SAs on G/PANI modified electrode compared to boron doped diamond electrode**

To compare the performance between the G/PANI modified screen-printed carbon electrode and boron-doped diamond electrode, the cyclic voltammograms of  $50 \mu\text{g mL}^{-1}$  SDZ, SMZ, SG, SSZ, SDM, SMM, SDX, and SMX in 0.1 M phosphate buffer solution pH 3 with the scan rate  $100 \text{ mV s}^{-1}$  have been investigated. The cyclic voltammograms of eight SAs was performed by G/PANI modified screen-printed carbon electrode and boron-doped diamond electrode are shown in Figure 4.13, 4.14, 4.15, 4.16, 4.17, 4.18, 4.19 and 4.20, respectively. The results showed that, G/PANI modified screen-printed carbon electrode provided the excellent sensitivity of eight SAs detection which was better than boron-doped diamond electrode. This can be concluded that graphene and polyaniline as nanocomposites on the electrode surface is successfully modified on screen-printed carbon electrode. G/PANI-modified electrode can improve the electrochemical detection for determination of SAs in the UFLC system compared to the expensive boron-doped diamond as a working electrode. Nonetheless, low cost G/PANI-modified electrode fabricated by in-house screen-printing techniques and electrospraying, respectively, provided high electrical conductivity, high mechanical strength and high sensitivity for determination of SAs.

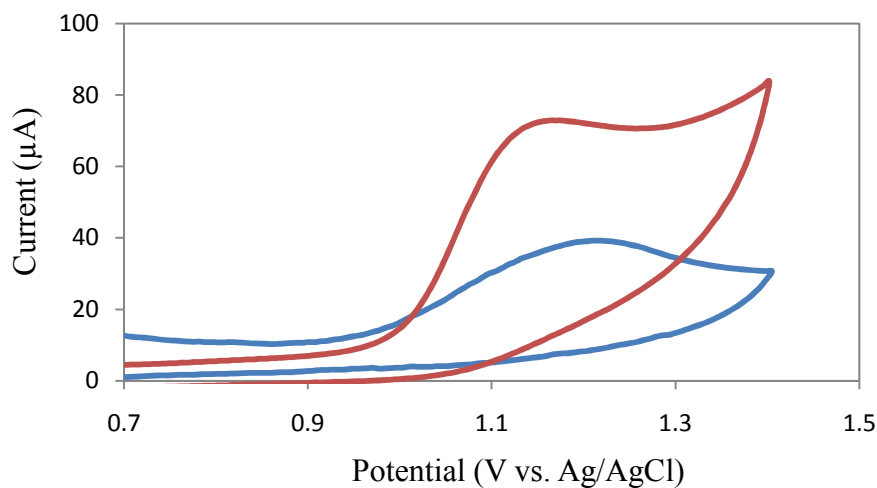


**Figure 4.13** Cyclic voltammograms for (—) G/PANI-modified carbon electrode and ( — ) boron-doped diamond electrode vs. Ag/AgCl in  $50 \mu\text{g mL}^{-1}$  SDZ, 0.1 M phosphate buffer solution pH 3.0 with scan rate  $100 \text{ mV s}^{-1}$ .

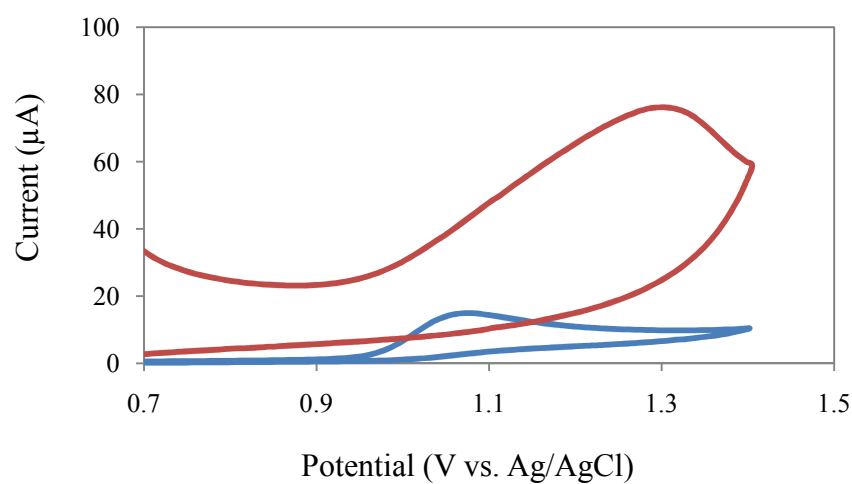


**Figure 4.14** Cyclic voltammograms for (—) G/PANI-modified carbon electrode and ( — ) boron-doped diamond electrode vs. Ag/AgCl in  $50 \mu\text{g mL}^{-1}$  SG, 0.1 M phosphate buffer solution pH 3.0 with scan rate  $100 \text{ mV s}^{-1}$ .

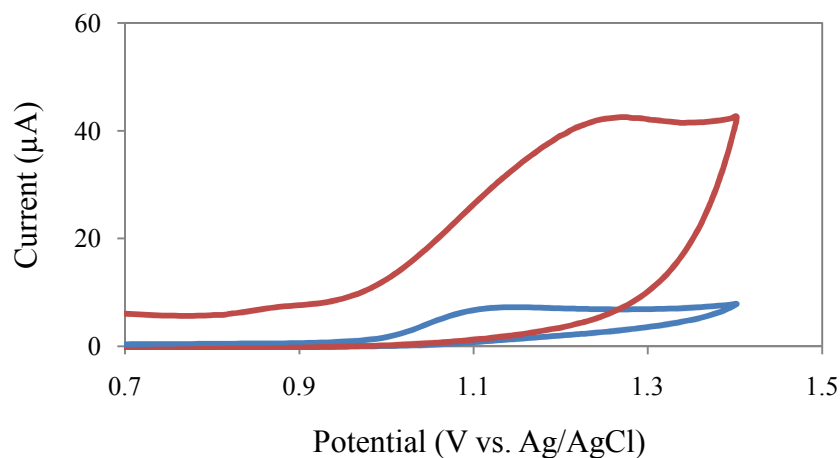


**Figure 4.15** Cyclic voltammograms for (—) G/PANI-modified carbon electrode and (—) boron-doped diamond electrode vs. Ag/AgCl in  $50 \mu\text{g mL}^{-1}$  SMM, 0.1 M phosphate buffer solution pH 3.0 with scan rate  $100 \text{ mV s}^{-1}$ .

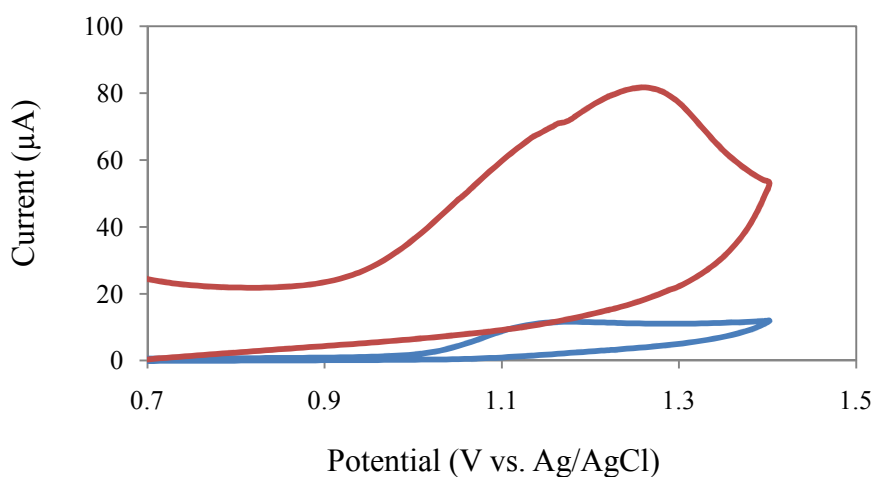


**Figure 4.16** Cyclic voltammograms for (—) G/PANI-modified carbon electrode and (—) boron-doped diamond electrode vs. Ag/AgCl in  $50 \mu\text{g mL}^{-1}$  SMX, 0.1 M phosphate buffer solution pH 3.0 with scan rate  $100 \text{ mV s}^{-1}$ .

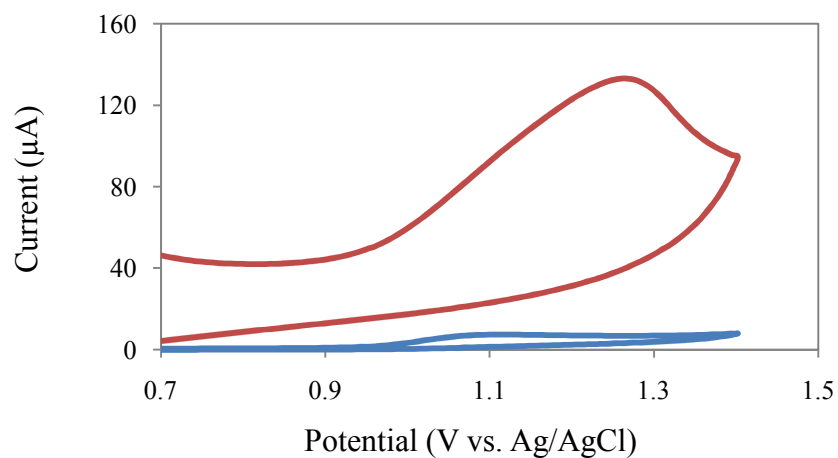


**Figure 4.17** Cyclic voltammograms for (—) G/PANI-modified carbon electrode and (—) boron-doped diamond electrode vs. Ag/AgCl in  $50 \mu\text{g mL}^{-1}$  SMZ, 0.1 M phosphate buffer solution pH 3.0 with scan rate  $100 \text{ mV s}^{-1}$ .

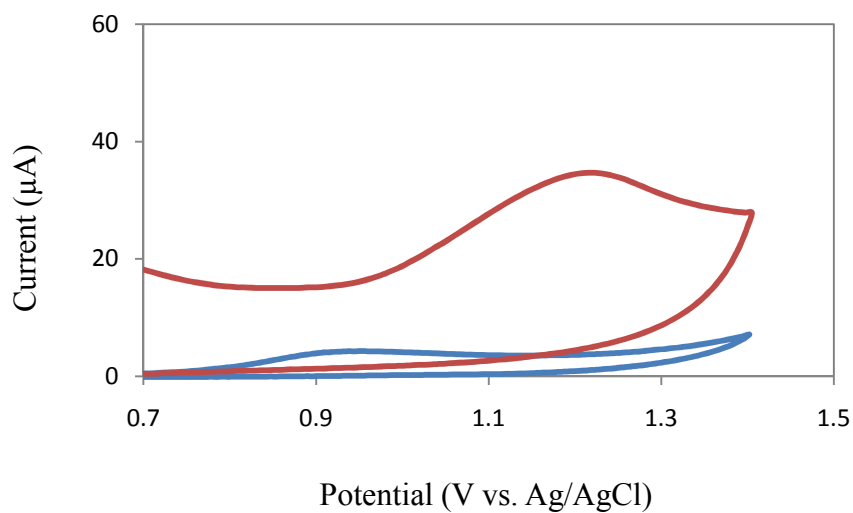


**Figure 4.18** Cyclic voltammograms for (—) G/PANI-modified carbon electrode and (—) boron-doped diamond electrode vs. Ag/AgCl in  $50 \mu\text{g mL}^{-1}$  SSZ, 0.1 M phosphate buffer solution pH 3.0 with scan rate  $100 \text{ mV s}^{-1}$ .

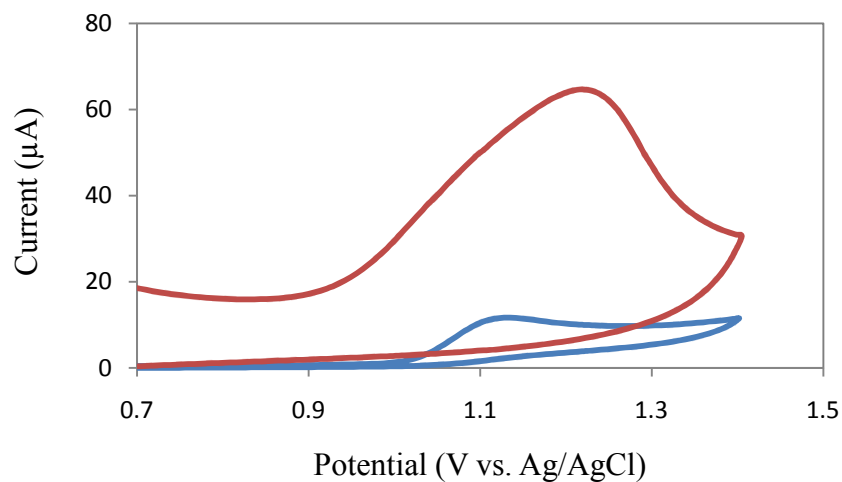


**Figure 4.19** Cyclic voltammograms for (—) G/PANI-modified carbon electrode and ( — ) boron-doped diamond electrode vs. Ag/AgCl in  $50 \mu\text{g mL}^{-1}$  SDX, 0.1 M phosphate buffer solution pH 3.0 with scan rate  $100 \text{ mV s}^{-1}$ .

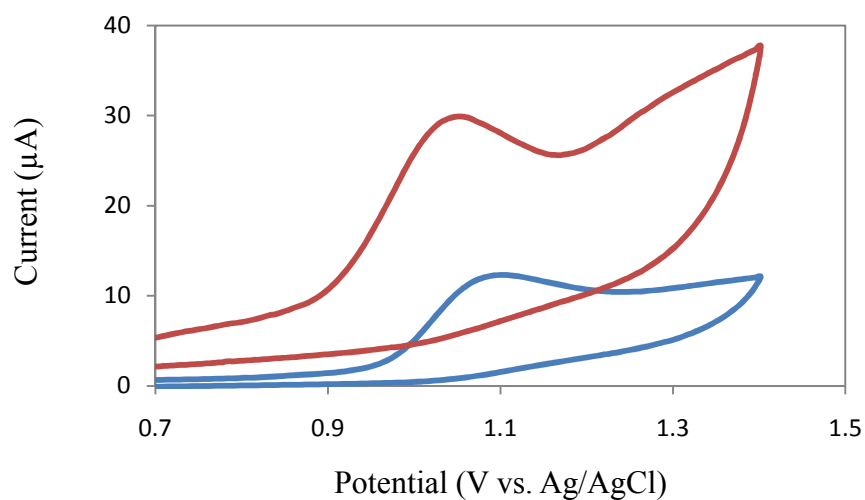


**Figure 4.20** Cyclic voltammograms for (—) G/PANI-modified carbon electrode and ( — ) boron-doped diamond electrode vs. Ag/AgCl in  $50 \mu\text{g mL}^{-1}$  SDM, 0.1 M phosphate buffer solution pH 3.0 with scan rate  $100 \text{ mV s}^{-1}$ .

### **4.3 Optimal conditions of UFLC-ECD**

#### **4.3.1 Optimization of the detection potential for SAs**

Hydrodynamic voltammetry was used to obtain the optimum potential in amperometric detection. The effect of detection potential for all eight SAs was studied by changing the detection potential in the range of 1.1 V to 1.5 V vs. Ag/AgCl. Figure 4.21 shows the hydrodynamic voltammetric *i*-E curve of eight SAs. The  $i_{pa}$  of all eight SAs increased when the detection potentials were increased until the detection potential of 1.4 V vs. Ag/AgCl. After that, the anodic current decreased. To obtain the high sensitivity of SAs detection on G/PANI modified screen-printed carbon electrode, the detection potential of 1.4 V vs. Ag/AgCl was chosen as optimal potential value for amperometric detection.



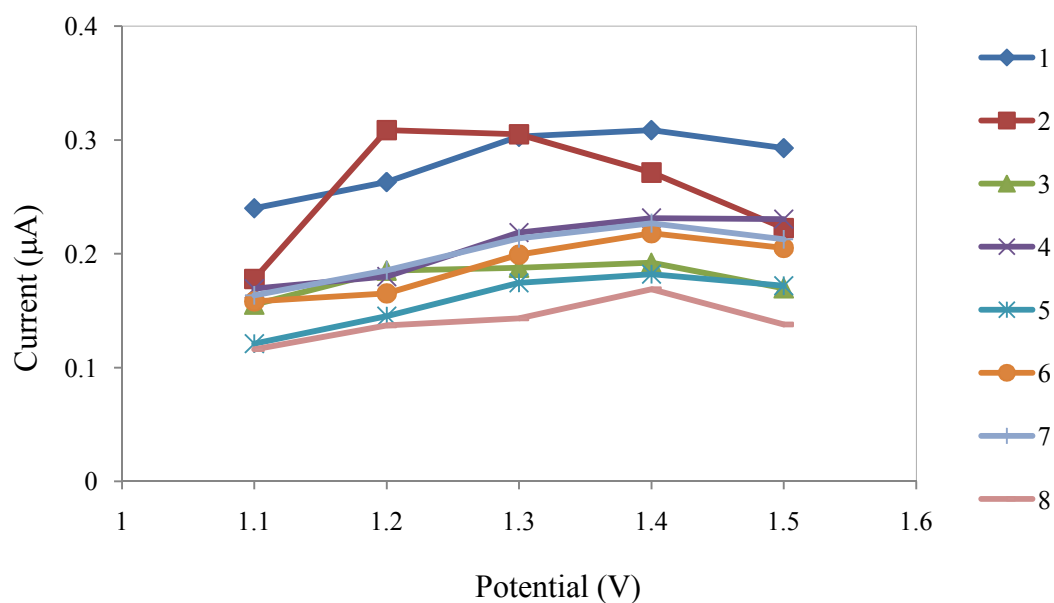


**Figure 4.21** Hydrodynamic voltammetric results using our proposed UFLC-ECD system for  $10 \mu\text{g mL}^{-1}$  of mixture of eight standard SAs (1) SG (2) SDZ (3) SMZ (4) SMM (5) SDX (6) SMX (7) SSZ (8) SDM at a flow rate of  $1.5 \text{ mLmin}^{-1}$ . The detection potential at 1.1 – 1.5 V vs. Ag/AgCl using G/PANI modified screen-printed carbon electrode.

### 4.3.2 The effect of pH

The effect of pH on the separation of sulfonamides by using UFLC coupled with amperometric detection was studied. The pH of supporting electrolyte was affected to the electrochemical oxidation of eight sulfonamides on G/PANI modified screen printed carbon electrode. Phosphate buffer solution with a different pH was used as the supporting electrolyte. To optimize the suitable pH of phosphate buffer solution, the pH was varied in the range of 3 to 7. The Figure 4.22, 4.23, 4.24, 4.25 and 4.26 show the chromatograms of eight sulfonamides with the different pH of potassium buffer solutions as the mobile phase for UFLC coupled with amperometric detection. From the results indicated that at pH 3 showed the best separation of eight sulfonamides. Increasing of pH provided the overlap of the peak because the higher pH has the effect to the structure of the sulfonamides. Due to the change of sulfonamide structure the overlap of the peak can occur at pH 4, 5, 6 and 7. From these results, pH 3 was selected as optimal pH value for the separation of eight sulfonamides by using UFLC couple with amperometric detection.

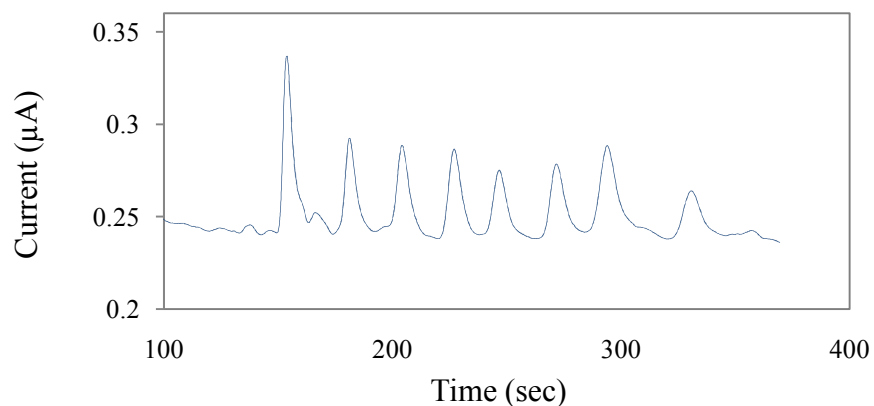


**Figure 4.22** UFLC-ECD chromatogram of eight SAs  $10 \mu\text{g mL}^{-1}$  at flow rate of  $1.5 \text{ mL min}^{-1}$  with 70:25:5(v/v/v) of potassium phosphate solution (pH 3): acetonitrile: ethanol as the mobile phase. The detection potential was 1.4 V vs. Ag/AgCl using G/PANI modified screen-printed carbon electrode.

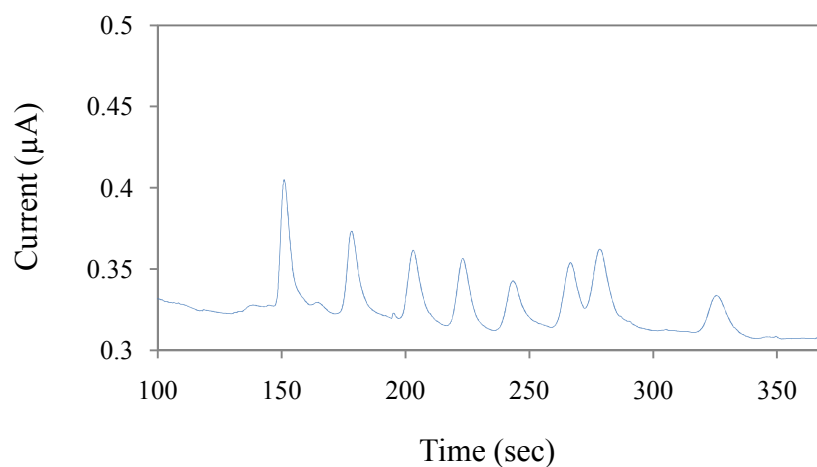


**Figure 4.23** UFLC-ECD chromatogram of eight SAs  $10 \mu\text{g mL}^{-1}$  at flow rate of  $1.5 \text{ mL min}^{-1}$  with 70:25:5(v/v/v) of potassium phosphate solution (pH 4): acetonitrile : ethanol as the mobile phase. The detection potential was 1.4 V vs. Ag/AgCl using G/PANI modified screen-printed carbon electrode.

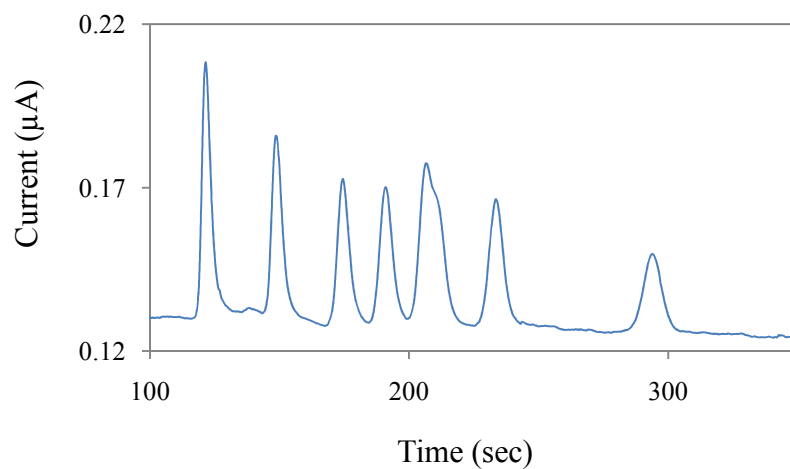


**Figure 4.24** UFLC-ECD chromatogram of eight SAs  $10 \mu\text{g mL}^{-1}$  at flow rate of  $1.5 \text{ mL min}^{-1}$  with 70:25:5(v/v/v) of potassium phosphate solution (pH 5): acetonitrile : ethanol as the mobile phase. The detection potential was 1.4 V vs. Ag/AgCl using G/PANI modified screen-printed carbon electrode.

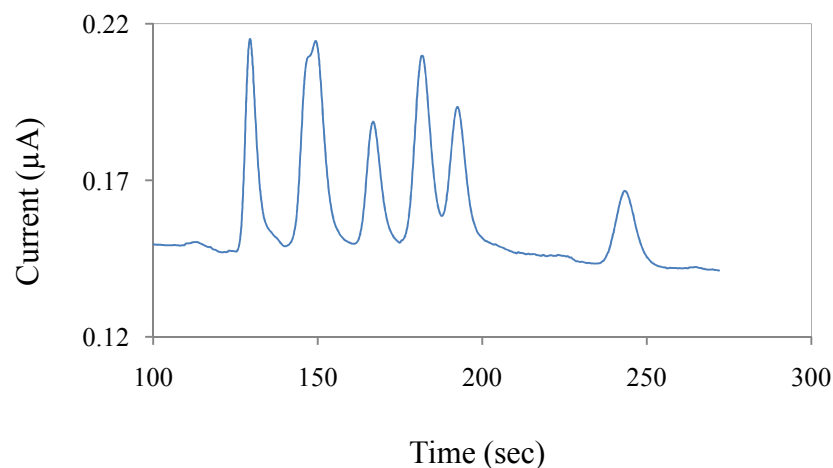


**Figure 4.25** UFLC-ECD chromatogram of eight SAs  $10 \mu\text{g mL}^{-1}$  at flow rate of  $1.5 \text{ mL min}^{-1}$  with 70:25:5(v/v/v) of potassium phosphate solution (pH 6): acetonitrile : ethanol as the mobile phase. The detection potential was 1.4 V vs. Ag/AgCl using G/PANI modified screen-printed carbon electrode.

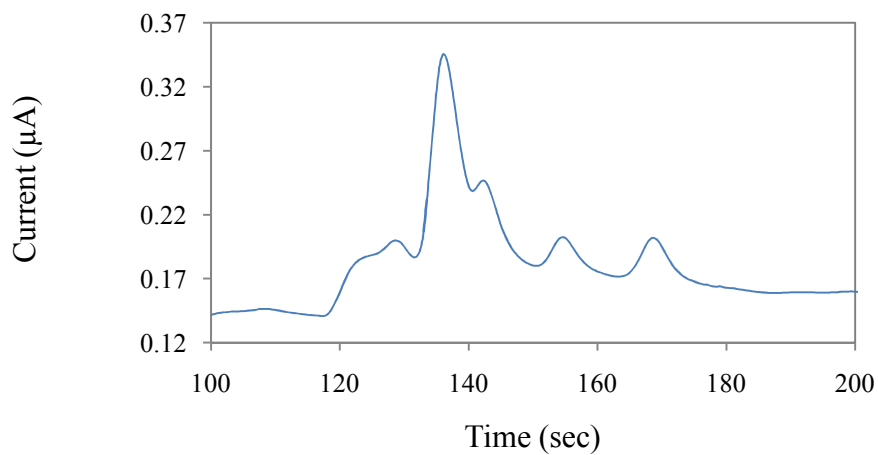


**Figure 4.26** UFLC-ECD chromatogram of eight SAs  $10 \mu\text{g mL}^{-1}$  at flow rate of  $1.5 \text{ mL min}^{-1}$  with 70:25:5(v/v/v) of potassium phosphate solution (pH7): acetonitrile : ethanol as the mobile phase. The detection potential was 1.4 V vs. Ag/AgCl using G/PANI modified screen-printed carbon electrode.

### 4.3.3 Optimal flow rate of mobile phase

The mixture of 0.05 M potassium hydrogen phosphate solution (pH3): acetonitrile: ethanol (70:25:5 v/v/v) was used as the mobile phase in chromatographic separation by using UFLC with amperometric detection. To obtain the clearly separation and rapid detection of eight SAs, the flow rate of the mobile phase was varied in the range of 0.5 - 2.0 mL min<sup>-1</sup>. The standard mixture of eight SAs at 10 µg mL<sup>-1</sup> with the injection volume of 25 µL was used to study the optimal flow rate of the mobile phase. The chromatograms of 10 µg mL<sup>-1</sup> with different flow rate of the mobile phase are shown in Figure 4.27. The results indicated that the flow rate of 1.5 mL min<sup>-1</sup> provided the best separation for all SAs within 7 min. The analysis time of the separation increased when the flow rate was decreased lower than 1.5 mL min<sup>-1</sup>. The overlapped peaks were obtained when the flow rate was higher than 1.5 mL min<sup>-1</sup>. As a result, the flow rate of mobile phase at 1.5 mL min<sup>-1</sup> was selected as the suitable flow rate of the separation for determination of eight SAs.

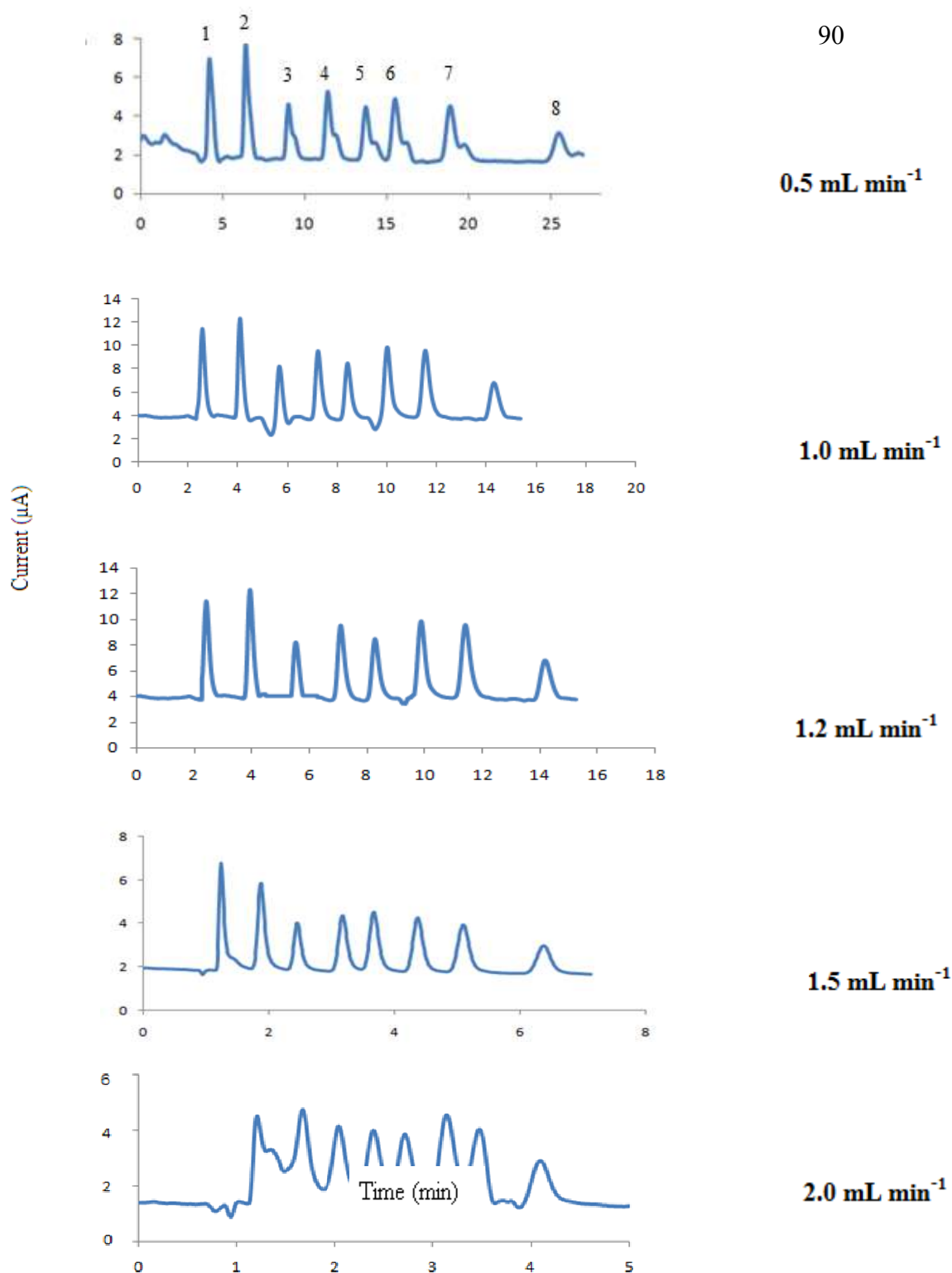


**Figure 4.27** UFLC-EC chromatogram of standard mixture of eight SAs ( $10 \mu\text{g mL}^{-1}$ ) (1) SG, (2) SDZ, (3) SMZ, (4) SMM, (5) SDX, (6) SMX, (7) SSZ and (8) SDM at G/PANI modified screen-printed carbon electrode with various of flow rate in the range of  $0.5 - 2.0 \text{ mL min}^{-1}$ .

#### 4.3.4 Optimal condition of the separation

To separate sulfonamides, Inertsil C4 column was used for UFLC analysis coupled with amperometric detection by G/PANI modified screen-printed carbon electrode. The optimal conditions in Table 4.1 were applied for complete separation of SG, SDZ, SMZ, SMM, SDX, SMX, SSZ and SDM by a novel system of UFLC-ECD. The chromatogram of 10  $\mu\text{g mL}^{-1}$  standard mixture of eight SAs is shown in Figure 4.28. The retention times of SG, SDZ, SMZ, SMM, SDX, SMX, SSZ and SDM were 1.69, 2.07, 2.62, 3.20, 3.91, 4.28, 5.14, and 6.23 minute, respectively. The proposed method was exhibited a rapid separation within 7 minutes.

**Table 4.1** The UFLC-ECD conditions for the detection of eight sulfonamides

UFLC parameters	UFLC conditions
Column	Inertsil C4 (150 x 4.6 mm)
Mobile phase	Phosphate buffer (pH 3): Acetonitrile: Ethanol (70:25:5, v/v/v)
Flow rate	1.5 mL/min
Injection volume	25 $\mu\text{L}$
Temperature	25 $^{\circ}\text{C}$
Detector	Amperometric detection at 1.4 V



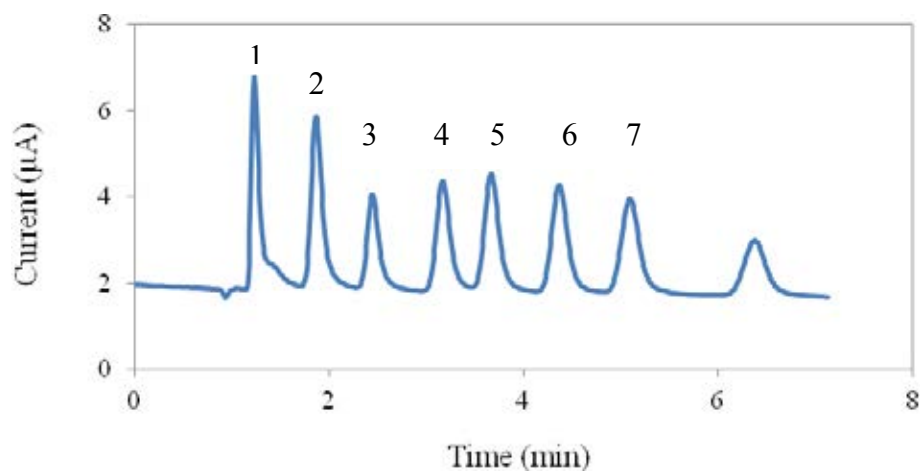


**Figure 4.28** UFLC-EC chromatogram of standard mixture of eight SAs ( $10 \mu\text{g mL}^{-1}$ ) (1) SG, (2) SDZ, (3) SMZ, (4) SMM, (5) SDX, (6) SMX, (7) SSZ and (8) SDM at G/PANI-modified carbon screen-printed electrode. The mobile phase was 0.05 M potassium hydrogen phosphate solution (pH 3): acetonitrile: ethanol (70:25:5 v/v/v). The injection volume was  $25 \mu\text{L}$ , and the flow rate was  $1.5 \text{ mL min}^{-1}$ .

## 4.4 Analytical Performance

### 4.4.1 Calibration and linearity

After completing the optimization of SAs separation and detection using our proposed system, calibration curve was established by measuring between current and concentration of the SAs. The calibration curves were obtained from triplicate injection of SAs in the range between 0.1 to 10  $\mu\text{g mL}^{-1}$ . These calibration curves of eight SAs show a good linearity between current and concentrations as shown in Figure 4.29, 4.30, 4.31, 4.32, 4.33, 4.34, 4.35 and 4.36, respectively. The results show that the coefficients of determination ( $r^2$ ) were higher than 0.99. Therefore, this novel system UFLC-ECD demonstrated a good linearity for determination of SAs.

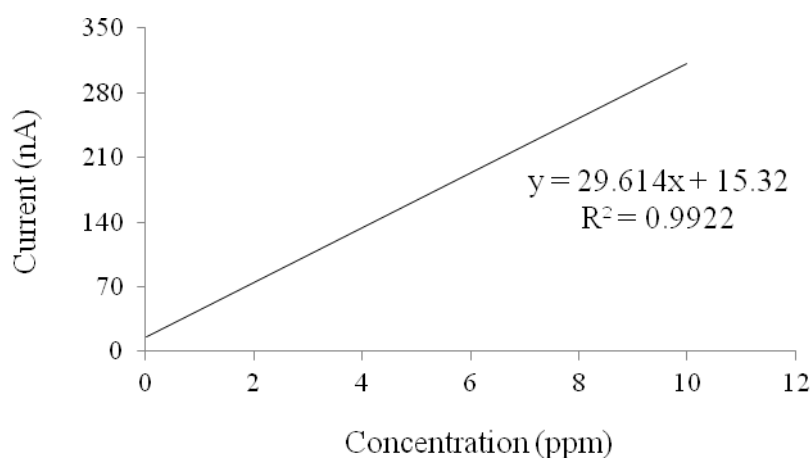


**Figure 4.29** Calibration curve of SMZ by UFLC-ECD using G/PANI-modified screen-printed carbon electrode in the concentration range of 0.1 to 10  $\mu\text{g mL}^{-1}$ .

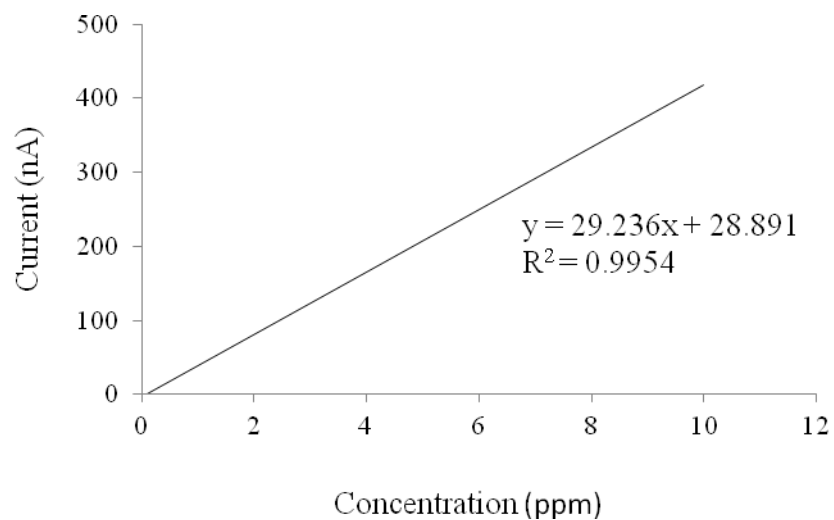


**Figure 4.30** Calibration curve of SMM by UFLC-ECD using G/PANI-modified screen-printed carbon electrode in the concentration range of 0.1 to 10  $\mu\text{g mL}^{-1}$ .

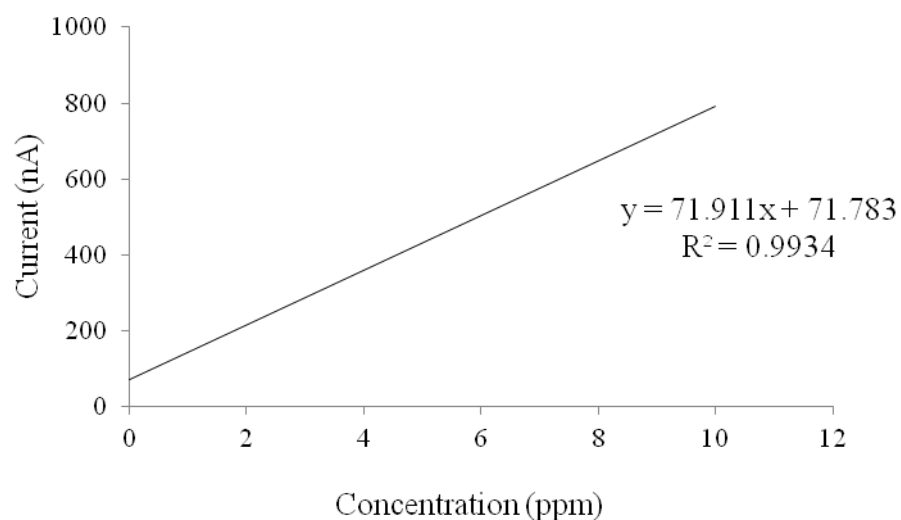


**Figure 4.31** Calibration curve of SG by UFLC-ECD using G/PANI-modified screen-printed carbon electrode in the concentration range of 0.1 to 10  $\mu\text{g mL}^{-1}$ .

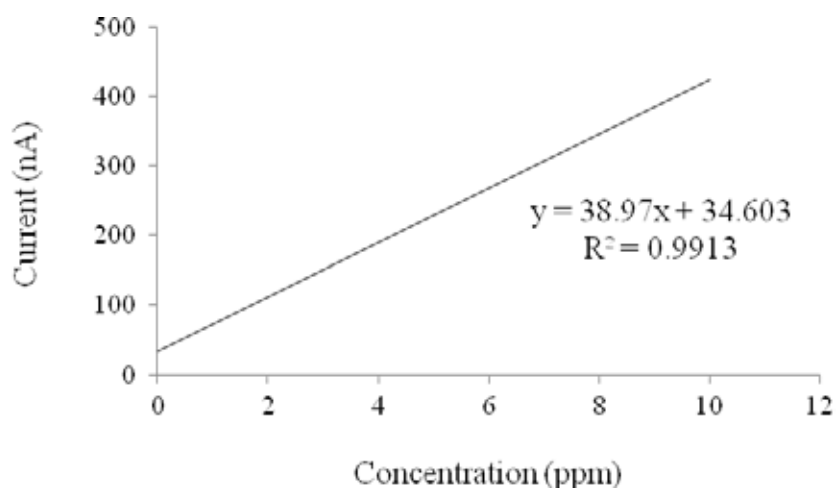


**Figure 4.32** Calibration curve of SDZ by UFLC-ECD using G/PANI-modified screen- printed carbon electrode in the concentration range of 0.1 to 10  $\mu\text{g mL}^{-1}$ .

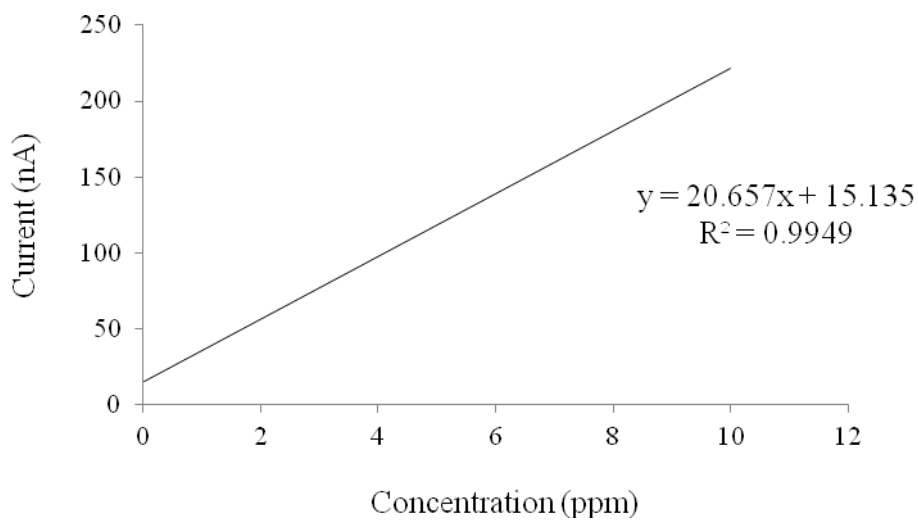


**Figure 4.33** Calibration curve of SDM by UFLC-ECD using G/PANI-modified screen- printed carbon electrode in the concentration range of 0.1 to 10  $\mu\text{g mL}^{-1}$ .

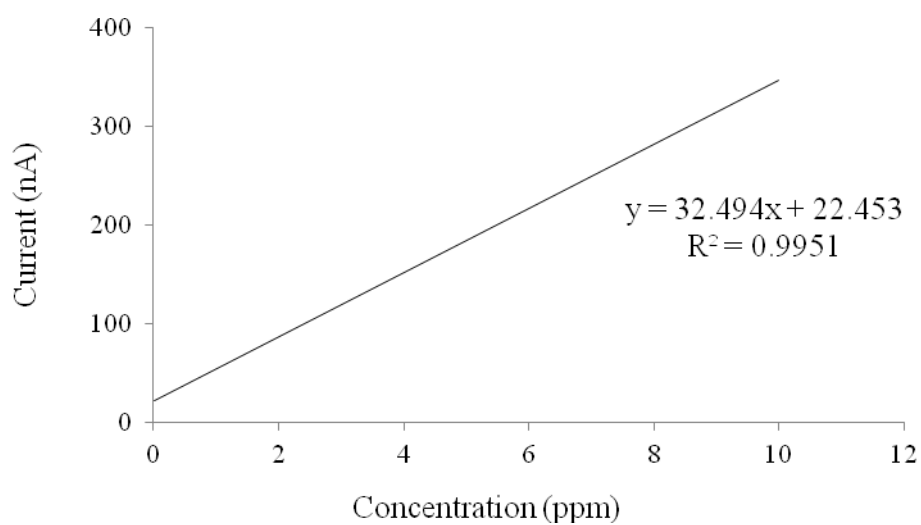


**Figure 4.34** Calibration curve of SSZ by UFLC-ECD using G/PANI-modified screen-printed carbon electrode in the concentration range of 0.1 to 10  $\mu\text{g mL}^{-1}$ .

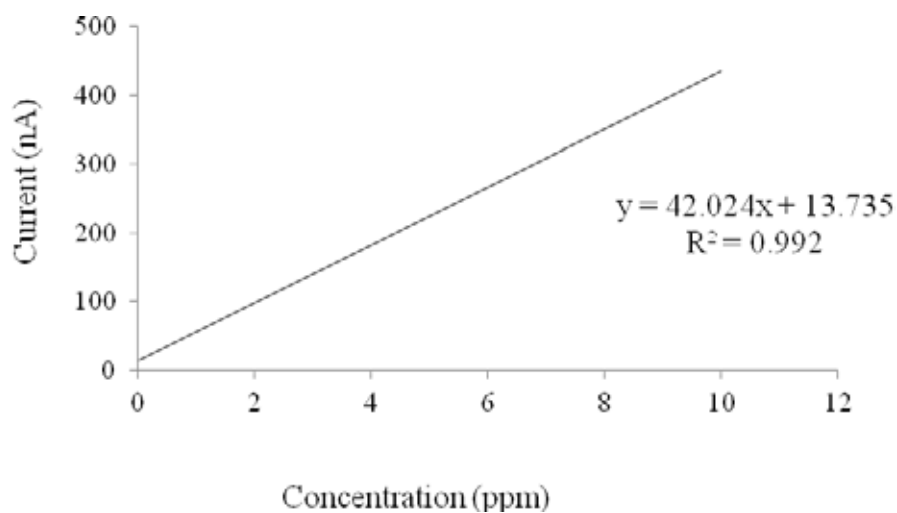


**Figure 4.35** Calibration curve of SMX by UFLC-ECD using G/PANI-modified screen-printed carbon electrode in the concentration range of 0.1 to 10  $\mu\text{g mL}^{-1}$ .

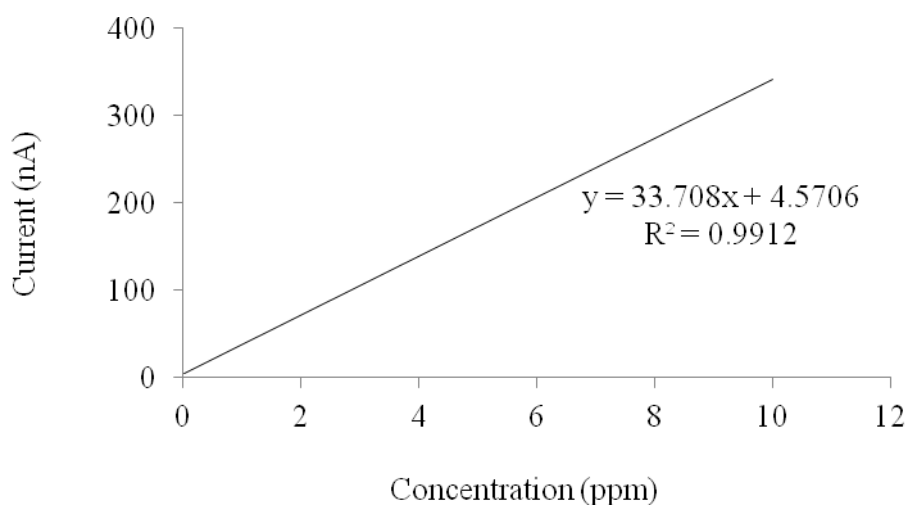


**Figure 4.36** Calibration curve of SDX by UFLC-ECD using G/PANI-modified screen printed carbon electrode in the concentration range of 0.1 to 10  $\mu\text{g mL}^{-1}$ .

#### 4.4.2 Limit of detection (LOD) and limit of quantification (LOQ)

The important analytical characteristics were the LOD and LOQ. The limit of detection (LOD) and limit of quantification (LOQ) were obtained from the calculation of  $3S_B/b$  and  $10S_B/b$ , where  $S_B$  is the standard deviation of the blank measurement ( $n=10$ ) and  $b$  is the sensitivity of the method or slope of the calibration curve. The LOD and LOQ of eight SAs were found in the range of 1.162 – 6.127  $\text{ng mL}^{-1}$  and 3.336 - 20.425  $\text{ng mL}^{-1}$ , respectively as shown on Table 4.2.

**Table 4.2** Analytical performance of eight SAs including linear range (LR), the limit of detection (LOD), slope ( $b$ ), and limit of quantification (LOQ).

SAs	LR ( $\mu\text{g mL}^{-1}$ )	Equation $y=bx+a$	$R^2$	LOD( $\text{ng mL}^{-1}$ )	LOQ( $\text{ng mL}^{-1}$ )
SG	0.01-10	$y = 71.911x+71.783$	0.9934	1.162	3.336
SDZ	0.01-10	$y = 38.970x+34.603$	0.9913	1.601	5.337
SMZ	0.01-10	$y = 29.614x+15.320$	0.9922	2.900	9.667
SMM	0.01-10	$y = 29.236x+28.891$	0.9954	2.467	8.224
SDX	0.01-10	$y = 33.708x+4.571$	0.9912	2.995	9.983
SMX	0.01-10	$y = 42.024x+13.735$	0.9920	2.513	8.376
SSZ	0.01-10	$y = 32.494x+22.453$	0.9951	3.287	10.957
SDM	0.01-10	$y = 20.657x+15.135$	0.9949	6.127	20.425

## 4.5 Application in real sample

Under the optimal condition of a novel system UFLC-ECD, the suitable condition was applied to determination of sulfonamides in shrimp sample. The  $\text{Na}_2\text{EDTA}$ -McIlvaine buffer (pH 4) was used as the extracting solution. Microcolumn Vertipak<sup>TM</sup> HCP was chosen for sample clean up and extraction in our proposed method.

### 4.5.1 Determination of SAs in shrimp

The proposed method was then applied to determine SAs in shrimp samples purchased from local supermarket in Thailand. The standard addition method was used for investigating reliability and accuracy of the developed method. The representative chromatogram obtained from the analysis of shrimp sample was demonstrated in Figure 4.37. The peaks were identified by comparison with the standard SAs which were reference compounds, determined by injection of standard solution. The method presented that the matrix compounds did not interfere with SDM, SMZ, SMM, SDX, SMX, SSZ and SDM. It can be explained that supernatant obtained from SPE procedure still contains very high concentrations of protein and lipid as shown in Figure 4.37 (a). Therefore, the method development of SPE system needs to study for further experiment. As a result, it can be concluded that this novel system of UFLC-ECD by using G/PANI- modified screen printed carbon electrode can be effectively used to detect sulfonamides in shrimp sample.



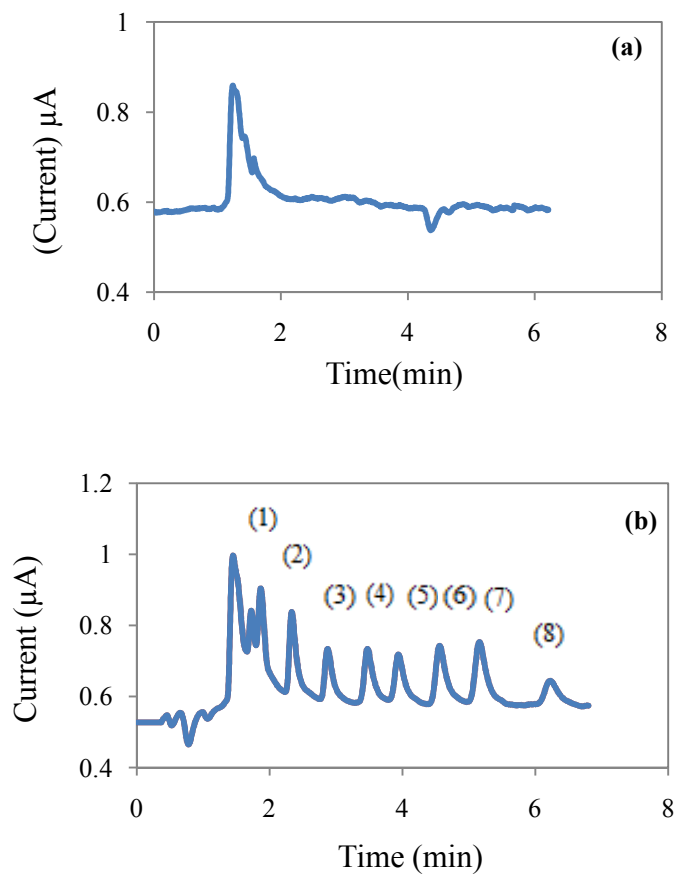


**Figure 4.37** UFLC-ECD chromatograms of (a) blank shrimp sample and (b) shrimp sample at spiked level  $5 \mu\text{g mL}^{-1}$  of (1) SG, (2) SDZ, (3) SMZ, (4) SMM, (5) SDX, (6) SMX, (7) SSZ and (8) SDM at G/PANI-modified carbon screen-printed electrode. The mobile phase was 0.05 M potassium hydrogen phosphate solution (pH 3): acetonitrile: ethanol (70:25:5 v/v/v). The injection volume was  $25 \mu\text{L}$ , and the flow rate was  $1.5 \text{ mL min}^{-1}$ .

#### 4.5.2 Accuracy and Precision

The precision of the analytical process was obtained by determining the relative standard deviation (RSD) from repeating detection of complete set of standard SAs solution. In order to assess the reproducibility in shrimp sample, the experiment was repeated for three times in each three concentration at 3, 5 and 9  $\mu\text{g mL}^{-1}$ . These selected concentrations represented low, medium and high levels in linear range of SAs detection. To evaluate the accuracy of the developed method, the percent recovery of spiking SAs in blank shrimp sample with level of 3, 5 and 9  $\mu\text{g mL}^{-1}$  were studied. The intra and inter-day precision and recovery of this novel system UFLC-ECD were summarized in Table 4.3 and Table 4.4, respectively. The results provided a good recovery and reproducible signal of all SAs. The RSD were below 5% and percent recovery was found in the range of 84.99-108.91 % for all SAs. It can be seen that the proposed method presented a percent recovery and %RSD value less than the AOAC International recommended value. Therefore, the novel UFLC-ECD system can be used to separate and detect all of SAs in shrimp sample with high accuracy and precision.

**Table 4.3** Intra-day precision and recoveries of SAs detection in shrimp samples (n=3)

Analyte	Spiked level	Recovery			mean±SD <sup>a</sup>	RSD (%)
		1	2	3		
1	3	98.81	104.00	102.72	101.84±2.70	2.65
	5	98.50	95.60	96.73	96.94±1.46	1.50
	9	100.48	99.11	99.09	99.56±0.80	0.80
2	3	85.56	91.46	92.58	89.86±3.77	4.20
	5	98.07	98.32	97.65	98.01±0.34	0.35
	9	99.50	101.00	101.67	100.73±1.11	1.10
3	3	83.69	84.4	86.88	84.99±1.68	1.97
	5	99.67	99.2	99.86	99.58±0.34	0.34
	9	101.02	99.81	99.62	100.15±0.75	0.75
4	3	95.94	96.82	96.80	96.52±0.50	0.52
	5	100.9	102.18	101.66	101.58±0.64	0.63
	9	99.91	98.79	99.58	99.43±0.57	0.50
5	3	88.26	84.72	87.48	86.82±1.86	2.15
	5	98.61	104.76	103.59	102.32±3.27	3.19
	9	100.42	97.96	99.06	99.15±1.23	1.24
6	3	84.77	86.24	88.36	86.46±1.80	2.08
	5	100.73	100.22	100.5	100.48±0.25	0.25
	9	102.21	101.01	100.81	101.37±0.73	0.72
7	3	87.21	88.92	89.69	88.60±1.27	1.43
	5	101.95	102.33	100.78	101.68±0.81	0.79
	9	102.52	101.0	100.75	101.42±0.95	0.94
8	3	111.17	108.53	107.02	108.91±2.10	1.93
	5	98.83	99.28	98.77	98.96±0.28	0.28
	9	100.98	101	101.39	101.02±0.35	0.34

<sup>a</sup> mean of recovery (%) ± standard deviation of triplicate measurements.

**Table 4.4** Inter-day precision and recoveries of SAs detection in shrimp samples (n=3)

Analyte	Spiked level	Recovery			mean $\pm$ SD <sup>a</sup>	RSD (%)
		1	2	3		
1	3	94.44	88.89	92.81	92.05 $\pm$ 2.85	3.10
	5	100.42	103.75	100.87	101.65 $\pm$ 1.83	1.79
	9	100.46	99.07	98.47	99.34 $\pm$ 1.01	1.02
2	3	87.69	88.18	87.99	87.95 $\pm$ 0.24	0.27
	5	102.76	102.55	102.90	102.74 $\pm$ 0.18	0.17
	9	99.57	100.58	100.51	100.22 $\pm$ 0.56	0.56
3	3	83.12	84.73	83.78	83.87 $\pm$ 0.81	0.96
	5	101.87	101.61	102.91	102.13 $\pm$ 0.68	0.67
	9	100.61	100.86	100.75	100.74 $\pm$ 0.12	0.12
4	3	93.24	92.31	92.02	92.52 $\pm$ 0.64	0.96
	5	102.46	104.04	106.16	104.22 $\pm$ 1.85	0.67
	9	100.96	100.48	100.26	100.57 $\pm$ 0.36	0.12
5	3	85.77	86.55	87.75	86.69 $\pm$ 0.99	1.15
	5	103.75	103.14	101.93	102.94 $\pm$ 0.93	0.9
	9	100.78	101.89	101.07	101.01 $\pm$ 0.21	0.2
6	3	87.28	87.42	88.02	87.57 $\pm$ 0.39	0.45
	5	97.09	96.82	96.45	96.79 $\pm$ 0.32	0.33
	9	102.14	102.22	102.27	102.21 $\pm$ 0.06	0.06
7	3	84.9	85.37	85.01	85.09 $\pm$ 0.24	0.28
	5	100.05	99.43	99.54	99.67 $\pm$ 0.32	0.32
	9	100.68	100.40	100.17	100.42 $\pm$ 0.26	0.25
8	3	91.61	91.58	91.38	91.52 $\pm$ 0.12	0.13
	5	94.68	94.75	95.51	94.98 $\pm$ 0.46	0.48
	9	103.79	103.15	102.25	103.06 $\pm$ 0.77	0.74

<sup>a</sup> mean of recovery (%)  $\pm$  standard deviation of triplicate measurements.

#### 4.5.3 Comparison of methods between the UFLC-ECD and UFLC-UV

The proposed method using G/PANI modified screen printed carbon electrode coupled with amperometric detection for determination of SG, SDM, SMZ, SMM, SDX, SMX, SSZ and SDM. To validate the developed method, the result of this novel system was compared to standard method using UFLC coupled with ultraviolet detection. The optimal conditions in Table 4.1 were also used to detect SAs in shrimp. Three shrimp samples consisting of blank shrimp, shrimp spiked SAs at  $3 \mu\text{g mL}^{-1}$  and  $5 \mu\text{g mL}^{-1}$  were performed for comparison of both methods. The results obtained from both methods are shown in Table 4.5. A paired t-test at 95% confidential interval was calculated using Microsoft Excel software. The statistic t-values for eight SAs were found to be 2.024 (spiked sample at  $3 \mu\text{g mL}^{-1}$ ) and 0.163 (spiked sample at  $5 \mu\text{g mL}^{-1}$ ). While the experimental t-value,  $t_{\text{calculated}}$  value two-tail were found to be 0.0826 (spiked sample at  $3 \mu\text{g mL}^{-1}$ ) and 0.875 (spiked sample at  $5 \mu\text{g mL}^{-1}$ ), respectively. The statistic t-value was higher than the experimental t-value. It is successfully found that there is no significant difference the two sets of results between a novel system and the standard method. Therefore, UFLC system coupled with G/PANI modified electrode as a novel method can be acceptable and reliable.

**Table 4.5** Comparisons results of two methods in shrimp sample.

Analyte	Concentration of SAs found	
	UFLC-ECD	UFLC-UV
Blank shrimp		
SG	ND	ND
SDZ	ND	ND
SMZ	ND	ND
SMM	ND	ND
SDX	ND	ND
SMX	ND	ND
SSZ	ND	ND
SDM	ND	ND
Spiking at level 3 $\mu\text{g mL}^{-1}$		
SG	3.06 $\pm$ 0.08	2.92 $\pm$ 0.05
SDZ	2.69 $\pm$ 0.11	3.10 $\pm$ 0.01
SMZ	2.55 $\pm$ 0.05	3.06 $\pm$ 0.01
SMM	2.90 $\pm$ 0.01	2.91 $\pm$ 0.01
SDX	2.60 $\pm$ 0.06	3.15 $\pm$ 0.04
SMX	2.59 $\pm$ 0.05	2.83 $\pm$ 0.01
SSZ	2.66 $\pm$ 0.04	3.16 $\pm$ 0.02
SDM	3.27 $\pm$ 0.06	3.00 $\pm$ 0.01
Spiking at level 5 $\mu\text{g mL}^{-1}$		
SG	4.84 $\pm$ 0.07	5.04 $\pm$ 0.09
SDZ	4.90 $\pm$ 0.02	4.94 $\pm$ 0.01
SMZ	4.97 $\pm$ 0.02	4.99 $\pm$ 0.01
SMM	5.07 $\pm$ 0.03	5.17 $\pm$ 0.01
SDX	5.11 $\pm$ 0.16	4.75 $\pm$ 0.06
SMX	5.02 $\pm$ 0.01	5.17 $\pm$ 0.01
SSZ	5.08 $\pm$ 0.04	4.87 $\pm$ 0.01
SDM	4.95 $\pm$ 0.01	5.15 $\pm$ 0.03

## CHAPTER V

### CONCLUSIONS

#### 5.1 Conclusions

G/PANI-modified screen-printed carbon electrode was firstly coupled with UFLC separation for rapid, selective, sensitivity, and simultaneous determination of sulfadiazine, sulfamerazine, sulfaquanidine, sulfisoxazole, sulfadimethoxine, sulfamonomethoxine, sulfadoxine, and sulfamethoxazole. G/PANI modified screen-printed carbon electrode was successfully prepared by a simply electrospraying technique. The surface morphology of G/PANI modified electrode was characterized by scanning electron microscope (SEM) to confirm the homogeneous distribution between graphene and polyaniline. Cyclic voltammetric results of  $[\text{Fe}(\text{CN})_6]^{3-}$  and  $[\text{Fe}(\text{CN})_6]^{4-}$  between G/PANI modified screen-printed carbon electrode and unmodified electrode demonstrated that the modified electrode exhibited a well-defined pair of oxidation-reduction peak higher than unmodified electrode, and electron transfer process provides linear relationship between current and square root of scan rate that can be indicating that the diffusion controlled process occurred on the G/PANI-modified screen-printed carbon electrode. The electrochemical behaviors of the eight SAs were investigated by cyclic voltammetry in phosphate pH 3. Comparison results of G/PANI-modified screen-printed carbon electrode, unmodified electrode and boron doped diamond electrode were found that G/PANI-modified screen-printed carbon electrode provided the highest sensitivity of electrochemical response for SAs detection. Moreover, the electrode developed in this novel system is much cheaper than boron doped diamond electrode and it can be simply fabricated.

By using the novel UFLC coupling with electrochemical detection, all SAs were completely separated and sensitivity detected within 7 minutes under the optimal

conditions including 0.05 M potassium hydrogen phosphate solution (pH 3): acetonitrile: ethanol (70:25:5 v/v/v), detection potential of 1.4 V, flow rate of 1.5 mL min<sup>-1</sup> and injection volume of 25 µL. Method validation of this novel system was presented in the linearity within the range of 0.1 to 10 µg mL<sup>-1</sup> with the correlation coefficient was 0.9934, 0.9913, 0.9922, 0.9954, 0.9912, 0.9920, 0.9951 and 0.9949 for SG, SDZ, SMZ, SMM, SDX, SMX, SSZ and SDM, respectively. And the limit of detection (LOD) and limit of quantification (LOQ) were found in the range of 1.162 – 6.127 ng mL<sup>-1</sup> and 3.336 – 20.425 ng mL<sup>-1</sup>, respectively for those eight SAs.

Furthermore, this proposed system could be applied for simultaneous determination of SAs in fresh shrimp sample. The results obtained from spiked SAs in shrimp sample at 3, 5 and 9 µg mL<sup>-1</sup> exhibited a good recovery in level of spiking solution. The intra and inter-day precision and recovery of this novel system UFLC-ECD were also studied, and the result provided a good recovery and reproducible signal of all SAs. The RSD were below 5% and percent recovery was found in the range of 84.99 - 108.91 % for all analyses. The proposed method presented a percent recovery and % RSD value less than the AOAC International recommended value. To validate the developed method, the result of this novel system was compared to standard method of UFLC coupled with ultraviolet detection. The statistic t-value was significant higher than the experimental t-value between two pairs of assays. It is successfully found that there was no significant difference the two sets of results between a novel system and the standard method. Therefore, all of SAs can be separated and simultaneously sensitive determine by our novel system.



## **5.2 Suggestion for future work**

In this research, the novel system UFLC coupled with G/PANI modified screen-printed carbon electrode was firstly applied to the separation and sensitive determination of sulfonamide in shrimp sample. Other sample of animal feed should be impetus us to study as well. Moreover, G/PANI modified screen-printed carbon electrode can be developed in biosensor study due to the modified electrode material, and polyaniline composite on the electrode surface have a basic structure of amine group that easily to apply for biosensor application.

## REFERENCES

- [1] Hruska, K., and Franek, M. Sulfonamides in the environment: a review and a case report. Veterinarni Medicina 57 (2012): 1-35.
- [2] Cheong, C.K., Hajeb, P., and Jinap, S. Sulfonamides determination in chicken meat products from Malaysia. International Food Research Journal 17 (2010): 885-892.
- [3] Commission of the European Community. The rules governing medical products in the European Community IV. Brussels: 1991.
- [4] Borrás, S., Companyo, R., and Guiteras, J. Analysis of Sulfonamides in Animal Feeds by Liquid Chromatography with fluorescence detection. Journal of Agricultural and Food Chemistry 59 (2011): 5240-5247.
- [5] Bruhn, H., and Beck, I. Effects of sulfonamide and tetracycline antibiotics on soil microbial activity and microbial biomass. Chemosphere 59 (2005): 457-465.
- [6] Gao, P., Munir, M., and Xagorarakis, I. Correlation of tetracycline and sulfonamide antibiotics with corresponding resistance genes and resistant bacteria in a conventional municipal wastewater treatment plant. Science of the Total Environment 421 (2012): 173-183.
- [7] Yang, T.C., Yang, I., and Liao, L. Determination of sulfonamide residues in milk by on-line microdialysis and HPLC. Journal of liquid chromatography and related technologies 27 (2004): 501-510.
- [8] Zhang, H., and Wang, S. Review on enzyme-linked immunosorbent assays for sulfonamide residues in edible animal products. Journal of Immunological Methods 350 (2009): 1-13.
- [9] Gerry, J., and Suarez, A. Development of a screening method for five sulfonamides in salmon muscle tissue using thin-layer chromatography. Journal of Chromatography A 555 (1991): 315-320.
- [10] Sherma, J. Thin-layer chromatography in food and agricultural analysis. Journal of Chromatography A 880 (2000): 129-147.

- [11] Haasnoot, W., Swanenburg, M. and Rhijna, H. Application of a multi sulfonamide biosensor immunoassay for the detection of sulfadiazine and sulfamethoxazole residues in broiler serum and its use as a predictor of the levels in edible tissue. *Analytica Chimica Acta* 552 (2005): 87-95.
- [12] Cháfer, C., Maquieira, A., Puchades, R., Miralles, J., and Moreno, A. Fast screening immunoassay of sulfonamides in commercial fish samples. *Analytical and Bioanalytical Chemistry* 296 (2010): 911-921.
- [13] Chiavarino, B., Crestoni, M.E., Marzio, A.D., and Fornarini, S. Determination of sulfonamide antibiotics by gas chromatography coupled with atomic emission detection. *Journal of Chromatography B* 706 (1998): 269-277.
- [14] Reeves, V.B. Confirmation of multiple sulfonamide residues in bovine milk by gas chromatography–positive chemical ionization mass spectrometry. *Journal of Chromatography B* 723 (1999): 127-137.
- [15] Fuh, M.S., and Chan, S. Quantitative determination of sulfonamide in meat by liquid chromatography–electrospray-mass spectrometry. *Talanta* 55 (2001): 1127-1139.
- [16] Xu, Y., Ding, J., Chena, H., and Ren, N. Fast determination of sulfonamides from egg samples using magnetic multiwalled carbon nanotubes as adsorbents followed by liquid chromatography–tandem mass spectrometry. *Food chemistry* 140 (2013): 83-90.
- [17] Galán, M.G., Cruz, M.S and Barceló, D. Determination of 19 sulfonamides in environmental water samples by automated on-line solid-phase extraction-liquid chromatography–tandem mass spectrometry (SPE-LC–MS/MS). *Talanta* 81 (2010): 355-366.
- [18] Minh, N., Stuetz, R.M., and Khan, S.J. Determination of six sulfonamide antibiotics, two metabolites and trimethoprim in wastewater by isotope dilution liquid chromatography/tandem mass spectrometry. *Talanta* 89 (2012): 407-416.

- [19] Cai, Z., Zhang, Y., Pan, H. Tie, X. and Ren, Y. Simultaneous determination of 24 sulfonamide residues in meat by ultra-performance liquid chromatography tandem mass spectrometry. Journal of Chromatography A 1200 (2008): 144-155.
- [20] Won, S.Y., Lee, C.H., Chang, H.S., Lee, S.H. and Kim, D.S. Monitoring of 14 sulfonamide antibiotic residues in marine products using HPLC-PDA and LC-MS/MS. Food Control 22 (2011): 1101-1107.
- [21] Galán, M.J., Rodríguez, C.E., Vicent, T., Caminal, G. and Barceló, D. Biodegradation of sulfamethazine by *Trametes versicolor*: Removal from sewage sludge and identification of intermediate products by UPLC–QqTOF-MS. Science of the Total Environment 409 (2011): 5505-5512.
- [22] Kaufmann, A., Butcher, P., Maden, K., and Widmer, M. Ultra-performance liquid chromatography coupled to time of flight mass spectrometry (UPLC–TOF): A novel tool for multiresidue screening of veterinary drugs in urine. Analytica Chimica Acta 586 (2007): 13-21.
- [23] Zotou, A., and Vasiliadou, C. Selective Determination of Sulfonamide Residues in Honey by SPE-RP-LC with UV Detection. Chromatographia 64 (2006): 307-311.
- [24] Kaufmann, A., Butcher, P., Maden, K., and Widmer, M. Identification of incurred sulfonamide residues in eggs: methods for confirmation by liquid chromatography-tandem mass spectrometry and quantitation by liquid chromatography with ultraviolet detection. Journal of Chromatography B 774 (2002): 39-52.
- [25] Chen, C., and Chen, Q. A tetra-sulfonamide derivative bearing two dansyl groups designed as a new fluoride selective fluorescent chemosensor. Tetrahedron Letters 45 (2004): 3957-3960.
- [26] Chen, C., and Chen, Q. A new and simple method to determine trace levels of sulfonamides in honey by high performance liquid chromatography with fluorescence detection. Journal of Chromatography A 1216 (2009): 7275-7280.

- [27] Furlong, E.T., Burkhardt, M.R., Gates, P.M. and Battaglin, W.A. Routine determination of sulfonylurea, imidazolinone, and sulfonamide herbicides at nanogram-per-liter concentrations by solid-phase extraction and liquid chromatography/mass spectrometry. The Science of the Total Environment 248 (2000): 135-146.
- [28] Orazio, G., Rocchi, S. and Fanali, S. Nano-liquid chromatography coupled with mass spectrometry: Separation of sulfonamides employing non-porous core-shell particles. Journal of Chromatography A 1255 (2012): 277-285.
- [29] Yu, C., and Hu, B. C18-coated stir bar sorptive extraction combined with high performance liquid chromatography-electrospray tandem mass spectrometry for the analysis of sulfonamides in milk and milk powder. Talanta 90 (2012): 77-84.
- [30] Lu, Y., Shen, Q., Dai, Z., Zhang, H., and Wang, H. Development of an on-line matrix solid-phase dispersion/fast liquid chromatography/tandem mass spectrometry system for the rapid and simultaneous determination of 13 sulfonamides in grass carp tissues. Journal of Chromatography A 1218 (2011): 929-937.
- [31] Nematollahi, D., and Maleki, A. Electrochemical oxidation of N,N-dialkyl-p-phenylenediamines in the presence of arylsulfonic acids. An efficient method for the synthesis of new sulfonamide derivatives. Electrochemistry Communications 11 (2009): 488-491.
- [32] Won, S., Chandra, P., Hee, T.S., and Shim, Y.B. Simultaneous detection of antibacterial sulfonamides in a microfluidic device with amperometry. Biosensors and Bioelectronics 39 (2013): 204-209.
- [33] Sangjarusvichai, H., Dungchaia, W., Siangproh, W., and Chailapakula, O. Rapid separation and highly sensitive detection methodology for sulfonamides in shrimp using a monolithic column coupled with BDD amperometric detection. Talanta 79 (2009): 1036-1041.
- [34] Preechaworapun, A., Chuanuwatanakul, S., Einaga, Y., Grudpan, K., Motomizu, S. and Chailapakul, O. Electroanalysis of sulfonamides by flow injection system/high-performance liquid chromatography

- coupled with amperometric detection using boron-doped diamond electrode. Talanta 68 (2006): 1726-1731.
- [35] Zhang, R.J., Lee, S.T., and Lam, Y.W. Characterization of heavily boron-doped diamond films. Diamond and Related Material 5 (1996): 1288-1294.
- [36] Pang, L., Chan, S., Chalkers, P. and Johnston, C. Thin film diamond metal-insulator field effect transistor for high temperature applications. Materials Science and Engineering B 46 (1997): 124-128.
- [37] Ensafi, A.A., Allafchian, A.R., Rezaei, B. and Mohammadzadeh, R. Characterization of carbon nanotubes decorated with NiFe<sub>2</sub>O<sub>4</sub> magnetic nanoparticles as a novel electrochemical sensor: Application for highly selective determination of sotalol using voltammetry. Materials Science and Engineering C 33 (2013): 202-208.
- [38] Li, X., Zhao, H., Quan, H., Zhang, Y. and Yu, H. Adsorption of ionizable organic contaminants on multi-walled carbon nanotubes with different oxygen contents. Journal of Hazardous Materials 186 (2011): 407-415.
- [39] Rozhkova, A.V., Giavaras, G., Bliokh, Y.P., Freilikher, V. and Nori, F. Electronic properties of mesoscopic graphene structures: Charge confinement and control of spin and charge transport. Physics Reports 503 (2011): 77-114.
- [40] Patole, A.S., Patole, S.P., Jung, S., and Yoo, J. Self assembled graphene/carbon nanotube/polystyrene hybrid nanocomposite by in situ microemulsion polymerization. European Polymer Journal 48 (2012): 252-259.
- [41] Pham, T.A., Kim, J.S., and Jeong, Y.T. One-step reduction of graphene oxide with l-glutathione. Colloids and Surfaces A: Physicochemical and Engineering Aspects 384 (2011): 543-548.
- [42] Sebaa, M., Nguyen, T.Y., Paul, R.K. and Liua, H. Graphene and carbon nanotube-graphene hybrid nanomaterials for human embryonic stem cell culture. Materials Letters 92 (2013): 122-125.

- [43] Stejskal, J., Sapurina, I., and Trchová, M. Polyaniline nanostructures and the role of aniline oligomers in their formation. Progress in Polymer Science 35 (2010): 1420-1481.
- [44] Jayamurugan, P., Mariappan, R., Ponnuswamy, V., and Manikandan, H. High-PL efficiency of polyaniline using various dopants. Optik 122 (2011): 2083-2085.
- [45] Janaki, V., Vijayaraghavan, K., Muthuchelian, K., and Ramasamy, A.K. Starch/polyanilinenanocomposite for enhanced removal of reactive dyes from synthetic effluent. Carbohydrate Polymers 90 (2012): 1437-1444.
- [46] Larimi, S.G., Darzi, H.H., and Darzi, G.N. Fabrication and characterization of polyaniline/xanthan gum nanocomposite: Conductivity and thermal properties. Synthetic Metals 162 (2012): 171-175.
- [47] Class drug overview [online]. Available from:  
<http://www.elmhurst.edu/~chm/vchembook/653sulfa.html> [2012, March]
- [48] Sulfonamide antibiotic [online]. Available from:  
<http://www.fpnotebook.com/id/pharm/Slfnd.htm> [2012, March]
- [49] Introduction, Chromatography Theory, and Instrument Calibration [online]. Available from:  
[http://people.whitman.edu/~dunnivfm/C\\_MS\\_Ebook/Downloads/CH1FINAL.pdf](http://people.whitman.edu/~dunnivfm/C_MS_Ebook/Downloads/CH1FINAL.pdf) [2012, March]
- [50] Robards, K., Haddad, P.R., and Jackson, P.E. Principles and practice of modern chromatographic method. London: Academic Press Limited, 1994.
- [51] Willard, H.H., Lynne L. Merritt, J.R., Dean, J.A., and Frank A. Settle, J.R. Instrumental methods of Analysis. 6<sup>th</sup> edition. California: Wadsworth Publishing Company, 1981.
- [52] Skoog, D.A., and Leary, J.J. Principles of instrumental analysis. 4th edition. United States of America: Saunders College Publishing, 1971.
- [53] Swartz, M.E. UPLC<sup>TM</sup>: An introduction and review. Journal of Liquid Chromatography & Related Technologies 28 (2005): 1253-1263.

- [54] The role of ion exchange chromatography in purification and characterization of molecules [online]. Available from:  
[http://cdn.intechopen.com/pdfs/40709/InTech-The\\_role\\_of\\_ion\\_exchange\\_chromatography\\_in\\_purification\\_and\\_characterization\\_of\\_molecules.pdf](http://cdn.intechopen.com/pdfs/40709/InTech-The_role_of_ion_exchange_chromatography_in_purification_and_characterization_of_molecules.pdf). [2012, March]
- [55] Wang, J. Analytical electrochemistry. 3<sup>rd</sup> edition. New Jersey, USA: John Wiley & Sons, 2006.
- [56] General principle of chromatography [online]. Available from:  
[http://vedyadhara.ignou.ac.in/wiki/images/e/e0/Unit\\_4\\_General\\_Principles\\_of\\_Chromatography.pdf](http://vedyadhara.ignou.ac.in/wiki/images/e/e0/Unit_4_General_Principles_of_Chromatography.pdf)[2012, March]
- [57] Affinity Chromatography [online]. Available from:  
<http://www.bio-sun.com.cn/download/1.pdf> [2012, March]
- [58] Chromatography - Royal Society of Chemistry [online]. Available from:  
<http://media.rsc.org/Modern%20chemical%20techniques/MCT5%20Chromatography.pdf> [2012, March]
- [59] General Principles of Chromatography [online]. Available from:  
[http://wolfson.huji.ac.il/purification/PDF/Others/T0SOH\\_PrinciplesChromatPoster.pdf](http://wolfson.huji.ac.il/purification/PDF/Others/T0SOH_PrinciplesChromatPoster.pdf)[2012, March]
- [60] An introduction to UPLC technology: Improve Productivity and Data Quality [online] Available from:  
<http://www.waters.com/webassets/cms/library/docs/720002425en.pdf> [2012, March]
- [61] Srivastava, B., Sharma, B.K., Uttam S.B., Yashwant, and Neha, S. Ultra performance liquid chromatography (UPLC) : A chromatography technique. International Journal of Pharmaceutical Quality Assurance 2 (2010): 19-25.
- [62] Swartz, M.E. Ultra Performance Liquid Chromatography (UPLC): An Introduction. LC GC North America (2005): 8-14.
- [63] Prominence UFLCXR [online]. Available from:  
[http://www.ssi.shimadzu.com/products/literature/HPLC/Prominence\\_UFLCXR.pdf](http://www.ssi.shimadzu.com/products/literature/HPLC/Prominence_UFLCXR.pdf) [2012, March]
- [64] UPLC in Pharmaceutical Process Development - Comparison with



- Theoretical Promise [online]. Available from:  
<http://www.pittcon.org/attendees/pdf/2012/UPLC%20in%20Pharmaceutical%20Process%20Development%20%20Comparison%20with%20Theoretical%20Promise.pdf> [2012, March]
- [65] Bard, A. J., and Faulkner, L. R. Electrochemical Methods: Fundamentals and Applications. 2nd Edition. New York: John Wiley and Sons, 2001.
- [66] Plambeck, J. A. Electroanalytical Chemistry Basic Principles and Applications. New York, USA: John Wiley, 1982.
- [67] Mass Transport Mechanisms [online]. Available from:  
[http://www.asdlib.org/onlineArticles/ecourseware/Kelly\\_Potentiometry/PDF-5-MassTransport.pdf](http://www.asdlib.org/onlineArticles/ecourseware/Kelly_Potentiometry/PDF-5-MassTransport.pdf) [2012, March]
- [68] Principle of Cyclic voltammetry [online]. Available from:  
[http://kb.psu.ac.th/psukb/bitstream/2553/1449/7/287951\\_ch1.pdf](http://kb.psu.ac.th/psukb/bitstream/2553/1449/7/287951_ch1.pdf)  
 [2012, March]
- [69] Thurman, E.M., and Mill, M.S. Solid-Phase Extraction Principles and Practice. Canada: John Wiley and Sons, 1994.
- [70] Fritz, J.S. Analytical Solid-Phase Extraction. Canada: John Wiley and Sons, 1999.
- [71] Titus, A.M., Msagati, J. and Ngila C. Voltammetric detection of sulfonamides at a poly (3-methylthiophene) electrode. Talanta 58 (2002): 605-610.
- [72] Fuh, S., and Chu, S. Quantitative determination of sulfonamide in meat by solid-phase extraction and capillary electrophoresis. Analytica Chimica Acta 499 (2003): 215-221.
- [73] Chinchilla, J.J, Gracia, L., Marzio, A.D., Campañai, M.M., and Ima, K. High performance liquid chromatography post-column chemiluminescence determination of sulfonamide residues in milk at low concentration levels using bis[4-nitro-2-(3,6,9-trioxadecyloxycarbonyl)phenyl] oxalate as chemiluminescent reagent. Journal of Chromatography A 1095 (2005): 60-67.
- [74] Souza, C.D., Braga, O.C., Marzio, A.D., Vieira, I.C., and Spinelli, A. Electroanalytical determination of sulfadiazine and sulfamethoxazole in

- pharmaceuticals using a boron-doped diamond electrode. Sensors and Actuators B135 (2008): 66-73.
- [75] Zhang, W., Duan, C., Marzio, and Wang, M. Analysis of seven sulphonamides in milk by cloud point extraction and high performance liquid chromatography. Food Chemistry 126 (2011): 779-785.
- [76] Won, S.Y., Lee, C.H., Chang, H.S., and Kim, D.S. Monitoring of 14 sulfonamide antibiotic residues in marine products using HPLC-PDA and LC-MS/MS. Food Control 222011 (2011): 1101-1107.
- [77] Hernandez, F.J, and Ozalp, V.C., Graphene and other nanomaterial-based electrochemical aptasensors. Biosensors 2 (2012): 1-14.

## **APPENDICES**

**APPENDIX A****Table A1** Paired-t-testvalue

<b>df</b>	<b>95%</b>	<b>99%</b>
1	12.71	63.66
2	4.30	9.93
3	3.18	5.84
4	2.78	4.60
5	2.52	4.03
10	2.23	3.17
15	2.13	2.95
20	2.09	2.85
30	2.04	2.75
$\alpha$	1.96	2.58

**Table A2** T-test: paired two sample for means at 3 mg L<sup>-1</sup> concentration

	<b>UPLC-ECD</b>	<b>UPLC-UV</b>
<b>Mean</b>	2.790019	3.018569
<b>Variance</b>	0.066605	0.014362
<b>Observations</b>	8	8
<b>Pearson Correlation</b>	-0.33926	
<b>Hypothesized Mean Difference</b>	0	
<b>df</b>	7	
<b>t Stat</b>	-2.02454	
<b>P(T&lt;=t) one-tail</b>	0.041288	
<b>t Critical one-tail</b>	1.894579	
<b>P(T&lt;=t) two-tail</b>	0.082576	
<b>t Critical two-tail</b>	2.364624	

**Table A3** T-test: paired two sample for means at 5 mg L<sup>-1</sup> concentration

	<b>UPLC-ECD</b>	<b>UPLC-UV</b>
<b>Mean</b>	4.997248	5.008968
<b>Variance</b>	0.009099	0.023772
<b>Observations</b>	8	8
<b>Pearson Correlation</b>	-0.28795	
<b>Hypothesized Mean Difference</b>	0	
<b>df</b>	7	
<b>t Stat</b>	-0.16304	
<b>P(T&lt;=t) one-tail</b>	0.437549	
<b>t Critical one-tail</b>	1.894579	
<b>P(T&lt;=t) two-tail</b>	0.875097	
<b>t Critical two-tail</b>	2.364624	

**APPENDIX B****Table B1** The acceptable precision, the data from AOAC manual for peer verified methods program, VA, NOV 1993

<b>Analyte concentration</b>	<b>%RSD</b>
100%	± 1.3
10%	± 2.7
1%	± 2.8
0.1%	± 3.7
100 ppm	± 5.3
10 ppm	± 7.3
1 ppm	± 11
100 ppb	± 15
10 ppb	± 21
1 ppb	± 30

**Table B2** The acceptable accuracy, the data from AOAC manual for peer verified methods program, VA, NOV 1993

<b>Analyte concentration</b>	<b>% recovery</b>
100%	98-102
10%	98-102
1%	97-103
0.1%	95-105
100 ppm	90-107
10 ppm	80-110
1 ppm	80-110
100 ppb	80-110
10 ppb	60-115
1 ppb	40-120



## VITA

- Name** : Miss Nupattaranee Thammasoontaree
- Date of Birth** : October 28, 1986
- Place of Birth** : Bangkok, Thailand
- Graduated** : 2006-2009 Bachelor Degree of Science  
 Program in Chemistry,  
 King Mongkut's Institute of  
 Technology Ladkrabang
- 2010-2012 Master Degree of Science  
 Program in Chemistry,  
 Chulalongkorn University
- Home address** : 415, Rama 4 Road, Klongton, Klongtoey,  
 Bangkok 10110, Thailand
- Poster Presentation** : 2012 STT 38, Bangkok
- Oral presentation** : 2013 PACCON 2013, Bangkok

**Proceeding and Publication :**

NupattaraneeThammasoontaree, OrawonChailapakul“Graphene modified carbon screen-printed electrode for the determination of sulfonamides by ultra fast liquid chromatography coupled with electrochemical detection” Proceedings of Congress on Science and Technology of Thailand 2012, The Empress Convention Center, Chiang Mai, Thailand, October 17-19, 2012, pp 1-6.

